DEVELOPMENTAL BIOLOGY OF HETERODERA GLYCINES (SOYBEAN CYST NEMATODE) AND OTHER PLANT - PARASITIC NEMATODES

BY

SITA THAPA

DISSERTATION

Submitted in partial fulfillment of the requirements
for the degree of Doctor of Philosophy in Crop Sciences
in the Graduate College of the
University of Illinois at Urbana-Champaign, 2018

Urbana, Illinois

Doctoral Committee:

Assistant Professor Nathan E. Schroeder, Chair
Associate Professor Kris N. Lambert
Associate Professor Leslie L. Domier
Professor A. Lane Rayburn

ABSTRACT

Nematodes are unsegmented round worms with a pseudocoelomate body cavity. Nematodes are omnipresent in nature. Most are free-living, living as bacterial or fungal feeders, while many nematodes species are parasitic to animals or plants and have a huge impact on human health and agriculture worldwide. Sedentary plant-parasitic nematodes (PPN) like *Heterodera glycines,* among the most damaging pathogens to agriculture production. The sedentary nematodes are more fecund and considered more damaging than their phylogenetically closest migratory relatives. A better understanding of their pre-hatch and post-infection developmental biology may help to target this economically important pathogen. The embryo development of PPN like *H. glycines,* less studied in comparison to the free-living nematode *Caenorhabditis elegans*. *H. glycines* has complicated hatching behavior. *H. glycines* hatching increases in the presence of a host plant or hatching stimulants, while some do not hatch in presence of a host. Furthermore, *H. glycines* females produce approximately one-third of their eggs into an egg sac (egg sac eggs), located at the posterior end of the female, and remaining eggs are retained within the female body (encysted eggs). Different hatching rates have been found between egg sac eggs and encysted eggs. I found that *H. glycines* develop from a single-cell egg stage to fully formed J2 in approximately seven days. I describe the timeline of *H. glycines* embryogenesis of encysted eggs and egg sacs eggs in different hatching stimulants. I found that hatching stimulants do not affect embryogenesis timeline. Furthermore, I found that stylet protractor muscles and the primary motor nervous system of *H. glycines* J2s continue to develop until late in pre-hatch J2s, suggesting their requirement in hatching.

Following infection and the establishment of a feeding site, sedentary nematodes females (*H. glycines, Meloidogyne incognita*, and *Rotylenchulus reniformis*) become immobile. Interestingly, loss of mobility after infection is reversed in adult (*H. glycines* and *Meloidogyne incognita*) males while females never regain mobility. In *C. elegans*, contraction and relaxation of most body wall muscles are regulated by motor neurons within the ventral nerve cord (VNC). I studied the VNC neurons of *H. glycines, M. incognita*, and *R. reniformis* using DAPI (4′,6-diamidino-2-phenylindole) stain throughout development. In *H. glycines*, I found a gradual reduction of VNC neurons (65 to 40) during development from the mobile J2 to sedentary J3 and J4 females. Some nuclei of the VNC in sedentary stages were located several microns away from the ventral midline. Strikingly, I found 70 neurons in the adult male VNC and a reorganization of the cord into a linear arrangement. Similar to *H. glycines* I found fewer VNC neurons in sedentary stages of *M. incognita* and *R. reniformis* in comparison to mobile stage. The number of VNC neurons remained stable in *P. penetrans*, a migratory nematode. My results suggest that VNC motor neuron degeneration is correlated with sedentary behavior.

Unlike most nematodes, sedentary nematode females grow disproportionately greater in width than in length developing into a saccate shaped adult. In *C. elegans,* body size is correlated with stem-cell-like divisions of laterally positioned stem cell-like 'seam' cells that contribute to an increase in the total number of epidermal nuclei. I examined the epidermis of both live and fixed *H. glycines* at regular time points after synchronized infection. First, I confirmed the presence of seam cells in *H. glycines*. Then I found that in post-infection *H. glycines* seam cells proliferate extensively during each developmental stages. I found that *H. glycines* adult female epidermis comprises a syncytium of approximately 1800 epidermal nuclei, comparison vermiform species *C. elegans* approximately 140. Saccate shaped development has evolved

multiple times among nematodes. To study the evolution of the saccate shape nematode, I study two other saccate shape nematodes, *M. incognita* and *R. reniformis. H. glycines* and *M. incognita* are phylogenetically distinct but have similar life cycles, whereas *H. glycines* and *R. reniformis* are phylogenetically close but have a different life cycle. I found that *M. incognita* seam cell also proliferates following infection, however, the pattern of the division was different than in *H. glycines*. Both *H. glycines* and *M. incognita* epidermal nuclei were polyploid. Interestingly, *R. reniformis* does not show increased seam cell proliferation compared with *C. elegans*.

My results on *H. glycines* hatching stimulants provide insight into the primary survival mechanism for this important parasite. I have found that VNC neuron degenerates in sedentary plant-parasitic nematode species. The nervous system of nematodes has been the primary target for nematode control. A better understanding of how the nervous system regulates the specific behavior may be used to develop targeted control strategies for these economically important plant-parasitic nematodes while avoiding off-target effects to beneficial nematodes and humans. My results on sedentary nematodes epidermis suggest distinct mechanisms evolved to produce a similar phenotype from a common ancestor. More information on sedentary plant-parasitic nematode epidermis may provide better insight into the evolution of these sedentary nematodes.

ACKNOWLEDGEMENTS

I would like to thank my major advisor Dr. Nathan E. Schroeder for his mentoring throughout out my Ph.D. He always made himself available and was willing to talk about my project. His suggestions were always helpful to move forward in my research projects. Nate has been a very helpful advisor, I could not have accomplished my degree without his support.

I would also like to thank my Ph.D. committee members Dr. Kris N. Lambert, Dr. Leslie L. Domier, and Dr. A. Lane Rayburn for their helpful suggestions on my Ph.D. proposal. All of their suggestions helped me to progress on my research projects.

I would like to thank my lab manager Ursula for taking care of all the lab materials required for my research. I thank the undergrad researcher Jayna for helping me during my hatching project. Her willingness to work during off-hour helped us many times to get more data on developmental timeline study. I would also like to thank Michael, my current undergrad research help for his help on different experiments. I am thankful to other doctoral students in my lab Paul, Bui, Becky, and Kristen for being friends with me and sharing all their research experiences.

I am thankful to the staff in the Department of Crop Sciences Dianne, Linda, and Tracey for helping me every-time during my school time. I would like to give a big thanks to the Schlumberger Foundation for funding my Ph.D., without their help I would not have achieved this degree.

This thesis is dedicated to my lovely daughter (Shriya) and my husband (Bijaya) for all of their love and support. My deepest gratefulness to my family in Nepal for supporting all my decisions and for celebrating my every achievement.

TABLE OF CONTENTS

CHAPTER 1: LITERATURE REVIEW: NEMATODE EMBRYOGENESIS AND POST-INFECTION BODY SIZE DEVELOPMENT

Nematodes and their impact on world crop-production

Nematodes are unsegmented round worms with a pseudocoelomate body cavity. Nematodes are omnipresent in nature, inhabiting a diversity of climates ranging from tropical to polar regions. The presence of over a million nematode species have been estimated, and around 30,000 species have been described (Kiontke and Fitch 2013). Most nematodes are free-living, living as bacterial or fungal feeders or as algivore-omnivore-predators in diverse environmental conditions (Blaxter et al. 1998; Williamson and Gleason 2003; Irshad et al. 2013). Additionally, there are numerous plant and animal-parasitic nematodes. Over 4,100 plant-parasitic nematodes (PPN) species have been described (Decreamer and Hunt 2006). These PPNs disrupt agricultural production by direct damaging crops or serving as vectors for plant viruses. The PPN wide host range causes a serious yield reduction in crop yields. PPN causes estimated $80 billion of crop loss worldwide annually (Nicol et al. 2011).

Nematode life cycle and feeding habits

The life cycle of PPNs consists of the egg, four juvenile stages (J1-J4), each followed by a molt, and an adult reproductive stage. Eggs may be deposited singly or in masses. Eggs in masses are held within the gelatinous matrix, commonly called egg sac (*Globodera* spp., *Heterodera* spp., and *Meloidogyne* spp.). *Globodera* spp. and *Heterodera* spp. retained some proportions of eggs within the body (encysted eggs). After the death of a female, a tough cyst formed from the body of the dead female provide additional protection to the encysted eggs. Most plant-parasitic nematodes, following embryogenesis, the first molt occurs within the egg,

giving rise to a J2. In most nematodes, J2s, J3s, and J4s resemble the adult female in morphology, differing in the absence of a mature reproductive system and in certain measurement and proportions (Decraemer and Hunt 2006). However, in some sedentary nematodes, there is disproportionate growth in their body width and length (cyst nematodes, root-knot, and reniform nematodes) and the adult female becomes saccate. PPNs show different types of plant parasitism: ectoparasitic, endoparasitic, semi-endoparasitic, and migratory. Ectoparasitic nematode such as *Longidorus* spp. remain in the soil and do not enter the plant tissues. It feeds by using a stylet to puncture plant cells. Semi-endoparasitic such as *Rotylenchulus reniformis* nematode enters only the anterior part of their body to penetrate the root, the posterior section remains in the soil (Lambert and Bekal 2002; Robinson et al.1997). Endoparasitic nematodes such as *Heterodera glycines* and *Meloidogyne incognita* penetrate the plant root tissue; establish a feeding site and their females become sedentary for the rest of the life (Lambert and Bekal 2002). Migratory endoparasites such as *Pratylenchus penetrans* retain their motility and have no fixed feeding site within the plant tissues. Establishment of a specialized feeding site enhances the flow of nutrients from the host, thereby allowing the females to become sedentary and obese in form and highly fecund (Decraemer and Hunt 2006).

Nematode hatching behavior and embryogenesis

In many nematode species, the egg is the main survival stage. Most nematode species lay eggs individually without any additional protection, whereas there are some exceptions like cyst nematodes (*Globodera* spp. and *Heterodera* spp.) retain some eggs inside the body and root-knot nematodes (*Meloidogyne* spp.) laid eggs in egg sac (egg sac eggs). The root-knot nematodes egg sac is made of glycoprotein materials, which shrinks and harden when dried and exert mechanical pressure on the eggs to inhibit hatching during drought conditions (Bird and

Soeffky1972). The cyst nematodes (*Globodera* spp. and *Heterodera* spp.) females after death become a tough cyst holding several hundred eggs and provide additional protection to encysted eggs (Perry 2002; Ishibashi et al.1973). Ishibashi et al (1973) also found that in *H. glycines* (soybean cyst nematode) the proportions of encysted eggs and egg sac eggs vary under different environmental conditions; more egg sac eggs in favorable conditions and more encysted eggs in unfavorable conditions. In plant endoparasitic nematode species, hatched larvae are very vulnerable to environmental stresses, they are viable in the soil for only a short period without feeding (Robinson, Atkinson and Perry, 1987), *H. glycines,* adult female retaining more encysted eggs at adverse environmental condition may be advantageous survival strategies. Among PPNs, the integration between the host and parasites to ensure successful invasion has progressed furthest in the cyst forming nematodes.

Hatching in some nematode species occurs without requiring specific cues emanating from the food source (Perry 2002). However, many parasitic nematodes include an infective stage in which development is arrested until a host is present and successfully infected (Wharton 2004). In many species, this arrest occurs before hatching. For example, eggs of the animal-parasitic nematode *Ascaris lumbricoides* do not hatch until after they have been ingested (Fairbairn 1961). This synchrony is often maintained by the host signals. In some animal-parasitic and insect-parasitic nematodes, the host gut provides the hatching conditions after ingestion (Fairbairn 1961). In some species of PPNs, the host roots provide the stimulus for hatching. Among PPNs, the requirements of host stimulus for hatching is most common in cyst nematodes, although other species such as *M. hapla* and *R. reniformis* also hatch in response to host stimulus (Perry, 2002). The host-parasite synchronization is mediated by root diffusates produced by host plants. In many cyst nematode species root diffusates increase the rate of

hatching, however, some proportions of eggs of these species can hatch freely in the water. *H. glycines,* has a complicated hatching behavior. *H. glycines* hatching increases in the presence of a host plant or hatching stimulants, while some do not hatch in presence of a host (Teft and Bone 1985; Teft, Rende, and Bone 1982, Clarke and Shepherd 1966). However, some *H. glycines* eggs can hatch freely in water (Perry 2002). Complicating this behavior. *H. glycines* females produce approximately one-third of their eggs into a egg sac, located at the posterior end of the female, while the remaining eggs are retained within the female body. It is reported that unsynchronized *H. glycines* egg sacs eggs hatch more rapidly than encysted eggs (Thompson and Tylka 1997).

The study of nematode biology allow us to learn how animals function. In most areas of modern biology, the free-living nematode *Caenorhabditis elegans* is one of the most important model organisms. *C. elegans* embryo development is well described (von Ehrenstein and Schierenberg 1980; Sulston et al. 1983). In comparison, the embryo development of most PPNs is not well-described. Several studies have found differences in early embryonic cleavage patterns among nematode species (Schlulze and Schierenberg 2011; Dolinski, Baldwinand Thomas 2001). Recent work on the early embryonic development of the nematode *M. incognita,* phylogenetically related to *H. glycines* (van Megan et al. 2009), provides a comparative species within the primary PPN clade to examine early cleavage events and a general timeline from a single-celled egg to hatching (Calderon-Urrea et al. 2016). In chapter 2, I describe the timeline of *H. glycines* embryogenesis of encysted eggs and egg sacs eggs in different hatching stimulants. Furthermore, I examined the development of the stylet and ventral nerve cord in pre-hatch J2s. I found that *H. glycines* develop from a single-cell egg stage to fully formed J2 in approximately 7 days. I also found that stylet protractor muscles and the primary motor nervous system of *H.*

glycines J2s continue to develop until late in pre-hatch J2s, suggesting their requirement in hatching.

Nematode motor neurons and their association with nematode motility

In some sedentary nematode species like *H. glycines* and *M. incognita*, newly hatched J2s are motile but become sedentary following infection. Interestingly, females remain sedentary for the rest of the life, whereas during the J4 molt adult males start to remodel into a vermiform shape and regain mobility. In a semi-endoparasite nematode species *R. reniformis*, adult females after the onset of parasitic life starts a sedentary life, the male never feeds and motile throughout the life. All other stages are motile. In another PPN *Pratylenchus penetrans*, both male and female are motile throughout the life-cycle. Locomotion in nematodes involves somatic muscles that are present below the cuticle and epidermis. The neuromuscular connection of nematodes is unusual. Processes from muscle cells synapse with neurons in the nerve cord rather than the neurons sending out the processes that connect with muscles (Bird 1967). *C. elegans* ventral nerve cord (VNC) comprises motor neurons between the head (retro-vesicular ganglion) and the tail (pre-anal ganglion), and these motor neurons regulate movement. The *C. elegans* VNC has 57 motor neurons innervating the body muscles on both the ventral and dorsal sides (White et al. 1976; Sulston 1976). Variation in nematode neuroanatomy has been reported (Han, Boas, and Schroeder 2016). In chapter 3, I examined the neuroanatomy, throughout the development of two sedentary nematode species (*H. glycines* and *M. incognita*), one semi-endoparasitic species (*R. reniformis*), and one migratory control endoparasitic species (*P. penetrans*). I found that during the sedentary developmental stages of *H. glycines*, *M. incognita*, and *R. reniformis*, motor neurons degenerate, whereas in motile species *P. penetrans* the number of motor neurons remained stable throughout development.

Nematodes as model systems in evolution and development

C. elegans is one of the most intensively studied animals. Nematode evolution and development studies can use knowledge about *C. elegans* as a baseline. Evo-devo investigates the evolution of developmental processes. Its research aims to understand the developmental basis of phenotypic change by investigating how during the course of evolution existing developmental structures are modified and how novel structures are generated (Simmer 2009; Wilkins 2002). Analyses of the cell lineages and developmental genetics have shaped knowledge about nematode evolution. Nematodes are widely considered to be eutelic, i.e., to have an adult cell number that does not vary among wild-type individuals because of an invariant cell lineage (Bird and Bird 1991). However, there is extensive evidence that at least some epidermal cell lineages are variable in nematodes (Azevedo et al. 2000). The nematode epidermis is a thin layer that lies immediately under the cuticle. In a cross-section of a nematode, the epidermis bulges into the body cavity dorsally, ventrally, and laterally **(Figure 1.1**). Azevedo et al. (2000) reported that the variance in cell number is influenced by the frequency of stem cell-like 'seam' cell lineage variants. In *C. elegans* the seam is composed of a longitudinal string of cells on each lateral side of the nematode **(Figure 1.2**). In a newly hatched *C. elegans*, there are 10 seam cells on each side of the animal (H0, H1, H2, V1-V6, T, **Figure 1.2**), whereas in another free-living nematode *Panagrellus redivivus,* H0 is missing (Sternberg and Horvitz 1982). All seam cells except H0 divide in a stem-like pattern before each molt. Most seam cell divisions generate an anterior daughter cell that fuses with the hyp 7 (syncytium in *C. elegans*) and a posterior daughter cell that becomes a seam cell. The seam cell lineages differ between *C. elegans* and *P. redivivus* (Sternberg and Horvitz 1982). *P. redivivus* is bigger than *C. elegans* and has more epidermal nuclei (Flemming et al. 2000). Body size evolution in nematodes is associated with

changes in cell number and ploidy level of their epidermal cells (Flemming et al. 2000; Hedgecock and White, 1985). However, Woodruff et al. (2018) found that in a close relative of *C. elegans, C*. sp. 34 body growth is related to the size of the cell not with the number of epidermal nuclei or ploidy level.

Sedentary PPNs (*Meloidogyne* spp., *Heterodera* spp. and *R. reniformis*) are among the most damaging pathogens to world agriculture production (Jones et al. 2013). Sedentary parasitism and its associated morphological changes have evolved multiple times (van Megan et al. 2009; Holterman et al. 2006). *H. glycines* and *M. incognita* are phylogenetically distinct but have similar life cycles. They hatch as vermiform J2s, establish a multinucleated feeding site and develop from vermiform J2s to saccate shaped female adults. In *C. elegans* seam cells are required for the formation of stage-specific cuticles, and cuticle play role in producing cuticle exudates (Thein, McCormack and Winter 2003). Fibrillar exudate has been found on the post-infection *H. glycines* cuticle surface (Endo 1993). This fibrillar exudate may have some role in host-parasite interaction (Aumann, 1991). A better understanding of saccate shape nematode epidermis may provide some information on host-parasite interaction. In chapter 4, I describe the epidermis of saccate shaped nematode *H. glycines* in detail to understand the method vermiform J2 would have used to grow disproportionately bigger in width than in most nematode species. I found that the *H. glycines* seam cell lineage has undergone an extensive evolutionary change to control its body shape. Furthermore, I found that while *M. incognita* also shows increased seam cell proliferative capacity, the pattern of the division is very different from that found in *H. glycines.* Interestingly, *R. reniformis* does not show increased seam cell proliferation compared with *C. elegans* or other vermiform nematodes (*A. avenae*, *Helicotylenchus* spp. and *P. penetrans*). Rather it appears that the growth of *R. reniformis* is associated with swelling of its

gonad. Our results suggest distinct mechanisms evolved to produce a similar phenotype from a common ancestor.

Management of plant-parasitic nematodes

The complexity of the soil environment makes the management of plant-parasitic nematodes complicated (Norton 1978). Some management strategies use a combination of chemical, biological, and cultural methods along with the use of host plant resistance (Heald 1987; Kerry 1987; Halbrendt and LaMondia 2004; Star and Robers 2004). All of these techniques have some pros and some cons. For example, chemical control has been one of the most important control methods, but its negative environmental and human health effects put its usage under review (Martin 2003). Usually, chemicals are applied as fumigant or non-fumigant. Fumigants are volatile compounds with nematicidal properties and are applied by injecting into the soil profile. These compounds evaporate and diffuse through the soil air spaces and result in effective contact with soil pathogens (Lembright 1990), but results are highly affected by soil conditions like soil texture, temperature, moisture, and soil organic matter. Moreover, fumigants like methyl bromide have been found to cause the depletion of the ozone (Zasada et al. 2010). Applications of the soil fumigants are strictly regulated because of public health and environment concerns. The most commonly used compounds for nematode control belong to organophosphorus and carbamates (Gupta 2006). Like fumigants, both organophosphorus and carbamate are toxic to vertebrates. These compounds are acetylcholinesterase inhibitors, which cause the death of nematodes. Acetylcholinesterase (AChE) is involved in the termination of impulse transmission by rapid hydrolysis of the neurotransmitter acetylcholine (ACh) in numerous cholinergic pathway in the central and peripheral nervous system (Colovic et al. 2013). ACh is involved in the regulation of locomotion, egg laying, pharyngeal pumping,

defecation cycling and male mating in *C. elegans*. Many *C. elegans* neurons have been found to be cholinergic through the detection of choline acetyltransferase (ChAT) expression (Pereira et al. 2015). The activity of AChE is more in the nervous system, higher in motor neurons than in sensory neurons. A detailed study on the nematode nervous system may provide insights into new control strategies avoiding potential off-target effects.

A better understanding of the nematode hatching behavior, their developmental biology, most importantly their nervous system can aid to target PPNs. Some plant-parasitic nematodes, like *H. glycines,* respond to host cues for hatching. Better understanding on which pre-hatch stage hatching stimulant act on can provide insight into their primary survival mechanism. Furthermore, understanding the biology of shape change of economically important sedentary PPNs like *H. glycines*, *M. incognita*, and *R. reniformis* may provide insights into evolution of saccate form nematodes. In this dissertation, chapter 2 describes *H. glycines* embryogenesis and the development of some structures required for hatching. It also describes that hatching stimulants have a critical period of activity. Chapter 3 is about motor neuron degenerations in some sedentary PPNs (*H. glycines, M. incognita*, and *R. reniformis*). Chapter 4 describes the changes in seam cell lineages and its association with nematode atypical body size evolution

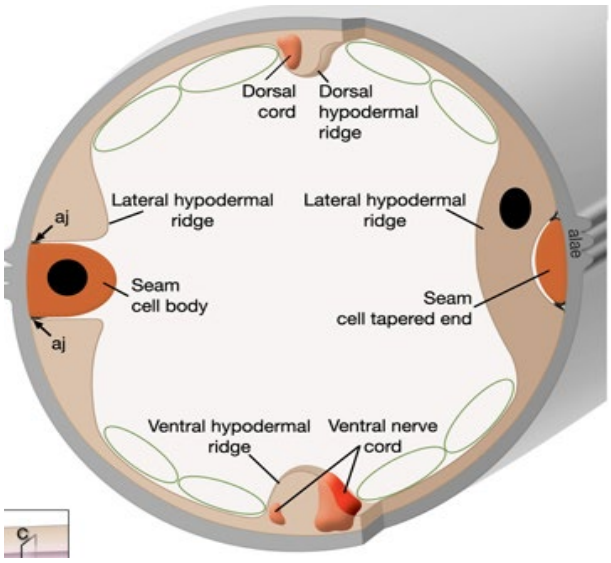

Figure 1.1. A cross-section of *C. elegans*. The epidermis is composed of four major longitudinal ridges (ventral, dorsal, and L/R lateral) that are joined circumferentially by thin sheets of cytoplasm. The body of the seam is lodged between the ventral and dorsal parts of the lateral hypodermal ridge.
Source:http://www.wormatlas.org/hermaphrodite/seam%20cells/mainframe.htm

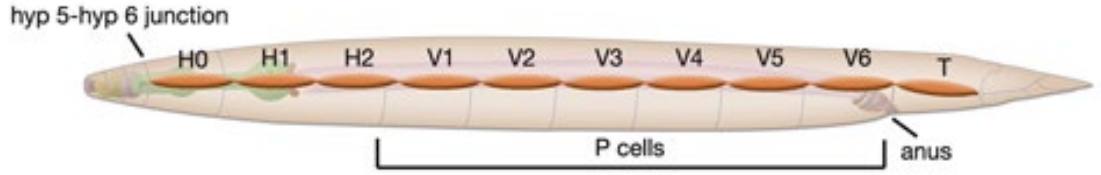

Figure 1.2. Longitudinal chain of seam cells in *C. elegans*. Schematic view of left lateral seam cells in an L1-stage larva. At this stage, ten embryonically born individual seam blast cells contact each other through adherens junctions. They are also in close contact with P blast cells on the ventral side.
Source:http://www.wormatlas.org/hermaphrodite/seam%20cells/mainframe.htm

REFERENCES

Alston, D. G., & Schmitt, D. P. (1988). Development of *Heterodera glycines* life stages as influenced by temperature. *Journal of Nematology*, *20*(3), 366.

Aumann, J., Robertson, W. M., & Wyss, U. (1991). Lectin binding to cuticle exudates of sedentary *Heterodera schachtii* (Nematoda: Heteroderidae). *Revue Nématol*, *14*(1), 113-118.

Azevedo, R. B., Cunha, A., Emmons, S. W., & Leroi, A. M. (2000). The demise of the platonic worm. *Nematology*, *2*(1), 71-79.

Bird, A. F. (1967). Changes associated with parasitism in nematodes. I. Morphology and physiology of preparasitic and parasitic larvae of *Meloidogyne javanica*. *The Journal of Parasitology*, 768-776.

Bird, A. F., & Bird, J. (2012). *The structure of nematodes*. Academic Press.

Bird, A. F., & Soeffky, A. (1972). Changes in the ultrastructure of the gelatinous matrix of *Meloidogyne javanica* during dehydration. *Journal of Nematology*, *4*(3), 166.

Blaxter, M. L., De Ley, P., Garey, J. R., Liu, L. X., Scheldeman, P., Vierstraete, A., & Vida, J. T. (1998). A molecular evolutionary framework for the phylum Nematoda. *Nature*, *392*(6671), 71.

Calderón-Urrea, A., Vanholme, B., Vangestel, S., Kane, S. M., Bahaji, A., Pha, K., & Gheysen, G. (2016). Early development of the root-knot nematode *Meloidogyne incognita*. *BMC Developmental Biology*, *16*(1), 10.

Clarke, A. J., & Shepherd, A. M. (1966). Inorganic ions and the hatching of *Heterodera* spp. *Annals of Applied Biology*, *58*(3), 497-508.

Colovic, M. B., Krstic, D. Z., Lazarevic-Pasti, T. D., Bondzic, A. M., & Vasic, V. M. (2013). Acetylcholinesterase inhibitors: pharmacology and toxicology. *Current Neuropharmacology*, *11*(3), 315-335.

Decraemer, W. & D.J. Hunt (2006). Structure and classification. In: Plant Nematology, pp: 4 - 32. Perry, R.N. and Moens, M (eds.). CABI1, Oxfordshire.

Dolinski, C. J. B. G., Baldwin, J. G., & Thomas, W. K. (2001). Comparative survey of early embryogenesis of Secernentea (Nematoda), with phylogenetic implications. *Canadian Journal of Zoology*, *79*(1), 82-94.

Ehrenstein, G. V., & Schierenberg, E. (1980). Cell lineages and development of *Caenorhabditis elegans* and other nematodes. *Cell Llineages and Development of Caenorhabditis elegans and other Nematodes.*, 1-71.

Endo, B. Y. (1993). Ultrastructure of cuticular exudates and related cuticular changes on juveniles in *Heterodera glycines*. *Journal of the Helminthological Society of Washington (USA)*.

Evans, K., & Stone, A. R. (1977). A review of the distribution and biology of the potato cyst-nematodes *Globodera rostochiensis* and *G. pallida*. *Pans*, *23*(2), 178-189.

Fairbairn, D. (1961). The in-vitro hatching of *Ascaris lumbricoides* eggs. *Canadian Journal of Zoology*, *39*(2), 153-162.

Flemming, A. J., Shen, Z. Z., Cunha, A., Emmons, S. W., & Leroi, A. M. (2000). Somatic polyploidization and cellular proliferation drive body size evolution in nematodes. *Proceedings of the National Academy of Sciences*, *97*(10), 5285-5290.

Halbrendt, J. M., & LaMondia, J.A. (2004). Crop Rotation and Other Cultural Practices. In: Nematology Advances and Perspectives: Vol. II Nematode Management and Utilization, pp. 909-930. Oxfordshire, UK: CAB International.

Han, Z., Boas, S., & Schroeder, N. E. (2016). Unexpected variation in neuroanatomy among diverse nematode species. *Frontiers in Neuroanatomy*, *9*, 162.

Heald, C.M. (1987). Classical nematode management practices. *In:* Vistas on Nematology, pp. 100–105.Veech, J. A. and Dickson, D. W. (eds.). Hyatssville, MD: Society of Nematologists.

Hedgecock, E. M., & White, J. G. (1985). Polyploid tissues in the nematode *Caenorhabditis elegans*. *Developmental Biology*, *107*(1), 128-133.

Irshad, U., Villenave, C., Brauman, A., Khan, S. A., Shafiq, S., & Plassard, C. (2013). Nitrogen and phosphorus flow stimulated by bacterial grazer nematodes in mycorrhizosphere of *Pinus pinaster*. *International Journal of Agriculture and Biology*, *15*(6), 1265-1271.

Ishibashi, N., Kondo, E., Muraoka, M., & Yokoo, T. (1973). Ecological Significance of Dormancy in Plant Parasitic Nematodes: I. Ecological Difference between Eggs in Gelatinous Matrix and Cyst of *Hetrodera glycines* Ichinohe: Tylenchida: Heteroderidae. *Applied Entomology and Zoology*, *8*(2), 53-63.

Kerry, B.R. (1987). Biological control. In: Principles and Practice of Nematode Control in Crops, pp. 223-263. Brown, R. H. and Kerry, B. R. (eds.) Sydney, Australia: Academic Press.

Kiontke, K., & Fitch, D. H. A. (2013). Nematodes. *Current Biology*, 23, 862–864.

Lambert, K., & Bekal, S. (2002). Introduction to plant-parasitic nematodes. *The Plant Health Instructor*, *10*, 1094-1218.

Lembright, H. W. (1990). Soil fumigation: principles and application technology. *Journal of Nematology*, *22*(4S), 632.

Martin, F. N. (2003). Development of alternative strategies for management of soilborne pathogens currently controlled with methyl bromide. *Annual Review of Phytopathology*, *41*(1), 325-350.

Nicol, J. M., Turner, S. J., Coyne, D. L., Nijs, L. Den, Hockland, S., Tahna Maafi, Z., et al. (2011). Genomics and Molecular Genetics of Plant-Nematode Interactions. In *Genomics and Molecular Genetics of Plant-Nematode Interactions*, p. 21–43. Available at: http://link.springer.com/10.1007/978-94-007-0434-3.

Norton, D. C., & Norton, D. C. (1978). *Ecology of plant-parasitic nematodes* (No. 632.65182/N883). New York: Wiley.

Pereira, L., Kratsios, P., Serrano-Saiz, E., Sheftel, H., Mayo, A. E., Hall, D. H., D.H., White, J.G., LeBoeuf, B., Garcia, L.R., Alon, U. and Hobert, O. (2015). A cellular and regulatory map of the cholinergic nervous system of *Caenorhabditis elegans*. *Elife*, *4*, e12432.

Perry, R.N. (2002). Hatching. In Lee, D, ed. The biology of nematodes. New York; Taylor and Francis. 147-69.

Robinson, A. F., Inserra, R. N., Caswell-Chen, E. P., Vovlas, N., & Troccoli, A. (1997). Rotylenchulus species: Identification, distribution, host ranges, and crop plant resistance. *Nematropica*, *27*(2), 127-180.

Robinson, M. P., Atkinson, H. J., & Perry, R. N. (1987). Influence of soil moisture and storage time on the motility, infectivity and lipid utilization of second stage juveniles of the potato cyst nematodes *Globodera rostochiensis* and *G. pallida*. *Revue de Nématologie*.

Schulze, J., & Schierenberg, E. (2011). Evolution of embryonic development in nematodes. *EvoDevo*, *2*(1), 18.

Sternberg, P. W., & Horvitz, H. R. (1982). Postembryonic nongonadal cell lineages of the nematode *Panagrellus redivivus*: description and comparison with those of *Caenorhabditis elegans*. *Developmental Biology*, *93*(1), 181-205.

Sulston, J. E., & Horvitz, H. R. (1977). Post-embryonic cell lineages of the nematode, *Caenorhabditis elegans*. *Developmental Biology*, *56*(1), 110-156.

Sulston, J. E., Schierenberg, E., White, J. G., & Thomson, J. N. (1983). The embryonic cell lineage of the nematode *Caenorhabditis elegans*. *Developmental Biology*, *100*(1), 64-119.

Tefft, P. M., & Bone, L. W. (1985). Plant-induced hatching of eggs of the soybean cyst nematode *Heterodera glycines*. *Journal of Nematology*, *17*(3), 275.

Tefft, P. M., Rende, J. F., & Bone, L. W. (1982). Factors influencing egg hatching of the soybean cyst nematode. In *Proceedings of the Helminthological Society of Washington* (Vol. 49, No. 2, pp. 258-265).

Thompson, J. M., & Tylka, G. L. (1997). Differences in hatching of *Heterodera glycines* egg-mass and encysted eggs in vitro. *Journal of Nematology*, *29*(3), 315.

van Megen, H., van den Elsen, S., Holterman, M., Karssen, G., Mooyman, P., Bongers, T., ... & Helder, J. (2009). A phylogenetic tree of nematodes based on about 1200 full-length small subunit ribosomal DNA sequences. *Nematology*, *11*(6), 927-950.

Woodruff, G. C., Willis, J. H., & Phillips, P. C. (2018). Dramatic evolution of body length due to postembryonic changes in cell size in a newly discovered close relative of *Caenorhabditis elegans*. *Evolution Letters*, *2*(4), 427-441.

Wharton, D.A. (2004). Survival strategies. In: Gaugler R, Bilgrami AL, editors. Nematode behavior. Chapter 13. Cambridge, MA: CABI International; p. 374–75.

White, J. G., Southgate, E., Thomson, J. N., & Brenner, S. (1986). The structure of the nervous system of the nematode *Caenorhabditis elegans*. *Philos Trans R Soc Lond B Biol Sci*, *314*(1165), 1-340.

Wilkins, A. S. (2002). *The evolution of developmental pathways*. Sunderland, Massachusetts, USA: Sinauer Associates Inc.

Williamson, V. M., & Gleason, C. A. (2003). Plant–nematode interactions. *Current Opinion in Plant Biology*, *6*(4), 327-333.

Zasada, I. A., Halbrendt, J. M., Kokalis-Burelle, N., LaMondia, J., McKenry, M. V., & Noling, J. W. (2010). Managing nematodes without methyl bromide. *Annual Review of Phytopathology*, *48*, 311-328.

CHAPTER 2: EMBRYOGENESIS IN THE PARASITIC NEMATODE *HETERODERA GLYCINES* IS INDEPENDENT OF HOST-DERIVED HATCHING STIMULATION

ABSTRACT

Many parasites regulate their development to synchronize their life cycle with a compatible host. The parasitic nematode *Heterodera glycines* displays incomplete host-mediated hatching behavior wherein some *H. glycines* individuals hatch only in the presence of a host-derived cue while others hatch in water alone. Furthermore, *H. glycine* shows variable hatching behavior based on oviposition location. The mechanisms regulating this hatching variability are unknown. In this study, we established a detailed timeline of the *H. glycines* pre-hatch development from early embryogenesis to the pre-hatched J2. These descriptive data were then used to test hypotheses regarding the effect of environment on pre-hatch development. We found that *H. glycines* develops from a single-cell egg to a fully formed J2 in approximately 172 hours. The stylet-based mouthpart, which is used to pierce the eggshell during hatching, is not completely formed until late in pre-hatch J2 development and is preceded in development by the stylet protractor muscles. We also found that the primary motor nervous system of *H. glycines* did not complete development until late in pre-hatch J2 development. These data suggest possible structural requirements for *H. glycines* hatching. As expected, exposure of *H. glycines* eggs to host-derived cues increased the percentage of nematodes that hatched. However, exposure to hatching cues did not affect pre-hatch development. Similarly, we found no obvious differences in the pre-hatch developmental timelines between eggs laid in an egg sac or retained within the mother. The pattern of early embryonic development in *H. glycines* was very similar to that recently described in the related parasitic nematode *Meloidogyne incognita.* However, the speed of *H. glycines* development was approximately three times faster than recently reported for

M. incognita. Our results suggest that hatching stimulants do not affect embryogenesis itself but only influence the hatching decision once J2 development is complete. Similarly, the oviposition location does not alter the rate of embryogenesis. These results provide insight into the primary survival mechanism for this important parasite.

Keywords: Soybean cyst nematode, SCN, root knot nematode, cleavage, post-embryonic development, ventral nerve cord

INTRODUCTION

The life cycle of most nematodes comprises embryogenesis followed by four juvenile stages (J1–J4) and the adult reproductive stage. Parasitic nematodes frequently include an infective stage in which development is arrested until a host is present and successfully infected (Wharton 2004). In many species, this arrest occurs before hatching. In the absence of a host, the nematode remains within the relatively protected eggshell until it has received appropriate signals from the host. For example, eggs of the animal-parasitic nematode *Ascaris lumbricoides* do not hatch until after they have been ingested (Fairbairn 1961). Most plant-parasitic nematodes hatch as J2s; following embryogenesis, they undergo the first molt within the egg. The egg of many plant-parasitic nematodes serves as the primary long-term survival stage. After leaving the protective environment of the eggshell, hatched J2s have limited energy reserves to find and infect a host (Perry 2002). To maximize the probability of success during this sensitive period, several species of plant-parasitic nematodes have evolved host-mediated hatching behaviors. Among plant-parasitic nematodes, the integration of host cues into the hatching process has progressed furthest in the cyst nematodes (*Globodera* spp., *Heterodera* spp.).

The hatching behavior of the parasitic nematode *Heterodera glycines* (commonly known as the soybean cyst nematode) is synchronized with its soybean host and, therefore, has a significant impact on control strategies (Charlson and Tylka 2003) *H. glycines* females produce several hundred eggs (Sipes, Schmitt, and Barker 1992). While some individual eggs will hatch in the absence of a host, the presence of soybean greatly increases the percentage of eggs that will hatch, thereby increasing the probability of emerging in the presence of a susceptible host. However, even in the presence of soybean and other conducive environmental conditions, many *H. glycines* individuals will remain in an arrested stage. This incomplete host-derived hatching stimulation is thought to serve as a hedge against a sudden deterioration in environmental conditions (Niblack, Lambert, and Tylka 2006). Complicating this behavior, approximately one third of *H. glycines* eggs are laid into a gelatinous sac (egg sac eggs), located at the posterior end of the female, while the remaining eggs are retained within the female body (encysted eggs). Upon death, the body of the dead female is referred to as a cyst, which serves as an additional layer of protection from the environment for the encysted eggs. There are differences in hatching behaviors between egg sac eggs and encysted eggs (Ishbashi et al. 1973; Thompson and Tylka 1997). The mechanisms regulating the complex hatching behavior of *H. glycines* are unclear.

To better understand the variability in hatching of *H. glycines*, it may be useful to have a more complete de- scription of pre-hatch development. Compared to the well-studied nematode *C. elegans,* the development of most parasitic nematodes is not well-described. Previous research has found substantial variation in early embryonic cleavage patterns among nematode species (Skiba and Schierenberg 1992; Dolinski, Baldwin, and Thomas,

2001). A previous description of the *H. glycines* life-cycle suggested that it took approximately six days for embryos to develop to J2s (Lauritis, Rebois, and Graney 1983). Separation of *H. glycines* eggs into embryos and juveniles can be accomplished using visual assessment via a dissecting microscope or through flow cytometry; this separation can then be used to increase developmental synchronization in hatching studies (Thompson and Tylka 1997; Tylka et al.1993; Masler, Rogers, and Chitwood 2013). For example, Masler et al. (2013) directly compared hatching in *Meloidogyne incognita* with *H. glycines* following separation of eggs into embryos and juveniles. However, a detailed description of the timing of early development in *H. glycines* is lacking and may be useful for understanding the hatching process. Recent work on the early embryonic development of the nematode *M. incognita* provides a comparative species within the primary plant-parasitic nematode clade to examine early cleavage events and a timeline from a single-celled embryo to hatching (Calderon-Urrea et al. 2016). Here, we describe a similar detailed timeline of pre-hatch development for *H. glycines*.

The development of structures required for hatching in nematodes is not well described. Unlike *C. elegans, H. glycines* has evolved a protractible stylet mouth part that is used for both infection and opening of the eggshell during hatching. The development of the secreted cuticular-based stylet and its associated musculature is not understood. We recently demonstrated that hatched J2 *H. glycines* contain several additional neurons in the primary motor nervous system compared to *C. elegans* (Han, Boas, and Schroeder 2016). In this study, we describe the pre-hatch development of the stylet and ventral nerve cord of *H. glycines.*

Since host cues greatly increase the hatching rate in *H. glycines*, we used our understanding of pre-hatch development to test the hypothesis if the presence of a host regulates the rate of *H.*

glycines embryogenesis. Several animal species use environmental cues to regulate developmental rates in order to achieve optimal hatching behaviors. For example, turtles adjust their rate of embryogenesis to establish synchronized hatching within a clutch (McGlashan and Spencer 2012; McGlashan et al. 2015). However, we found that host-derived cues and the location of egg deposition do not impact the rate of pre-hatch development in *H. glycines.*

MATERIALS AND METHODS

H. glycines: *H. glycines* were grown on soybean (cv. Williams) in a 1:1 sand to soil mixture. Females were collected by mixing roots and soil with water and pouring over stacked 850 and 250-µm-pore sieves. Females were separated from root fragments and other debris by centrifugation in a 68% ($^{w}/_{v}$) sucrose solution to remove root debris (Riggs, Schmitt, and Mautomoustakos 1997). The supernatant was poured again on 250-µm-pore sieves, washed, and recovered females were collected. For the pre-hatch development study, encysted and egg sac eggs were separated. Egg sacs were soaked for 1 minute in 0.5% NaOCl to dissolve the gelatinous matrix and poured over stacked 250 and 25-µm-pore sieves (Thomas and Tylka 1997; Hussey and Barker 1973). Egg sac eggs were then collected from the 25-µm-pore sieve. To collect encysted eggs, we opened cysts manually. All eggs were obtained from three to four-week old females. Two-celled eggs were handpicked under a dissecting microscope and used within one day following extraction.

Hatching stimulant preparation: Soybean root exudate was collected based on previous methods (Charlson and Tylka 2003; Levene, Owen, and Tylka 1998). Soybeans (cv. Williams) were grown in a 2:1 sand to soil mixture. After six weeks, the plants were removed from the soil mix, and the roots were rinsed with tap water to remove soil particles. The roots of four plants

were incubated for 48 h in 400 ml of distilled water at 24°C. The roots were excised at the hypocotyl, blot dried, and weighed. The concentration of host exudate was adjusted to 1.3 root-gram-hour (RGH) as calculated by the formula $\frac{root\ mass\ (g) \times incubation\ time\ (h)}{amount\ of\ root\ exudate\ obtained\ (ml)}$ (Teft and Bone 1985). Host exudate was sterilized by passing through a 0.2-µm cellulose acetate sterile syringe filter (VWR), and stored at -20° C.

***H. glycines* hatching experiment:** Hatching chambers consisted of a 30-µm nylon mesh (Genesee Scientific, CA) held between 30-mm (l) × 38-mm (d) and 15-mm (l) × 40-mm (d) plastic cylinders (Bhem et al. 1995). Hatching chambers were placed on the bottom of a 5-cm Petri dishes (VWR). Approximately 1,000 eggs of mixed developmental stages were dispensed in hatching chambers with water or hatching stimulants. Hatching chambers were stored at 25°C. Each treatment was randomly assigned and had three replications. Every 24 h, the hatching chambers were transferred to new Petri dishes and hatched J2s recovered from the Petri dish were counted. The experiment was repeated once. The data were analyzed in SAS with PROC MIXED for repeated measures with a compound symmetry covariance structure (Wolfinger and Chang 1995).

***H. glycines* early embryo development and pre-hatch developmental timeline:** Several methods were used to examine pre-hatch development. The pre-hatch development timeline was initially observed using a hanging drop method with modifications (Gilarte et al. 2015). Single eggs were added to 6 µl of either water or a hatching stimulant in a concave well microscope slide and covered with a coverslip. We found that *H. glycines* embryos were very sensitive to pressure. Therefore drops of petroleum jelly were placed at each corner of the coverslip to serve as spacers. Slides were kept in a humidity chamber at 25°C between imaging.

Development was observed using an inverted microscope (Zeiss Axiovert 200) with Differential Interference Contrast (DIC) microscopy at 400x magnification. A pre-hatch developmental timeline was created in both water and hatching stimulants based on at least 15 animals for each treatment. High-resolution images of major stages of the developing embryo were collected using an upright compound microscope at 1000x magnification. To further confirm our results with the inverted microscope and obtain higher resolution images, the early embryonic development of three animals from the fusion of the male and female pronuclei to the eight-celled stage was observed. Single eggs were placed on a 4% agarose pad. Coverslips were sealed with parafilm, rehydrated as needed, and incubated at 25°C in a dark humidity chamber when not imaging. Images were taken every 30 minutes using an upright compound microscope with a mechanized stage (Zeiss M2 AxioImager and Zen software). Cell divisions were labeled based on *M. incognita* and *C. elegans* (Calderon-Urrea et al. 2016; Sulston et al. 1983).

***H. glycines* post-embryonic stylet and VNC development:** Two-celled eggs were incubated in water at 25°C for 6-7 days to obtain pre-hatched J2s. Eggshells were gently opened in phosphate buffered saline with Triton X-100 (PBST: 8 g NaCl, 0.2 g KCl, 1.43 g Na_2HPO_4, 0.05% ($^{v}/_{v}$) Triton X-100 in 1L) using pressure from fine forceps. These pre-hatch J2s were fixed in 2% formaldehyde at 4°C overnight in 1-ml microcentrifuge tubes. The stylet protractor muscles were visualized by staining fixed nematodes with Alexa Fluor 488 phalloidin. Nematodes were transferred onto a 4% Noble agar pads with 20 µl of 5% ($^{v}/_{v}$) phalloidin. The nematode cuticle was punctured with a Micropoint laser to aid in the penetration of phalloidin. Slides were kept in a moist chamber overnight at room temperature and imaged the next morning. The VNC was observed with 4′, 6-diamidino-2-phenylindole (DAPI) using a modification of previous methods (Han, Boas, and Schroeder 2016). Twenty early and late pre-

hatched J2s were fixed in 2% formaldehyde, washed three times with PBST, and incubated in 50% methanol for 30 min. Nematodes were then washed three times with PBST and incubated in 0.2-0.5 µg/ml of DAPI overnight in the dark at room temperature. Twenty-eight hatched J2s were fixed in 4% formaldehyde and incubated in 100% methanol for at least four hours followed by overnight incubation in DAPI. Nematodes were stored at 4°C before examination. Images were taken using a Zeiss M2 AxioImager with DIC and fluorescence. The ventral nerve cord (VNC) was identified based on their size and morphology (Han, Boas, and Schroeder 2016; Sulston 1983). DAPI stained neurons appeared as highly condensed round fluorescent puncta (Han, Boas, and Schroeder 2016; Sulston 1983). The VNC was categorized as including neurons from immediately posterior of the retro-vesicular ganglion to immediately anterior of the pre-anal ganglion (Han, Boas, and Schroeder 2016).

RESULTS

***H. glycines* embryos develop much faster than *M. incognita*, but with a similar cleavage pattern:** To better understand the hatching behavior of *H. glycines*, we first resolved the timeline of pre-hatch development using several observational techniques. Single cell eggs were rarely found. We, therefore, started most of our observations at the two-celled stage. We observed a similar sequence of pre-hatch developmental stages (2, 3, and 4-celled stages, gastrula, tadpole, J1, and J2) as recorded in other plant-parasitic nematodes (Calderon-Urrea et al. 2016; Dolinski, Baldwin and Thomas 2001). Furthermore, we traced the early cell lineage of some embryos. The first cell division was transverse and slightly unequal, producing the P_1 and AB blastomeres **(Figure 2.1, 7 h)**. This asymmetry determined the anterior-posterior axis. P_1 divided to produce EMS and P_2 **(Figure 2.1, 10.5 h)**. Following this division, AB divided to

form the ABa (a-anterior) and ABp (p-posterior) blastomeres **(Figure 2.1, 13.5 h)**. Similar to other previously described Clade 12 nematodes, we observed a linear arrangement of a four-celled embryo (ABa, ABp, EMS, and P_2) indicative of an I_3-Type blastomere arrangement (Schulze and Schierenberg 2011). Following the four-celled linearly arranged embryo, the P_2 cell divided to produce C and P_3 **(Figure 2.1, 21.5 h)**. ABa and ABp then divided to produce anterior and posterior pairs (ABaa, ABap, ABpa, ABpp) **(Figure 2.1, 24 h**). Following the AB cell divisions, EMS divided to form MS and E, resulting in an eight-celled embryo **(Figure 2.1, 27 h**). The cell lineage of individual animals was not traced following the eight-cell stage due to the refractive optical properties of the embryo, as described for other plant-parasitic nematodes (Dolinski, Baldwin and Thomas 2001).

Following the early cell divisions, rapid longitudinal and transverse cell divisions led to recognizable developmental stages. The onset of gastrulation occurred approximately three days following the beginning of our observations **(Figure 2.2)**. After approximately four days, the embryo began to move during the tadpole stage, and soon after formed a worm-shaped J1 **(Figure 2.2)**. At this time the body was readily differentiated into two zones of dissimilar densities. The light zone is presumed to form the anterior end of the nematode while the dark zone is thought to develop into the intestine. A well-developed stylet was observed in J2s **(Figure 2.2)**. The fully formed unhatched J2 moved within the egg. It kept circulating within the eggshell, with occasional bouts of quiescence, exploring locations to make a slit near a pole of the egg from which to emerge. Recently**,** the pre-hatch development and early cell lineage were described in the root-knot nematode *Meloidogyne incognita* (Calderon-Urrea et al. 2016). While *Meloidogyne* spp. and *Heterodera* spp. are both plant-parasitic species and found in the same phylogenetic clade, they display many differences in their biology and are thought to have

evolved from different immediate common ancestors (van Megen et al. 2009). Interestingly, while the pattern of major pre-hatch development was similar in both species the speed of development was much faster in *H. glycines.* For example, in *H. glycines* the E cell was produced in approximately one day at 25˚C while *M. incognita* requires almost five days at 22˚C (Calderon-Urrea et al. 2016).

***H. glycines* pre-hatch development is not affected by hatching stimulants or oviposition location**: Compared with the N2 *C. elegans* laboratory strain, *H. glycines* strains are genetically variable. To confirm that our strain of *H. glycines* displays a host-mediated hatching response and to ensure the efficacy of our host exudate extraction methods, we tested the effect of different hatching stimulants on an asynchronous population of *H. glcyines* eggs. As expected, the number of eggs that hatched in soybean root exudate and $ZnCl_2$, a known hatching stimulant, was significantly higher than in water ($P < 0.0001$) **(Figure 3.3)**. Numerous studies have demonstrated that *H. glycines* hatching increases in the presence of a host plant or other stimulants (Perry 2002; Teft and Bone 1985; Teft, Rende and Bone 1982; Clarke and Shepherd 1966). It is unknown whether this is due to manipulation of the rate of embryogenesis or due to stimulation once the J2 has completely developed. To test this, we examined the rate of embryogenesis in synchronized eggs exposed to different hatching stimulants. There were no obvious differences in the pre-hatch developmental timelines among eggs in water, host exudate, or $ZnCl_2$ **(Table 2.1)**. It was also previously reported that unsynchronized *H. glycines* eggs from egg sacs hatch more rapidly than encysted eggs (Thompson and Tylka 1997). One possible explanation is that egg sac eggs develop faster than encysted eggs. Alternatively, egg sac eggs may be older and therefore reach the fully formed J2 stage earlier. To test these possibilities, we examined the development of synchronized eggs from each source beginning at the two-cell

stage. Similar to our hatching stimulant data, we found no difference between the pre-hatch developmental timelines of encysted eggs and egg sac eggs **(Table 2.2)**. Despite our synchronization, there was substantial variability in the development timeline among individual eggs within a treatment. This may be due to slight differences in environmental conditions or to genetic differences among eggs.

***H. glycines* stylet and ventral nerve cord continue to develop in pre-hatched J2s:** Most plant-parasitic nematodes hatch following the molt from J1 to J2. During our studies, we observed that the anatomy of unhatched J2s did not appear identical to hatched J2s. Specifically, we noted pre-hatch J2s with a partially shed J1 cuticle, indicative of the first molt, but which did not have a fully developed stylet **(Figure 2.4 A)**. The *H. glycines* J2 stylet is a protractible hollow spear used to cut open the eggshell during hatching and for later infection. As the pre-hatched J2s continuously moved within the egg, it was difficult to observe this structure over time. Therefore, to better understand changes during J2 pre-hatch development, we carefully opened eggs containing J2s at various time points following the first molt. Nematodes were fixed and stained with DAPI and phalloidin to label nuclei and filamentous actin, respectively, and then examined with fluorescent and DIC optics. Based on our observations, we could separate J2s into distinct groups we call “early” and “late” J2. Early J2s have only the anterior cone component of the stylet **(Figure 2.4 B)**. As development progresses, the shaft becomes visible followed by the stylet knobs. The stylet knobs initially appear as a slight enlargement of the shaft. Over time the stylet knobs expand in diameter and begin to show a slight curvature similar to that seen in hatched J2s **(Figure 2.4 C)**. We hypothesized that the change of curvature might be due to attachment of the stylet protractor muscles and a physical deformation of the knobs. In fully developed J2s, the contractile portion of the three stylet protractor muscle cells attach to the

stylet knobs and extend as ten separate elements to the cephalic framework (Endo 1983). Interestingly, our phalloidin staining showed that the stylet protractor muscles were present before the formation of the stylet knobs, suggesting that knob curvature is independent of muscle attachment **(Figure 2.5)**. We also observed differences in the structure of the cuticle between early and late pre-hatch J2s. Early pre-hatched J2s lacked obvious ridges (alae) along the lateral field of the cuticle **(Figure 2.4 D)** as seen in hatched J2s **(Figure 2.4 E)**.

We observed phalloidin staining, indicative of F-actin, in the nerve ring of one early pre-hatch J2 *H. glycines* (**Figure 2.6 A**). In *C. elegans,* actin and actin-associated proteins are often found in the nerve ring during early development (Legouis et al. 2000; Van Troys et al. 2004; Polet et al. 2006). This observation may suggest that the neurodevelopment of recently molted J2s is not complete. To test this further, we examined the ventral nerve cord of pre-hatched and hatched J2s. We found that the number of VNC neurons increased slightly from early J2s (average=62; n=20) to hatched J2s (average=65; n=20). More strikingly, the VNC of early pre-hatched J2s appeared more disorganized than in hatched J2s **(Figure 2.6 B and C)**. These data support our hypothesis of continued neuronal development following the J1 to J2 molt.

DISCUSSION

Hatching is the result of highly regulated metabolic and developmental events that are responsive to both endogenous and environmental factors (Warkentin 2011). In addition to the importance of temperature on developmental rate, some animals are capable of modulating their hatching based on less obvious environmental cues (Tsutsumi and Sakurai 1966). Certain species of freshwater snails are capable of suppressing pre-hatch development based on signals received from conspecific individuals (Voronezhskaya, Khabarova, and Nezlin 2004). Similarly, turtles

can adjust their development to synchronize hatching via embryo-embryo communication (McGlashan et al. 2015). The cyst nematodes, including *H. glycines,* regulate hatching based on the presence of a host (Perry 2002; Tsutsumi and Sakura 1952). The hypothesis that differences in embryogenesis affect the host-responsive hatching behavior seen in *H. glycines* was unresolved.

Our results do not support the hypothesis that hatching stimulants affect *H. glycines* embryo development. We found no obvious differences in the timing of pre-hatch development of *H. glycines* when exposed to hatching stimulants. Instead, the stimulants appear to influence the hatching decision once the fully formed J2 has developed. Our data are most consistent with the presence of an environmentally mediated dormancy. Similar to our hatching stimulant data, we found no obvious differences in the timing of pre-hatch development between egg sac eggs and encysted eggs. Thompson and Tylka (1997) found that asynchronous egg sac eggs hatch sooner than encysted eggs. They suggested that rapid hatching of egg sac eggs compared to encysted eggs may be due to the gelatinous egg sac containing more mature eggs (Thompson and Tylka 1997). Anecdotally, we also observed a greater proportion of mature eggs in the egg sac than in cysts. One caveat to ours and other studies is that manipulation of eggs within the lab may lead to artifacts in development and behavior not seen in nature. An additional question that remains to be addressed is the mechanism and types of quiescence that occur in pre-hatched J2s. Approximately 30% of eggs were unresponsive to hatching stimulants **(Figure 2.3)**. This may suggest these eggs are in a state of long-term dormancy distinct from that found in eggs which respond to stimulation (Yen, Niblack and Wiebold 1995).

Our data show that while the pattern of embryogenesis is very similar to most previously described plant-parasitic nematodes, the rate of development is variable. Previous research has

shown variability in early embryogenesis among diverse nematode species (Dolinski, Baldwin and Thomas, 1993; Schulze and Schierenberg, 2011; Von Ehrenstein and Schierenberg 1980). *C. elegans* embryos develop to the eight-cell stage in less than one hour (Sulston et al. 1983). Although the cleavage pattern of early embryogenesis varies among nematodes, we found *H. glycines* has a very similar cleavage pattern to *M. incognita* (Calderon-Urrea et al. 2016). However, the embryonic development of *H. glycines* timeline was substantially faster than *M. incognita* (Calderon-Urrea et al. 2016). We found that *H. glycines* developed from a one cell egg to eight cells in approximately one day, and hatched after eight days. *M. incognita* took approximately five days to form the eight-cell embryo and hatched after 21 days (Calderon-Urrea et al. 2016). This difference in timing may be due to the incubation temperature. While we maintained our eggs at 25°C, Calderón-Urrea et al. (2016) incubated their *M. incognita* eggs at 22°C. Interestingly, an earlier study suggested that *M. incognita* formed J2s within seven days at 20°C (Vrain and Barker 1978). Unlike, the laboratory maintained N2 strain of *C. elegans,* laboratory-maintained populations of plant-parasitic nematodes are established from diverse locations and likely exhibit genetic and phenotypic diversity. It will be interesting to directly examine the variability in embryogenesis and hatching among diverse populations of *H. glycines*.

A protractible stylet mouthpart is an adaptation found in all plant-parasitic nematodes. The stylet is used for infection and, in some species, for hatching. The mechanisms regulating the development of this important structure are unknown. Unlike *C. elegans,* most plant-parasitic nematodes undergo the first molt within the egg and hatch as J2s. We observed the developing stylet cone during the first molt of *H. glycines*. Our observations are similar to those previously described in the plant-parasitic nematode *Hoplolaimus columbus* (Fassuliotis 1975). Furthermore, we found that individual structures like the stylet and stylet protractor muscles

continued to develop in pre-hatch J2s. We did not specifically test if hatching stimulants affect the progression of development during this stage. However, our earlier analysis suggested there were no differences among different hatching stimulants in the time to reach either the J1 or the J2 **(Table 2.1)**.

The stylet protractor muscles were present in early pre-hatch J2s before the formation of stylet knobs. In *C. elegans,* esophageal muscles are thought to secrete the cuticle lining the stoma lumen (Albertson and Thomson 1976). It is tempting to speculate that *H. glycines* stylet protractor muscles secrete the cuticle that forms the stylet. However, Endo (1985) suggested that the cuticle-based stylet is secreted by arcade epithelial cells. It may be possible to ablate individual stylet protractor muscle cells to test these hypotheses. In addition to our finding of post-molt stylet development, we also uncovered changes to the nervous system. It is uncertain from our data whether these changes to the nervous system are required for hatching behavior. Further investigation into pre-hatch development may lead to strategies for manipulating hatch behavior that could be useful for controlling this parasite.

Conclusions: Embryogenesis in the parasitic nematode *H. glycines* is decoupled from hatching stimulants or oviposition location. While the pattern of early embryonic development in *H. glycines* was very similar to the closely related parasitic nematode *M. incognita,* the rate of *H. glycines* development was substantially faster. The continued development of the stylet, nerve ring, and the ventral nerve cord in pre-hatched J2s may suggest they are required structures for *H. glycines* hatching.

TABLES AND FIGURES

Table 2.1. Hatching stimulants do not affect the pre-hatch development timeline of *Heterodera glycines*.

Developmental stage	Water (n)	Zinc chloride (n)	Soybean root exudate (n)
3 cell	2.67 ± 1.15 (3)	3.24 ± 1.25 (4)	3.20 ± 1.3 (6)
4 cell	4.67 ± 2.08 (3)	5.33 ± 1.53 (3)	5.25 ± 0.96 (7)
Gastrula	75.71 ± 9.25 (6)	72.60 ± 1.51 (5)	70.60 ± 4.35 (7)
Tadpole	100.50 ± 8.31 (6)	97.25 ± 4.57 (4)	93.80 ± 5.77 (5)
J1 stage	112 ± 7.66 (7)	113.80 ± 9.49 (5)	107.72 ± 10.12 (10)
J2 stage	168.29 ± 7.16 (7)	165.20 ± 9.76 (5)	166.14 ± 10.16 (11)

Fifteen synchronized two-celled eggs were placed in water, soybean root exudate or 3 mM $ZnCl_2$ and examined at variable time points. Data are means ± s.d. of hours to reach a specific developmental stage following the two-cell stage. Numbers in parentheses indicate number of animals observed at that specific stage out of the fifteen. For some animals, observation of the specific stage was missed. The J2 stage was assessed by the presence of a fully formed stylet. No statistically significant differences were found among treatments.

Table 2.2. Pre-hatch developmental timeline of *Hetrodera glycines* is not affected by oviposition location.

Developmental stages	Encysted eggs (n)	Egg sac eggs (n)
3 cell	2.67 ± 1.15 (3)	3.50 ± 0.84 (6)
4 cell	4.67 ± 2.08 (3)	4.71 ± 0.49 (8)
Gastrula	75.71 ± 9.25 (6)	69.86±2.97 (7)
Tadpole	100.50 ± 8.31 (6)	95 ± 0 (5)
J1 stage	112 ± 7.66 (7)	126.20±9.56 (10)
J2 stage	168.29 ± 7.16 (7)	172.54±9.34 (10)

Fifteen synchronized two-celled eggs from the egg sac or the cyst were examined daily in water. Data are mean ± s.d. of hours after the two-celled stage. Numbers the parentheses indicate number of animals observed at that specific stage out of the fifteen. For some animals, observation of the specific stage was missed. The J2 stage was assessed by the presence of a fully formed stylet. No statistically significant differences were found between treatments.

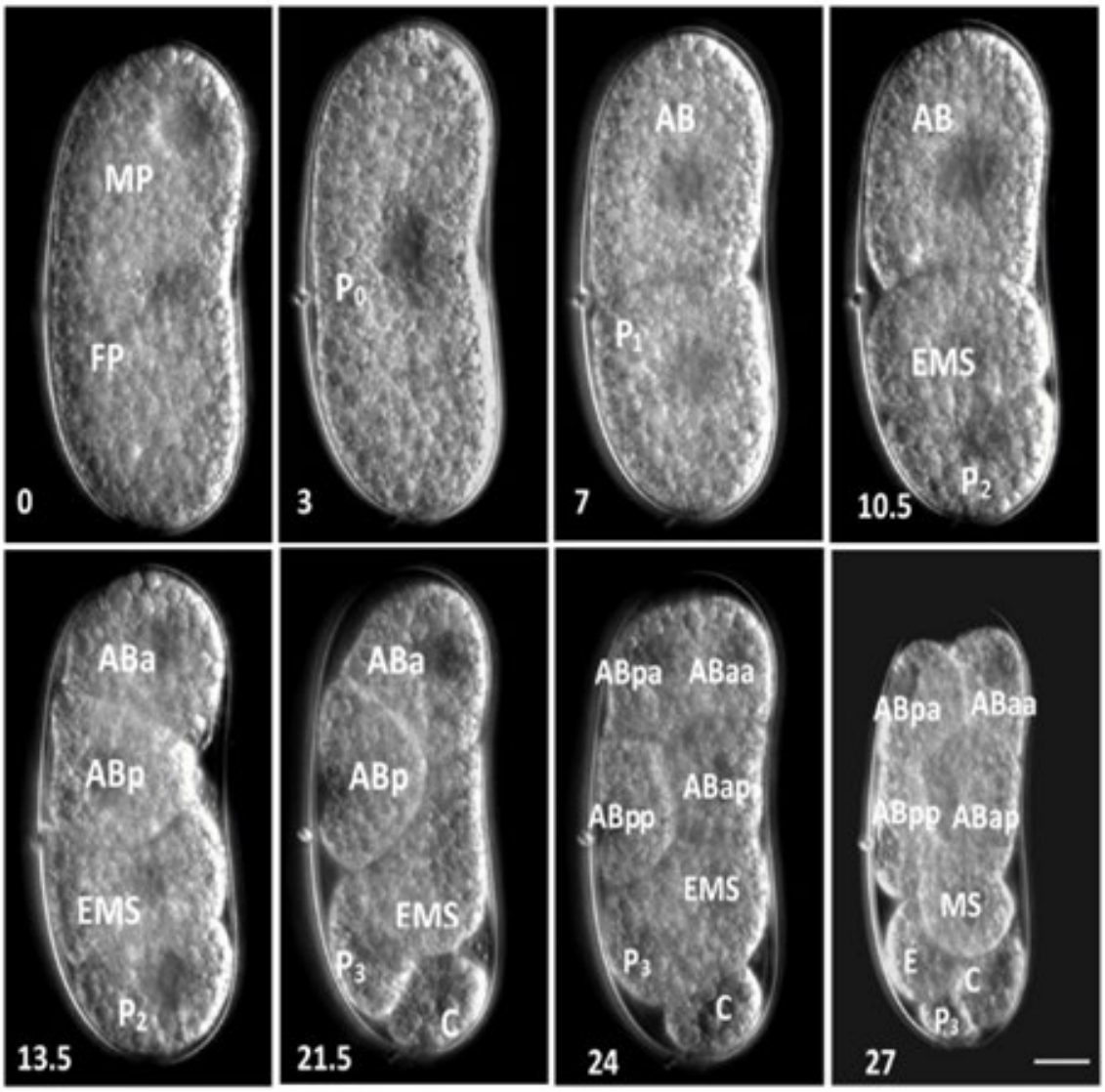

Figure 2.1. Representative DIC micrographs of *Heterodera glycines* early embryo development. Individual eggs were observed every half hour until the eight-cell stage. The time in hours (lower left corner) was recorded for each of the cell divisions. Cell labels are based on *Caenorhabditis elegans* and inferred based on positional homology in other nematode species (Dolinski, Baldwin, and Thomas 2001; Lauritis, Rebois, and Graney 1983; Bhem et al. 1995; Sulston, 1976). Scale, 15µm.

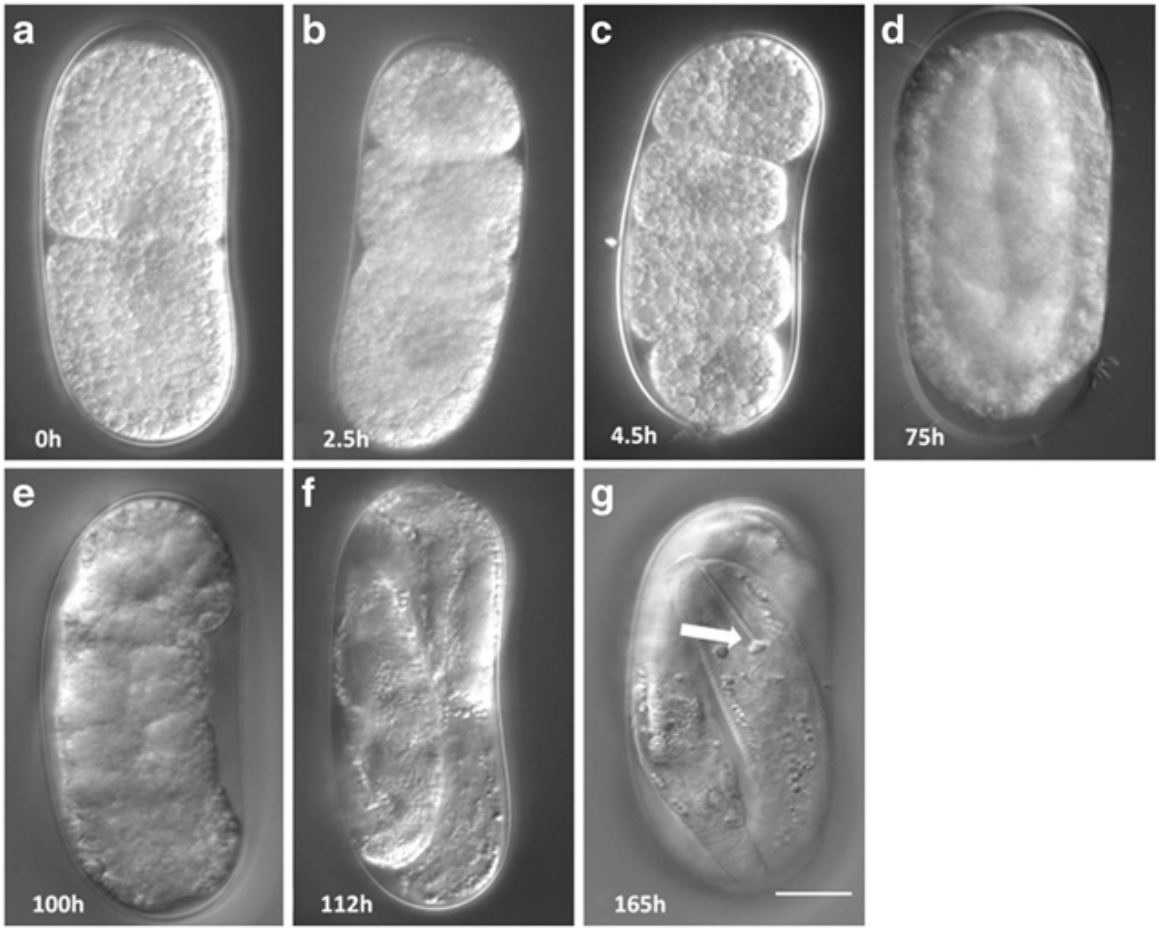

Figure 2.2. Representative DIC micrographs of selected developmental stages in *Heterodera glycines* and their corresponding timeline in hours after the 2-cell egg. Major pre-hatch development stages were determined through long-term imaging in hanging drops. (A) 2-cell stage; (B) 3-cell stage; (C) 4-cell stage; (D) gastrula; (E) tadpole; (F) first stage juvenile; (G) J2 with fully formed stylet (arrow). Scale, 15 µm.

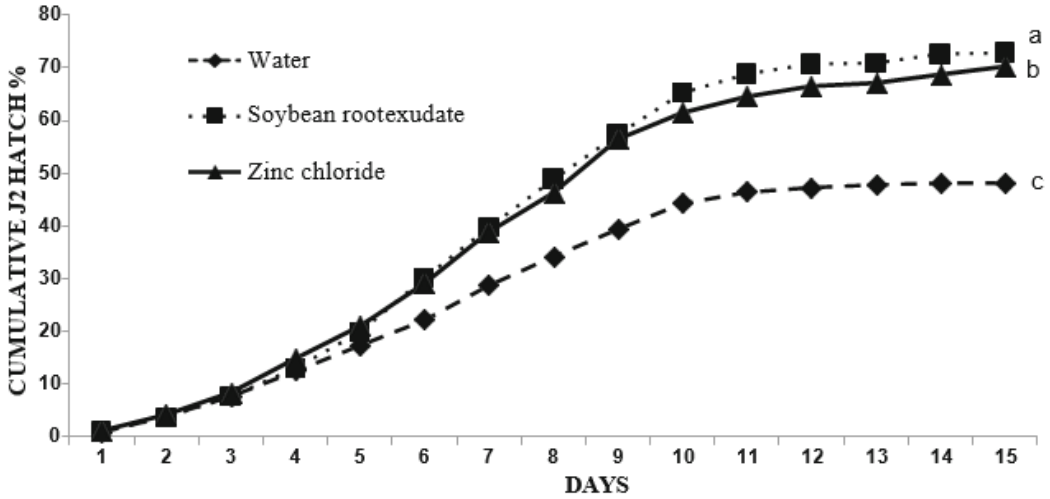

Figure 2.3. *Heterodera glycines* hatching is increased by the presence of soybean root exudate or $ZnCl_2$. Asynchronous eggs were examined for hatching each day for 15 days in sterile distilled water, soybean root exudate, and $ZnCl_2$. The experiment was repeated once with three replications, each replication consists of 1000 eggs. Different letters at the end of the curves indicate statistically significant differences ($P < 0.001$), at $\alpha = 0.05$.

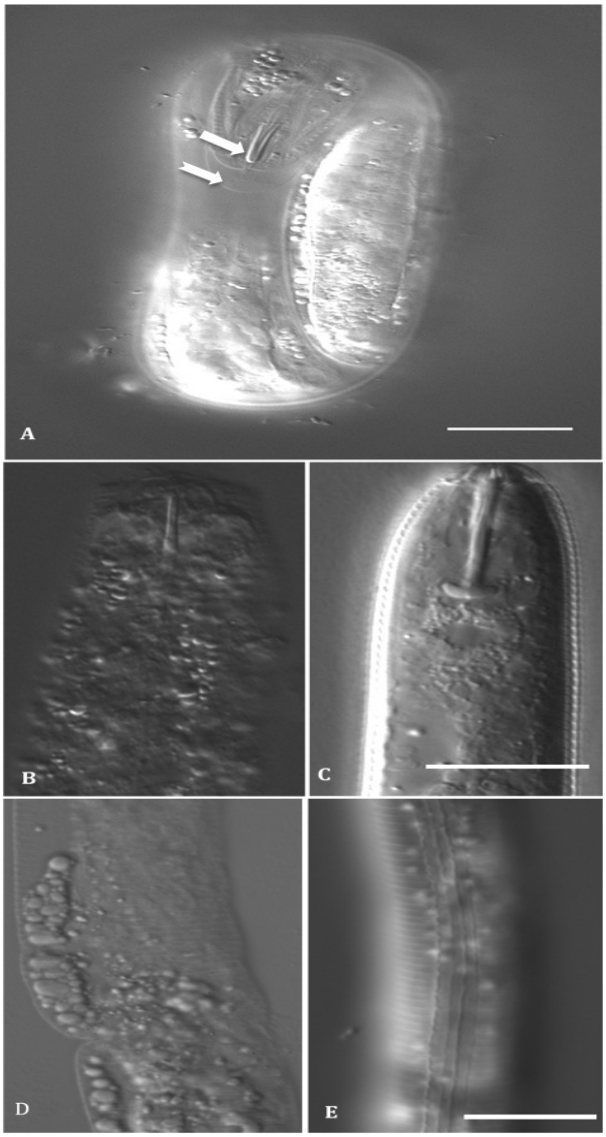

Figure 2.4. The stylet and cuticle development of pre-hatched J2 *Hetrodera glycines* continues beyond the J1 to J2 molt. Pre-hatch J2s immediately following the J1 to J2 molt (A) retain their old J1 cuticle (lower arrow) and do not show a completely developed stylet (upper arrow). Early pre-hatched J2s mechanically removed from the eggshell (B and D) show an incomplete stylet, including a complete lack of the stylet shaft and knobs (B) and a lack of longitudinal ridges (alae) along the lateral field of the cuticle (D). In comparison, a fully formed J2 has a complete stylet (C) and well developed alae (E). Scale, 15µm.

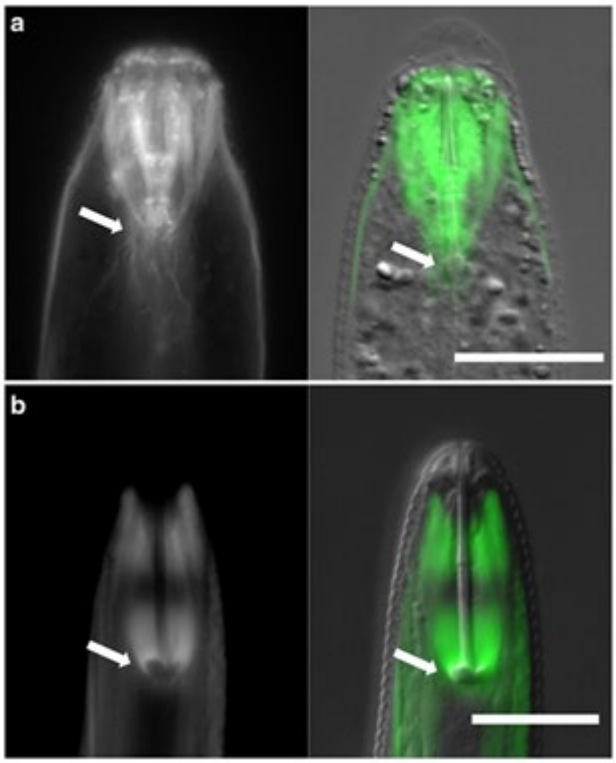

Figure 2.5. The stylet protractor muscle development precedes the complete development of the stylet. Pre-hatched (A) and hatched (B) J2 *Heterodera glycines were* stained with phalloidin and imaged using fluorescence (left) and DIC optics (right). The stylet protractor muscles were present prior to the complete formation of the stylet knobs (arrows). Scale, 15µm.

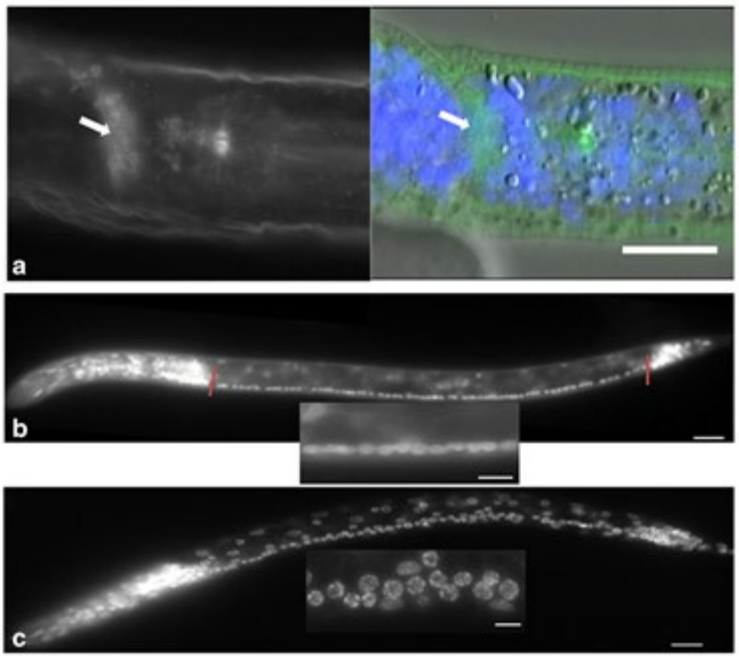

Figure 2.6. The neurodevelopment of *Heterodera glycines* early pre-hatched J2 is not complete. Pre-hatched J2 (A and C) were mechanically removed from their egg shell and stained with phalloidin and/or DAPI and compared to hatched J2s (B). In one early pre-hatched J2 (A) we observed F-actin binding phalloidin staining (left and green in right) in the nerve ring (arrows). The nerve ring was identified by position and a lack of cell nuclei (blue DAPI staining in right). An increase in the number of ventral nerve cord (VNC) nuclei and linearity was seen between pre-hatch (C) and hatched (B) J2. The VNC consists of a series of motor neurons that extends from the retro-vesicular ganglion to the pre-anal ganglion (marked with red lines in B). Pre-hatched J2s showed an average of 62 VNC and a less linear organization (inset) compared to the 65 VNC nuclei arranged in a highly linear manner as observed in hatched J2s. A-C scale, 15µm. Inset scale, 5µm.

REFERENCES

Albertson, D. G., & Thompson, J. N. (1976). The pharynx *of Caenorhabditis elegans*. *Philosophical Transactions of the Royal Society of the London. 275*(938), 299-325.

Behm, J. E., Tylka, G. L., Niblack, T. L., Wiebold, W. J., & Donald, P. A. (1995). Effects of zinc fertilization of corn on hatching of *Heterodera glycines* in soil. *Journal of Nematology*, *27*(2), 164.

Calderón-Urrea, A., Vanholme, B., Vangestel, S., Kane, S. M., Bahaji, A., Pha, K., Garcia, M., Snider, A. and Gheysen, G. (2016). Early development of the root-knot nematode *Meloidogyne incognita*. *BMC developmental Biology*, *16*(1), 10.

Charlson, D. V., & Tylka, G. L. (2003). *Heterodera glycines* cyst components and surface disinfestants affect H. glycines hatching. *Journal of Nematology*, *35*(4), 458.

Clarke, A. J., & Shepherd, A. M. (1966). Inorganic ions and the hatching of Heterodera spp. *Annals of Applied Biology*, *58*(3), 497-508.

Dolinski, C. J. B. G., Baldwin, J. G., & Thomas, W. K. (2001). Comparative survey of early embryogenesis of Secernentea (Nematoda), with phylogenetic implications. *Canadian Journal of Zoology*, *79*(1), 82-94.

Endo, B. Y. (1985). Ultrastructure of the head region of molting second-stage juveniles of *Heterodera glycines* with emphasis on stylet formation. *Journal of Nematology*, *17*(2), 112.

Endo, B. Y. (1983). Ultrastructure of the stomatal region of the juvenile stage of the soybean cyst nematode, *Heterodera glycines*. *Proceedings of the Helminthological Society of Washington*, *50*(1), 43-61.

Fairbairn, D. (1961). The in vitro hatching of *Ascaris lumbricoides* eggs. *Canadian Journal of Zoology*, *39*(2), 153-162.

Fassuliotis, G. E. O. R. G. E. (1975). Feeding, egg-laying, and embryology of the Columbia lance nematode, *Hoplolaimus columbus*. *Journal of Nematology*, *7*(2), 152.

Gilarte, P., Kreuzinger-Janik, B., Majdi, N., & Traunspurger, W. (2015). Life-history traits of the model organism *Pristionchus pacificus* recorded using the hanging drop method: comparison with *Caenorhabditis elegans*. *PloS One*, *10*(8), e0134105.

Han, Z., Boas, S., & Schroeder, N. E. (2016). Unexpected variation in neuroanatomy among diverse nematode species. *Frontiers in Neuroanatomy*, *9*, 162.

Hussey, R. S. (1973). A comparison of methods of collecting inocula of Meloidogyne spp., including a new technique. *Plant Disease Reporter, 57*, 1025-1028.

Ishibashi, N., Kondo, E., Muraoka, M., & Yokoo, T. (1973). Ecological Significance of Dormancy in Plant Parasitic Nematodes: I. Ecological Difference between Eggs in Gelatinous Matrix and Cyst of *Hetrodera glycines* Ichinohe: Tylenchida: Heteroderidae. *Applied Entomology and Zoology*, *8*(2), 53-63.

Lauritis, J. A., Rebois, R. V., & Graney, L. S. (1983). Development of *Heterodera glycines* Ichinohe on soybean, Glycine max (L.) Merr., under gnotobiotic conditions. *Journal of Nematology*, *15*(2), 272.

Legouis, R., Gansmuller, A., Sookhareea, S., Bosher, J. M., Baillie, D. L., & Labouesse, M. (2000). LET-413 is a basolateral protein required for the assembly of adherens junctions in *Caenorhabditis elegans*. *Nature Cell Biology*, *2*(7), 415.

Levene, B. C., Owen, M. D., & Tylka, G. L. (1998). Influence of herbicide application to soybeans on soybean cyst nematode egg hatching. *Journal of Nematology*, *30*(3), 347.

Masler, E. P., Rogers, S. T., & Chitwood, D. J. (2013). Effects of catechins and low temperature on embryonic development and hatching in *Heterodera glycines* and *Meloidogyne incognita. Nematology*, *15*(6), 653-663.

McGlashan, J. K., Loudon, F. K., Thompson, M. B., & Spencer, R. J. (2015). Hatching behavior of eastern long-necked turtles (*Chelodina longicollis*): The influence of asynchronous environments on embryonic heart rate and phenotype. *Comparative Biochemistry and Physiology Part A: Molecular & Integrative Physiology*, *188*, 58-64.

McGlashan, J. K., Spencer, R. J., & Old, J. M. (2011). Embryonic communication in the nest: metabolic responses of reptilian embryos to developmental rates of siblings. *Proceedings of the Royal Society of London B: Biological Sciences*, *279*(1734), 1709-1715.

Niblack, T. L., Lambert, K. N., & Tylka, G. L. (2006). A model plant pathogen from the kingdom animalia: *Heterodera glycines*, the soybean cyst nematode. *Annual Review of Phytopathology*, *44*, 283-303.

Perry, R.N. (2002). Hatching. In: Lee D, editor. The biology of nematodes. New York: Taylor and Francis; pp. 147–69.

Polet, D., Lambrechts, A., Ono, K., Mah, A., Peelman, F., Vandekerckhove, J., Baillie, D.L., Ampe, C. and Ono, S. (2006). *Caenorhabditis elegans* expresses three functional profilins in a tissue-specific manner. *Cell Motility and the Cytoskeleton*, *63*(1), 14-28.

Riggs, R. D., Schmitt, D. P., & Mauromoustakos, A. (1997). Comparison of extraction and shipping methods for cysts and juveniles of *Heterodera glycines*. *Journal of Nematology*, *29*(1), 127.

Schulze, J., & Schierenberg, E. (2011). Evolution of embryonic development in nematodes. *EvoDevo*, *2*(1), 18.

Sipes, B. S., Schmitt, D. P., & Barker, K. R. (1992). Fertility of three parasitic biotypes of *Heterodera glycines*. *Phytopathology.82*, 999-1001.

Skiba, F., & Schierenberg, E. (1992). Cell lineages, developmental timing, and spatial pattern formation in embryos of free-living soil nematodes. *Developmental Biology*, *151*(2), 597-610.

Sulston, J. E., Schierenberg, E., White, J. G., & Thomson, J. N. (1983). The embryonic cell lineage of the nematode *Caenorhabditis elegans*. *Developmental Biology*, *100*(1), 64-119.

Sulston, J. E. (1976). Post-embryonic development in the ventral cord of *Caenorhabditis elegans*. *Philosophical Transaction of the Royal Society of London B*, *275*(938), 287-297.

Tefft, P. M., & Bone, L. W. (1985). Plant-induced hatching of eggs of the soybean cyst nematode *Heterodera glycines*. *Journal of Nematology*, *17*(3), 275.

Teft, P. M., Rende, J. F., & Bone, L. W. (1982). Factors Influencing Egg Hatching of the Soybean Cyst Nematode. In *Proceeding of the Helminthology Society of Washington* (Vol. 49, No. 2, pp. 258-265.

Thompson, J. M., & Tylka, G. L. (1997). Differences in hatching of *Heterodera glycines* egg-mass and encysted eggs in vitro. *Journal of Nematology*, *29*(3), 315.

Tsutsumi, M. (1966). Influence of root diffusates of several host and non-host plants on the hatching of the soybean cyst nematode, *Heterodera glycines* Ichinose, *Japanese Journal of Applied Entomology and Zoology*, *10*, 129-137.

Tylka, G. L., Niblack, T. L., Walk, T. C., Harkins, K. R., Barnett, L., & Baker, N. K. (1993). Flow cytometric analysis and sorting of *Heterodera glycines* eggs. *Journal of Nematology*, *25*(4), 596.

van Megen, H., van den Elsen, S., Holterman, M., Karssen, G., Mooyman, P., Bongers, T., Holovachov, O., Bakker, J. & Helder, J. (2009). A phylogenetic tree of nematodes based on about 1200 full-length small subunit ribosomal DNA sequences. *Nematology*, *11*(6), 927-950.

Van Troys, M., Ono, K., Dewitte, D., Jonckheere, V., De Ruyck, N., Vandekerckhove, J., Ono, S. & Ampe, C. (2004). Tetrathymosinβ is required for actin dynamics in *Caenorhabditis elegans* and acts via functionally different actin-binding repeats. *Molecular Biology of the Cell*, *15*(10), 4735-4748.

Voronezhskaya, E. E., Khabarova, M. Y., & Nezlin, L. P. (2004). Apical sensory neurons mediate developmental retardation induced by conspecific environmental stimuli in freshwater pulmonate snails. *Development*, *131*(15), 3671-3680.

Von Ehrenstein, G., Schierenberg, E. (1980). Cell lineages and development of *Caenorhabditis elegans* and other nematodes. In: Zuckerman BM (eds.) Nematodes as biological models Vol. I. Behavioral and

developmental model, pp. 2-68. New York: Academic.

Vrain, T. C., & Barker, K. R. (1978). Influence of low temperature on development of *Meloidogyne incognita* and *M. hapla* eggs in egg masses. *Journal of Nematology*, *10*(4), 311.

Warkentin, K. M. (2011). Plasticity of hatching in amphibians: evolution, trade-offs, cues and mechanisms. *Integrative and Comparative Biology*, *51*(1), 111-127.

Wharton, D.A. (2004). Survival strategies. In: Gaugler, R., Bilgrami, A.L. (eds) Nematode behavior. Chapter 13. Cambridge, MA: CABI International.

Wolfinger, R., & Chang, M. (1998). Comparing the SAS GLM and MIXED procedures for repeated measures. Available from: http://www.ats.ucla.edu/stat/sas/library/mixedglm.pdf

Yen, J. H., Niblack, T. L., & Wiebold, W. J. (1995). Dormancy of *Heterodera glycines* in Missouri. *Journal of Nematology*, *27*(2), 153.

CHAPTER 3: VENTRAL NERVE CORD NEURONS DEGENERATION IS ASSOCIATED WITH SEDENTARY LIFE CYCLE OF PLANT-PARASITIC NEMATODES

ABSTRACT

The sedentary plant-parasitic nematodes are considered among the most economically damaging pathogens of plants. The sedentary nematodes are more fecund and considered more damaging than their phylogenetically closest migratory relatives. Following infection and the establishment of a feeding site, sedentary nematodes become immobile. Interestingly, in some sedentary cyst nematodes like *Heterodera glycines*, loss of mobility after infection is reversed in adult males while females never regain mobility. The structural basis for this change in mobility is unknown. In *Caenorhabditis elegans*, contraction and relaxation of most body wall muscles are regulated by motor neurons within the ventral nerve cord (VNC). The VNC consists of a series of motor neurons that innervate nematode body-wall muscles and regulate movement. In this chapter, we examined the VNC neurons of three sedentary plant-parasitic nematodes (*H. glycines, Meloidogyne incognita*, and *Rotylenchulus reniformis*) belonging to clade 12. Within this phylogenetic clade, comprising most plant-parasitic nematode, the sedentary life-style has arisen at least twice. We used DAPI (4′, 6-diamidino-2-phenylindole) staining to examine the VNC neurons throughout the developmental cycle of these nematodes. We include *Pratylenchus penetrans,* a migratory nematode as a control. In *H. glycines*, we found a gradual reduction of VNC neurons (65 to 40) during development from the mobile J2 to sedentary J3 and J4 females. Some nuclei of the VNC in sedentary stages were located several microns away from the ventral midline. Strikingly, we found 70 neurons in the adult male VNC and a reorganization of the cord into a linear arrangement. It appears that, the VNC neurons in the VNC of both sexes of *H. glycines* degenerate during sedentary stages of development. However, males undergo

neuronal remodeling that includes the addition of neurons. Similar to *H. glycines* we found fewer VNC neurons in sedentary stages of *M*. *incognita. H. glycines* and *M. incognita* has similar life cycles. *R. reniformis* has different life-cycle than *H. glycines*, its J3, J4 and adult stages are mobile, only adult female after the onset of parasitism become sedentary. The number of VNC neurons in *R. reniformis* degenerates in sedentary female stage only. As expected, the number of VNC neurons in mobile stages of *R. reniformis* remained stable like in *P. penetrans*, migratory nematode. Our results suggest that VNC neuron degeneration is correlated with sedentary behavior.

INTRODUCTION

The nematode has simple anatomy, which makes it suitable for the neuroanatomy study (Chitwood and Chitwood 1938). The free-living nematode *Caenorhabditis elegans* is well studied, its nervous system consists of only 302 neurons in the adult hermaphrodite (White et al. 1986). The *C. elegans* ventral nerve cord (VNC) consists of series of motor neurons that innervate nematode body-wall muscles and regulate movement (White et al. 1976). The *C. elegans* VNC has 57 motor neurons innervating the body muscles on both the ventral and dorsal sides (White et al. 1976; Sulston 1976). In *Ascaris suum*, 55 neurons in the VNC innervate approximately 50,000 muscle cells (Stretton 1976; Stretton et al. 1978). Locomotion in nematodes involves somatic muscles that are present below the cuticle and epidermis.
In *C*. *elegans*, movement is generated through muscle contractile force propagated to the outer cuticle through a thin basal lamina and epidermal layer via fibrous organelles (Francis and Waterston 1991). Muscle contractions are produced via the innervation of excitatory cholinergic and inhibitory GABAergic VNC motor neuron (Mclntire, Jorgensen and Horvitz 1993; Mclntire

et al. 1993). Previously, our lab has found neuroanatomical variation within and among nematodes clades (Han, Boas and Schroeder 2016). Furthermore our lab found variation in the developmental timing of the VNC among nematode species (Han, Boas and Schroeder 2016). Not much information is available on plant-parasitic nematodes (PPNs) VNC.

Sedentary PPNs are among the most damaging pathogens to agricultural crop production worldwide (Jones et al. 2013). For example, the soybean cyst nematode, *Heterodera glycines,* is estimated to account for over a billion dollars in yield loss annually (Koenning and Wrather 2010). *H. glycines* hatches as an infective, mobile second-stage juvenile (J2). Following infection, *H. glycines* establishes a multinucleated feeding site, both males and females develop from a vermiform J2 to sausage-shaped J3 male and female (**Figure 3.1**). While feeding, both sexes are restricted in movement to slight head motion at their feeding (Wyss and Zunke 1986). During J4, males undergo extensive morphological remodeling back to a vermiform morphology. Following the final molt, the adult male is fully mobile (**Figure 3.1**). Unlike the adult male, adult *H. glycines* females do not regain its mobility. The root-knot nematode species, *Meloidogyne incognita,* has a very similar life cycle to *H. glycines*, its adult male regains its mobility at adult stage, while adult females remain sedentary. Another semi-endoparasite nematode, *Roylenchulus reniformis,* has an interesting life cycle. The J2 hatches from the eggs and undergoes three successive molts without feeding and develops into vermiform males or females. All these stages are motile. The young adult female penetrates the roots, inserting about one-third of its body into the plant, and establishes a multinucleated feeding site similar to *H. glycines.* After establishing the feeding site, the females lose mobility.

Within the phylogenetic clade comprising most PPNs, the sedentary life-style has arisen at least twice (van Megan et al. 2009; Holterman et al. 2006). While having a similar life-cycle,

M. incognita and *H. glycines* are phylogenetically diverged. *R. reniformis* and *H. glcyines* are phylogenetically close but have different life cycles (van Megan et al. 2009; Holterman et al 2006) (**Figure 3.2).** The sedentary nematodes are more fecund and considered more damaging than their phylogenetically closest "migratory" PPNs relatives (Jones et al. 2013; Hastings 1936). A better understanding of their neuroanatomy modifications that occur during sedentary nematode development could provide novel targets for control. For example, the resumption of mobility by male cyst nematodes could be targeted without affecting non-target nematodes that do not undergo this unusual development. We examined the VNC neurons in some Tylenchomorpha nematodes from clade 12 throughout their developments (van Megan et al. 2009; Holterman et al. 2006) (**Figure 3.2**). My study included sedentary PPNs (*H. glycines, M. incognita*, and *R. reniformis*) and a migratory control *Pratylenchus penetrans*.

MATERIALS AND METHODS

Nematode culture

H. glycines were isolated from a soybean field in Illinois, USA and maintained on susceptible soybean (cv. Macon) in the greenhouse. To collect synchronized developmental stages of *H. glycines,* soybean seeds were germinated in moist paper towels for three days. Soybean seedlings were then placed in pluronic gel F-127 with freshly hatched J2s for 24 hours (Wang et al,). Soybean roots were washed gently with water to remove nematodes that had not infected roots within 24 hours of inoculation. *H. glycines*-infested roots were then planted in sandy loam soil and kept in a growth chamber at 22-24°C and 12-hour light cycle until extraction. After inoculation, the infested roots were grown for 6-7 days to collect J3s, 9-10 days to collect J4 females and males, and 11-13 days for an adult female (Dong et al. 2014). Developmental stages and sex were determined by overall body size and gonad

morphology (Raski 1950). Infested roots were macerated with a hand blender to obtain *H. glycines* at specific time points. The mixture was poured over stacked 850, 250, and 25-µm-pore sieves. *H. glycines* adult males were extracted from the soil after 15 days of inoculation.

M. incognita (gift from Dr. Jason Bond) was originally isolated from soybean and maintained on 'Rutgers' tomato in the greenhouse. To collect synchronized developmental stages of *M. incognita*, two week old tomato seedlings were inoculated with freshly hatched J2s. Tomato seedlings were gently pulled from the soil and washed with water to remove nematodes that had not infected roots within 48 hours following inoculation. *M. incognita* infested roots were then planted in sandy loam soil and kept in a growth chamber with temperature 22-24°C and 12-hour light cycle until extraction. The nematodes were extracted using a hand blender to collect different developmental time points of the post-infective J2 stage from 6 -14 days after inoculation (Triantaphyllou and Hirschmann 1960).

R. reniformis (gift from Dr. Martin Wubben) was maintained in sandy loam soil in 'Macon' cultivar of soybean in the greenhouse. To study the non-parasitic stages, eggs were incubated at 30°C in a glass Petri dish. Different developmental stages were identified based on their morphology and number of cuticles that were present (Bird 1984). Parasitic adult females were extracted as previously described (Ganji et al. 2013).

P. penetrans (gift from Dr. Terry Niblack) were cultured on corn root explants on Murashige and Skoog (MS) media (Rebois and Huettel 1986). Specific developmental stages of *P. penetrans* were isolated by synchronizing populations from eggs. *P. penetrans* eggs were extracted as previously described (Dunn 1973). Freshly hatched J2s were collected and placed on corn root explants on MS media. Developmental stages of *P. penetrans* were determined based on body size and gonad morphology.

4′, 6-diamidino-2-phenylindole (DAPI) staining

H. glycines were fixed in Carnoy's fixative (60% ethanol, 30% acetic acid, 10% chloroform) overnight in a 1.5 ml centrifuge tube and allowed to settle in the bottom of the tube (Flemming et al. 2000; Hedgecock and White 1985). The supernatant was removed and transferred to 75% ethanol before staining with 0.2–0.5 µg/ml of DAPI overnight in the dark at room temperature. All other nematodes (*M. incognita, R. reniformis,* and *P. penetrans)* were fixed in Carnoy's fixative for 2 hours and then transferred to 50% methanol and stained with 0.2–0.5 µg/ml of DAPI overnight in the dark at room temperature until imaging. All images were captured with Zen software on a Zeiss M2 AxioImager with differential interference contrast (DIC) and fluorescence optics and examined in FIJI using ImageJ software. The VNC nuclei were identified based on their size and morphology (Sulston 1976; White et al.1976). Counts of neuronal nuclei were made from immediately posterior of the retro-vesicular ganglion to immediately anterior of the pre-anal ganglion (**Figure 3.3**)

RESULTS AND DISCUSSION

***H. glycines* motor neurons degenerate during development:** In *C. elegans*, contraction and relaxation of most body wall muscles are regulated by motor neurons within the VNC (White et al. 1976; Chalfie et al. 1985). We, therefore, examined the VNC during *H. glycines* development. We previously found that mobile J2 *H. glycines* contain 65 VNC neurons (Han, Boas and Schroeder 2016; Thapa et al. 2017). Here, using DAPI staining we found a gradual reduction of VNC neurons during development from the mobile J2 to sedentary J3 and J4 females (**Table 3.1; Figure 3.4**). In addition, the overall pattern of the VNC in sedentary stages deviates from the linear pattern seen during mobile stage. Some nuclei in the

VNC of sedentary stages are located several microns away from the ventral midline (**Figure 3.4 B**). Strikingly, we found 70 neurons in the adult male VNC and a reorganization of the cord into a linear arrangement (**Table 3.1; Figure 3.4 C**). It appears that, the motor neurons in the VNC of both sexes of *H. glycines* degenerate during sedentary stages of development. However, males undergo neuronal remodeling that includes formation of the addition neurons. This addition of neurons results in more VNC neurons in adult males than in mobile J2s. Similar to *C. elegans*, the males of *H. glycines* may include sex-specific motor neurons in the VNC (Sulston and Horvitz 1977).

Developmentally associated neurodegeneration evolved in phylogenetically separate parasitic nematodes: Among Tylenchomorpha nematodes, sedentary behavior is found in multiple genera. The root-knot nematodes (*Meloidogyne* spp.) also become immobile soon after infecting the plant host (Bird 1967). However, *Meloidogyne* spp. are phylogenetically diverged from *H. glycines* **(Figure 3.2)**. *R. reniformis* is a phylogenetically closer relative of *H. glycines* **(Figure 3.2)**. Their adult females also become immobile after infecting plant host. Sister lineages to *Meloidogyne* spp. *Heterodera* spp. and *R. reniformis* are mobile during all post-embryonic stages (van Megan et al. 2009; Holterman et al. 2006). We examined the VNC of mobile and immobile developmental stages of *M. incognita* and *R. reniformis* with DAPI to determine if motor neurons degeneration is correlated with sedentary behavior in phylogenetically diverged species. Similar to *H. glycines,* we found fewer VNC neurons in sedentary stages of *M. incognita* **(Table 3.1; Figure 3.5)**. As expected, we found that the number of VNC motor neurons remained stable during *R. reniformis* mobile stages (J3s, J4s and female stages) **(Table 3.1; Figure 3.6**). However, following infection of the host plant, we observed a reduction in the number of VNC motor neurons in *R. reniformis* females **(Table 3.1; Figure 3.6).** Interestingly,

R. reniformis sedentary stage female VNC motor neurons follow a linear pattern, unlike *H. glycines* sedentary female motor neurons, which were away from ventral line. Finally, as a control group, we examined the ventral cord of *P. penetrans* at different developmental stages. *P. penetrans* is classified in the same phylogentic clade as *H. glycines*, *M. incognita and R. reniformis* (van Megan et al. 2009; Holterman et al. 2006) **(Figure 3.1)**, but is mobile at all stages. We found that the number of ventral cord neurons in *P. penetrans* remained stable throughout development **(Table 3.1; Figure 3.7)**. Our results suggest that VNC degeneration in *H. glycines*, *M. incognita*, and *R. reniformis* is specifically correlated with sedentary behavior.

The sedentary PPNs are among the most damaging pathogens to agricultural crop production worldwide (Jones et al. 2013). Our findings on motor neuron degeneration may be used to develop targeted control strategies for these devastating sedentary parasitic nematodes while avoiding potential off-target effects to other nematodes.

TABLE AND FIGURES

Table 3.1. Developmental changes to the ventral nerve cord in sedentary and mobile nematodes.

Nematode species	Stages	Average number[1] of neurons	Range	Sample size
Heterodera glycines	J2[2]	65	59-70	20
	J2 Post-infection	63	56-68	15
	J3 male	53	48-58	15
	J3 female	45	40-54	11
	J4 female	40	32-52	20
	Adult male	70	62-81	14
Meloidogyne incognita	J2	59	57-65	10
	J2 Post-infection	50	44-56	9
	Molting to J3	41	35-47	9
	J4/adult female	43	37-47	10
Rotylenchus reniformis	J2	69	63-73	10
	J2 molting	62	55-67	10
	Pre-parasitic adult female	59	54-66	9
	Parasitic/sedentary female	39	34-49	11
Pratylenchus penetrans	J2	58	53-60	10
	J3	58	53-61	8
	J4 female	59	54-62	10
	Adult female	59	54-62	10
	Adult male	63	59-68	8

[1] Neurons were counted between the retro-vesicular ganglion and the pre-anal ganglion of DAPI stained animals. [2] Second stage juveniles (J2) of *H. glycines* data is from 2nd chapter. J3, third stage juvenile and J4, fourth stage juvenile.

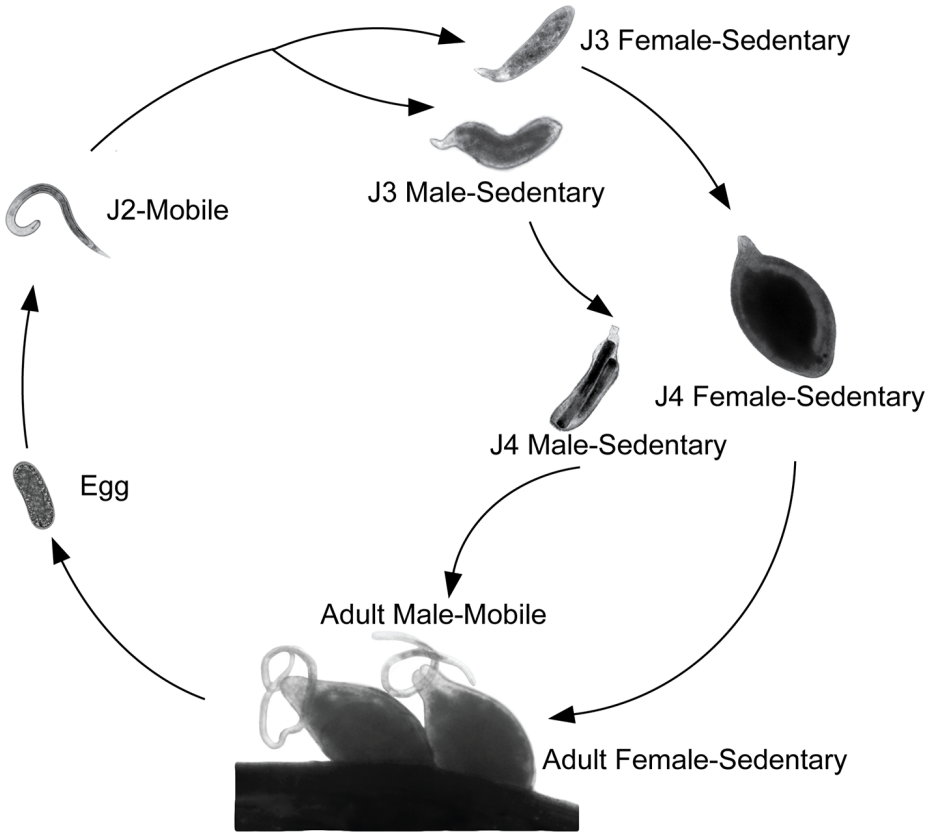

Figure 3.1. The life cycle of *Heterodera glycines.* *H. glycines* hatch as mobile second-stage juveniles (J2s), migrate to the host roots, infect and initiate feeding. Following the establishment of a feeding site, J3s remain sedentary and continue feeding. Following the final molt, adult males are fully mobile and seek out females to inseminate. Adult females remain immobile and continue to feed. Each life stage is not represented to scale.

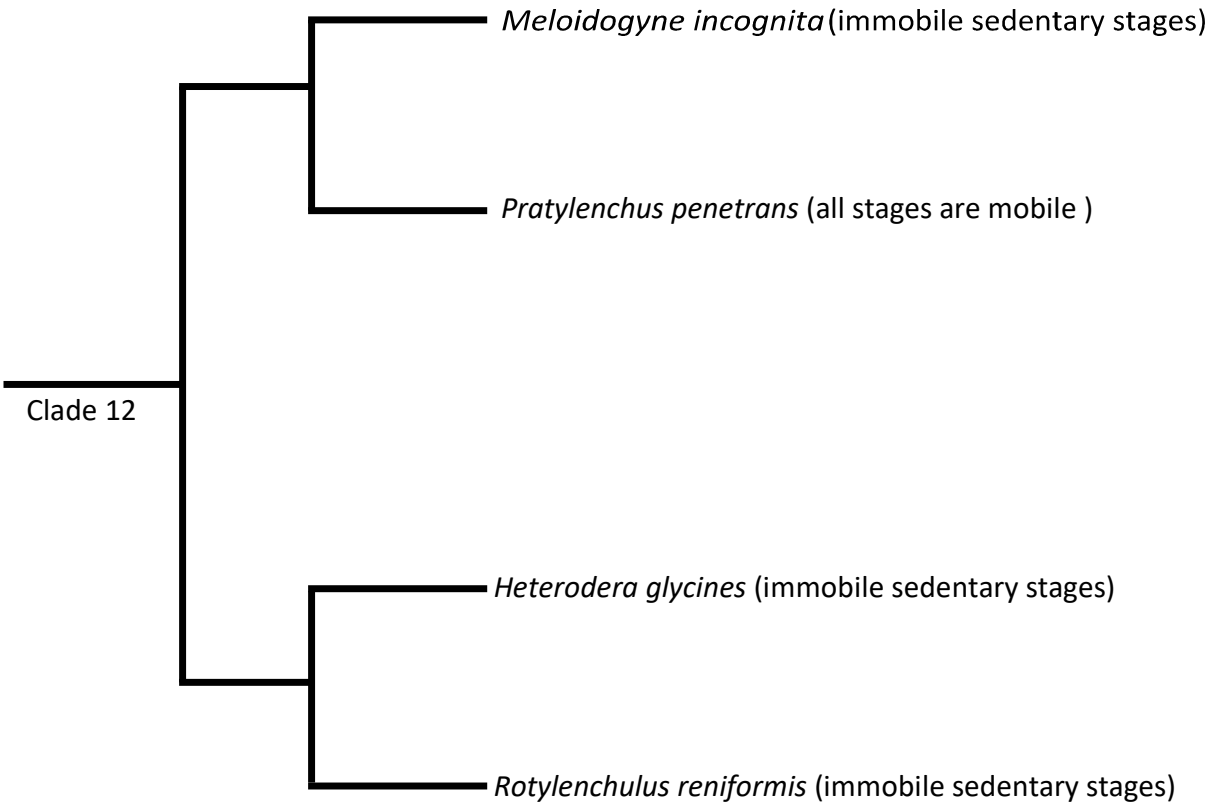

Figure 3.2. Phylogeny of the genera of nematode discussed in this study. The phylum nematode is currently divided into 12 clades (van Megan et al. 2009).

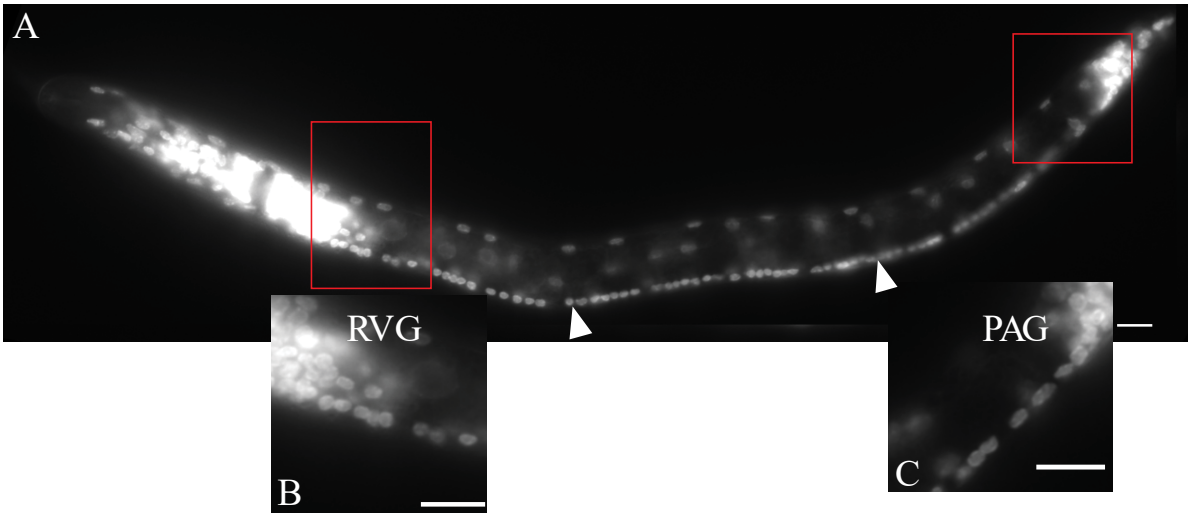

Figure 3.3. DAPI (4′, 6-diamidino-2-phenylindole*)* staining of *Heterodera glycines* pre-infective J2 stage. The ventral nerve cord (VNC) consists of a line of motor neurons (arrowheads) extending along the ventral midline from the retro-vesicular ganglion (RVG) to the pre-anal ganglion (PAG). (**A**) Ventral view of DAPI stained animal. (**B**) Region surrounding end of RVG. (**C**) Division between pre-anal ganglion and VNC. Scale bars = 10 µm.

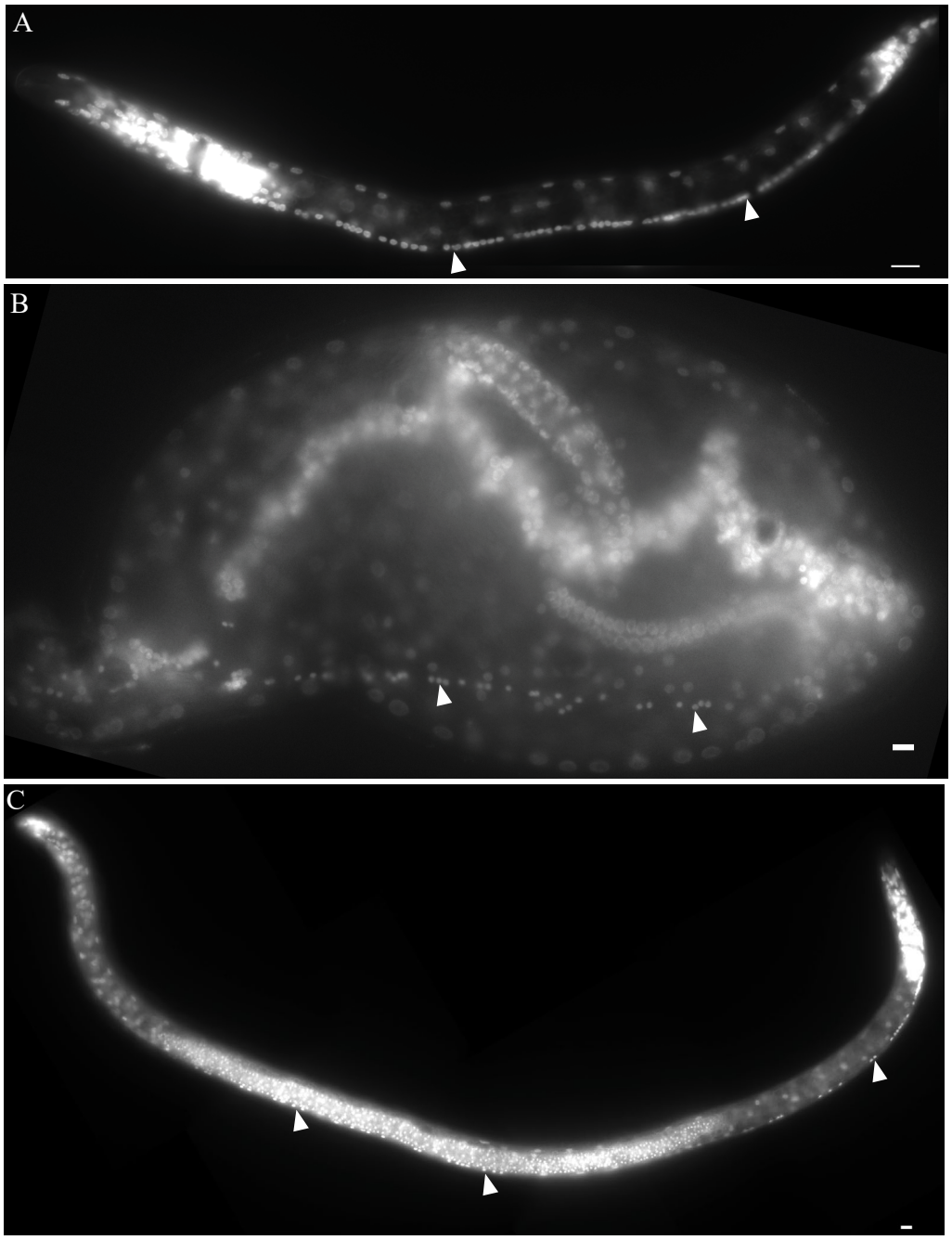

Figure 3.4. Motor neurons degeneration in the ventral nerve cord of *Heterodera glycines* is sex-specific. Ventral and sub-ventral micrographs of DAPI-stained mobile J2 (A) and sedentary J4 female (B), and adult mobile male (C). Central nerve cord (VNC) neuronal nuclei (arrowheads) are highly condensed fluorescent puncta. VNC nuclei in immobile J4 females deviate from the linear pattern seen in mobile J2s. VNC nuclei in mobile adult male is linear pattern similar to J2s. Fluorescence from sperm nuclei make it difficult to discern VNC nuclei. Scale bars = 10 µm.

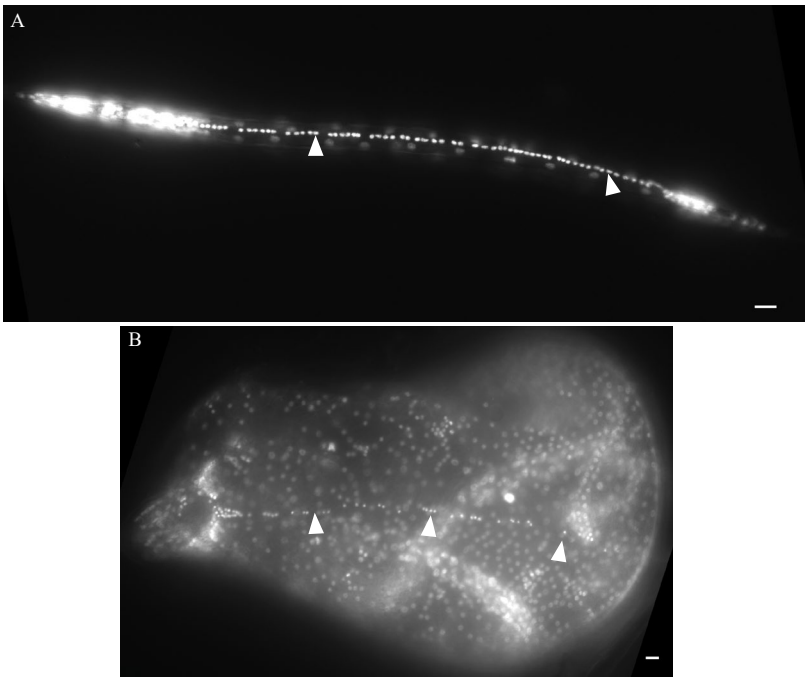

Figure 3.5. Similar to *Heterodera glycines*, motor neurons degenerate in the ventral nerve cord during *Meloidogyne incognita* development. DAPI (4′, 6-diamidino-2-phenylindole) stained mobile J2 (top) and sedentary adult female (bottom), respectively. VNC neuronal nuclei (arrowheads) are highly condensed fluorescent puncta. VNC nuclei in immobile adult females deviate from the linear pattern seen in mobile J2s. Scale bars = 10 μm.

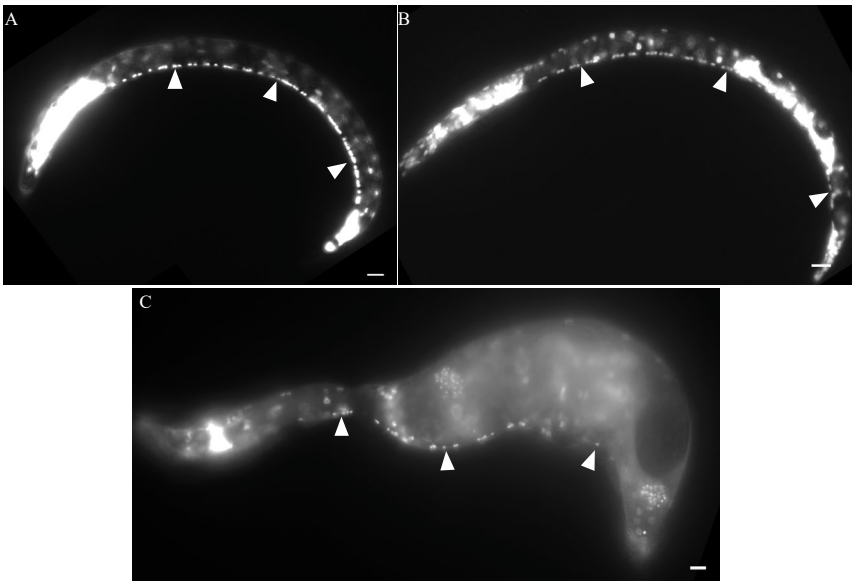

Figure 3.6. Similar to *Heterodera glycines* and *Meloidogyne incognita*, motor neurons degenerate in the ventral nerve cord of *Rotylenchus reniformis* adult female after onset of sedentary life style. DAPI (4′, 6-diamidino-2-phenylindole) -stained mobile J2 (A), adult female motile stage (B), and sedentary adult female stage (C). VNC neuronal nuclei (arrowheads) are highly condensed fluorescent puncta. VNC nuclei in immobile adult female do not deviate from the linear pattern seen in mobile J2s. Scale bars = 10 µm.

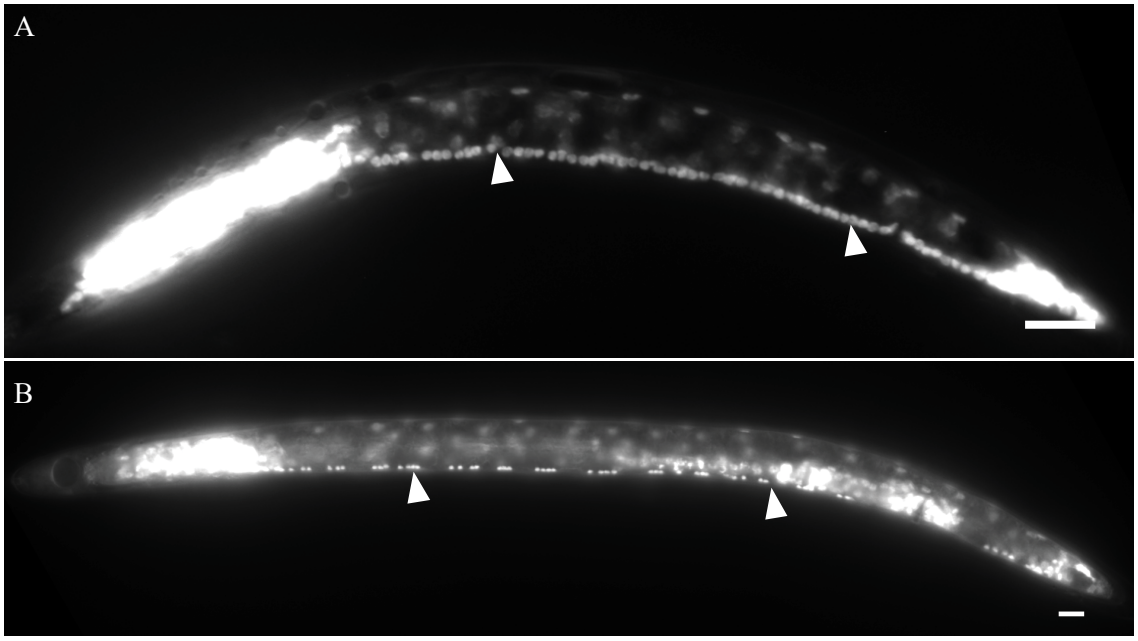

Figure 3.7. Motor neurons do not degenerate in the ventral nerve cord during *Pratylenchus penetrans* development. DAPI (4′, 6-diamidino-2-phenylindole) -stained mobile J2 (top) and mobile J4 molting female (bottom), respectively. VNC neuronal nuclei (arrowheads) are highly condensed fluorescent puncta. Scale bars = 10 µm

REFERENCES

Bird, A. F. (1967). Changes associated with parasitism in nematodes. I. Morphology and physiology of pre-parasitic and parasitic larvae of *Meloidogyne javanica*. *The Journal of Parasitology*, 53(4),768-776.

Chalfie, M., Sulston, J. E., White, J. G., Southgate, E., Thomson, J. N., & Brenner, S. (1985). The neural circuit for touch sensitivity in *Caenorhabditis elegans*. *Journal of Neuroscience*, *5*(4), 956-964.

Chitwood, B. G., & Chitwood, M. B. (1938). An Introduction to Nematology. Section I. Part II. *An Introduction to Nematology. Section I. Part II.*

Dong, L., Li, X., Huang, L., Gao, Y., Zhong, L., Zheng, Y., & Zuo, Y. (2013). Lauric acid in crown daisy root exudate potently regulates root-knot nematode chemotaxis and disrupts Mi-flp-18 expression to block infection. *Journal of Experimental Botany*, *65*(1), 131-141.

Dunn, R. A. (1973). Extraction of eggs of *Pratylenchus penetrans* from alfalfa callus and relationship between age of culture and yield of eggs. *Journal of Nematology*, *5*(1), 73.

Francis, R., & Waterston, R. H. (1991). Muscle cell attachment in *Caenorhabditis elegans*. *The Journal of Cell Biology*, *114*(3), 465-479.

Han, Z., Boas, S., & Schroeder, N. E. (2016). Unexpected variation in neuroanatomy among diverse nematode species. *Frontiers in Neuroanatomy*, *9*, 162.

Hastings, R. J. (1939). The biology of the meadow nematode *Pratylenchus pratensis* (de Man) Filipjev 1936. *Canadian Journal of Research*, *17*(2), 39-44.

Holterman, M., van der Wurff, A., van den Elsen, S., van Megen, H., Bongers, T., Holovachov, O., Bakker, J & Helder, J. (2006). Phylum-wide analysis of SSU rDNA reveals deep phylogenetic relationships among nematodes and accelerated evolution toward crown clades. *Molecular Biology and Evolution*, *23*(9), 1792-1800.

Jones, J. T., Haegeman, A., Danchin, E. G., Gaur, H. S., Helder, J., Jones, M. G., Kikuchi, T., Manzanilla López, R., Palomares Rius, J.E., Wesemael, W.M. & Perry, R. N. (2013). Top 10 plant-parasitic nematodes in molecular plant pathology. *Molecular Plant Pathology*, *14*(9), 946-961.

Koenning, S. R., & Wrather, J. A. (2010). Suppression of soybean yield potential in the continental United States by plant diseases from 2006 to 2009. *Plant Health Progress*, *10*.

Mclntire, S. L., Jorgensen, E., Kaplan, J., & Horvitz, H. R. (1993). The GABAergic nervous system of *Caenorhabditis elegans*. *Nature*, *364*(6435), 337.

Raski, D. J. (1950). The life history and morphology of the sugar-beet nematode, *Heterodera schachtii* Schmidt. *Phytopathology*, *40*(2), 135-152.

Rebois, R. V., & Huettel, R. N. (1986). Population dynamics, root penetration, and feeding behavior of *Pratylenchus agilis* in monoxenic root cultures of corn, tomato, and soybean. *Journal of Nematology*, *18*(3), 392.

Stretton, A. O. (1976). Anatomy and development of the somatic musculature of the nematode Ascaris. *Journal of Experimental Biology*, *64*(3), 773-788.

Stretton, A. O., Fishpool, R. M., Southgate, E., Donmoyer, J. E., Walrond, J. P., Moses, J. E., & Kass, I. S. (1978). Structure and physiological activity of the motor neurons of the nematode Ascaris. *Proceedings of the National Academy of Sciences*, *75*(7), 3493-3497.

Sulston, J. E., & Horvitz, H. R. (1977). Post-embryonic cell lineages of the nematode, *Caenorhabditis elegans*. *Developmental Biology*, *56*(1), 110-156.

Thapa, S., Patel, J. A., Reuter-Carlson, U., & Schroeder, N. E. (2017). Embryogenesis in the parasitic nematode *Heterodera glycines* is independent of host-derived hatching stimulation. *BMC Developmental Biology*, *17*(1), 2.

Triantaphyllou, A. C., & Hirschmann, H. (1960). Post infection development of *Meloidogyne incognita* Chitwood 1949 (Nematoda-Heteroderidae). In *Annales de l'Institut Phytopathologique Benaki*, 3 (1). 1-11.

van Megen, H., van den Elsen, S., Holterman, M., Karssen, G., Mooyman, P., Bongers, T., Bakkar, J & Helder, J. (2009). A phylogenetic tree of nematodes based on about 1200 full-length small subunit ribosomal DNA sequences. *Nematology*, *11*(6), 927-950.

Wang, C., Bruening, G., & Williamson, V. M. (2009). Determination of preferred pH for root-knot nematode aggregation using pluronic F-127 gel. *Journal of Chemical Ecology*, *35*(10), 1242-1251.

White, J. G., Southgate, E., Thomson, J. N., & Brenner, S. (1976). The structure of the ventral nerve cord of *Caenorhabditis elegans*. *Philosophical Transactions of the Royal Society B, 275*(938), 327-348.

Wyss, U., & Zunke, U. (1986). Observations on the behavior of second stage juveniles of *Heterodera schachtii* inside host roots. *Revue Nematol*, *9*(2), 153-165.

CHAPTER 4: PROLIFERATION OF STEM CELL-LIKE SEAM CELLS IS ASSOCIATED WITH THE EVOLUTION OF ATYPICAL BODY SHAPES IN SOME NEMATODES

ABSTRACT

How do body shapes evolve? The vast majority of nematode species have vermiform (worm-shaped) body plans throughout post-embryonic development. Within the phylogenetic clade comprising most plant-parasitic nematodes, the development of an atypical body shape has arisen at least twice. The plant-parasite Tylenchomorpha nematode *Heterodera glycines* hatches as a vermiform infective juvenile. Following infection and the establishment of feeding site *H. glycines* grows disproportionately greater in width than length, developing into a saccate shaped adult. Body size in *Caenorhabditis elegans* was previously shown to correlate with post-embryonic divisions of laterally positioned stem cell-like 'seam' cells and endoreduplication of the seam cell epidermal daughter. To test if a similar mechanism produces the unusual body shape of saccate parasitic nematodes, we compared seam cell development and epidermal ploidy levels of *H. glycines* to *C. elegans*. Finally, to study the evolution of body shape development, we examined seam cell development of four additional Tylenchomorpha species. First we confirmed the presence of seam cell homologs in *H. glycines*. We found that *H. glycines* adult female epidermis comprises a syncytium of approximately 1800 epidermal nuclei compared with the 139 nuclei in the primary epidermal syncytium of *C. elegans*. We found a significant association between *H. glycines* body volume and the number and ploidy level of epidermal nuclei. Furthermore, we found that while the saccate *M. incognita* seam cells also proliferate following infection; however, the pattern of division differed substantially from that seen in *H. glycines*. Interestingly, *R. reniformis* does not undergo increased seam cell proliferation during

its development into a saccate form. Our data reveal that seam cell development has undergone extensive evolutionary changes from *C. elegans* and that the proliferation of *H. glycines* epidermal nuclei and its ploidy level correlates with growth in size. Our finding of different seam cell division patterns in the independently evolved saccate species *M. incognita* and *H. glycines* provides an example of convergent evolution acting through homologous cells. However, *R. reniformis* does not demonstrate seam cell proliferation following infection suggesting distinct mechanisms evolved to produce a similar phenotype from a common ancestor. We hypothesize that *R. reniformis* may serve as an extant transitional model for the evolution of atypical body shapes.

Keywords: Soybean cyst nematode, Root-knot nematode, Reniform nematode, post-infection development, pyriform

INTRODUCTION

How do body shapes evolve? Most nematodes are vermiform (i.e. worm-shaped) throughout post-embryonic development. However, several diverse nematode species develop from a vermiform juvenile into saccate adult females. For example, females of the avian parasitic Tetrameridae family have a distended shape (Schmidt, 1962). Similarly, the shark-parasitic nematode *Phlyctainophora squali* develops into a coiled and globose female (Adamson et al., 1987). Among Tylenchomorpha nematodes, several of the most economically damaging plant-parasitic nematode species develop into saccate-shaped adult females following infection (Jones et al. 2013). *Heterodera glycines* hatches as a vermiform infective second-stage juvenile (J2). Following infection and the establishment of a feeding site *H. glycines* females grow disproportionately greater in width than length, developing into a saccate shaped adult. Male *H.*

glycines initially grow disproportionally in width following infection. During the final juvenile stage (J4), males remodel into a vermiform adult.

Not all saccate-shaped nematode undergo the same sequence of developmental events as *H. glycines.* The closely related species *Rotylenchulus reniformis* hatches as a vermiform J2. Interestingly, *R. reniformis* does not infect following hatching, but rather molts through subsequent juvenile stages without feeding. Upon molting into a vermiform adult female *R. reniformis* infects a host and subsequently develops into a saccate shaped and gravid female.

Based on the current hypothesized phylogeny of nematodes, development into saccate adults among Tylenchomorpha nematodes evolved at least twice **(Figure 4.1)** (Holterman et al., 2006; Van Megen et al., 2009). Similar to *H. glycines,* the independently evolved root knot nematodes, *Meloidogyne* spp. grow from a vermiform J2 into a saccate adult female following infection. Unlike *H. glycines,* much of the growth in *M. incognita* occurs prior to the molt into J3 that is quickly followed by the molts into J4 and adult female without intervening feeding. After molting into the adult, the female resumes feeding and further growth. The mechanisms regulating the development of saccate body shapes in nematodes are unknown.

In the bacterial-feeding nematode *Caenorhabditis elegans,* the epidermis is considered a major regulator of body size (Flemming et al. 2000). Most of the *C. elegans* epidermis comprises a single large syncytium (hyp 7) that grows during postembryonic development as a succession of nuclei fuse with it (Shemer and Podbilewicz, 2000). The postembryonic hyp 7 nuclei are daughters of the seam cells, a series of laterally positioned epidermal cells with stem cell-like properties (Sulston and Horvitz, 1977). Newly hatched J1 *C. elegans* have 10 seam cells on each lateral ridge that divide in a stem cell-like pattern before each molt **(Figure 4.2)** (Sulston and Horvitz, 1977). Most seam cell divisions generate an anterior daughter nucleus that fuses with

hyp 7 and a posterior daughter seam cell. Following the final molt, the seam cells terminally differentiate and fuse to form a separate syncytium (Sulston and Horvitz, 1977; Singh and Sulston 1976).

The evolution of nematode body size was suggested to be due to changes in seam cell proliferation and endoreduplication of nuclei within the epidermal syncytium (Flemming et al. 2000; Azevedo et al. 2000). However, a recent report demonstrated that a newly isolated *Caenorhabditis* species evolved increased length due to increased cytoplasmic volume rather than nuclear number or ploidy (Woodruff). We hypothesized that the *H. glycines* seam cell lineage has undergone extensive evolutionary changes to grow from a vermiform juvenile to a saccate adult female. To understand the evolution of the saccate-shaped nematode, we examined the development of the closely related *R. reniformis* and the independently-evolved saccate species *M. incognita.* As comparisons, we examined three Tylenchomorpha nematodes with typical vermiform shapes throughout development.

MATERIALS AND METHODS

Nematode cultures

H. glycines were isolated from a soybean field in Illinois, USA and maintained on susceptible soybean (cv. Macon) in the greenhouse. To collect synchronized developmental stages of *H. glycines,* soybean seeds were germinated in moist paper towels for three days. Soybean seedlings were then placed in pluronic gel F-127 with freshly hatched J2 for 24 hours (Wang et al, 2009). Soybean roots were washed gently with water to remove nematodes that had not infected roots within 24 hours of inoculation. Then *H. glycines*-infested roots were planted in

sandy loam soil and kept in a growth chamber at 22-24ºC and 12-hour light cycle until extraction. After inoculation, the infested roots were grown for 6-7 days to collect J3s, 9-10 days to collect J4s, 11-13 days for adult females, and 15 days for adult males (Dong et al, 2014). Infested roots were macerated with a hand blender to obtain *H. glycines* at specific time points. The mixture was poured over stacked 850, 250, and 25-µm-pore sieves. The developmental stage and sex of each individual was determined based on overall body size and gonad morphology (Raski, 1950).

Meloidogyne incognita (gift from Dr. Jason Bond) was originally isolated from soybean and maintained on tomato (cv. Rutgers) in the greenhouse. To collect synchronized developmental stages of *M. incognita*, two weeks old tomato seedlings were inoculated with freshly hatched J2s. Tomato seedlings were gently pulled from the soil and washed with water to remove nematodes that had not infected roots within 48 hours following inoculation. *M. incognita* infested roots were then planted in sandy loam soil and kept in a growth chamber at 22-24ºC and 12-hour light cycle until extraction. The nematodes were extracted using a hand blender to collect different developmental time points of the post-infective J2 stage from 6 -14 days after inoculation (Triantaphyllou and Hirschmann, 1960).

Rotylenchus reniformis (gift from Dr. Martin Wubben) was maintained in sandy loam soil on soybean (cv. Macon) in the greenhouse. To study the non-parasitic stages, eggs were incubated at 30ºC in a glass Petri dish. Different developmental stages were identified based on their morphology and number of cuticles (Bird, 1984). *R reniformis* parasitic adult females were extracted the same way as *H. glycines* post-infection stages using a hand blender.

Aphlenchus avenae was originally isolated from the rhizosphere of garlic plants and identified using morphological characters. *A. avenae* was cultured on 1/8 strength Potato

Dextrose Agar (PDA) with the fungus *Botrytis cinerea* (De Soyza, 1973). To collect the synchronized *A. avenae* eggs, gravid females were incubated in 5% M9 buffer (Stiernagle, 2006). After five hours, females were removed, and eggs were incubated at room temperature for approximately 48 hours for hatching. Freshly hatched J2s were transferred to 1/8 strength PDA with *B. cinerea.* Developmental stages were determined based on body size and gonad morphology.

Pratylenchus penetrans (gift from Dr. Terry Niblack) was cultured on corn root explants on Murashige and Skoog (MS) media (Rebois and Huettel, 1986). Specific developmental stages of *P. penetrans* were isolated by synchronizing populations from eggs. *P. penetrans* eggs were extracted as previously described (Dunn, 1973). Freshly hatched J2s were collected and placed on corn root explants on MS media. To recover the different developmental stages, the *P. penetrans* cultured plate was flooded with water for few hours, water was drained in a glass Petri dish, and animals were handpicked under dissecting scope. Developmental stages of *P. penetrans* were determined based on body size and gonad morphology.

Helicotylenchus sp. was isolated from soybeans at the University of Illinois research farm and maintained on soybean (cv. Macon) in sandy loam soil in the greenhouse. J4 molting stage animals were determined based on the presence of a shedding cuticle, body size, and gonad morphology.

Live nematode imaging

Nematodes were mounted on a 4% agarose pad on microscope slides incubated at room temperature in a dark humidity chamber when not imaging. Slides were rehydrated as needed. Images were taken after every hour for two days, using an upright compound microscope with a mechanized stage (Zeiss M2 AxioImager and Zen software). Seam cells were identified based on

their location and morphology (Sulston and Horvitz, 1977). At least four animals at each developmental stage were observed.

DAPI (4′, 6-diamidino-2-phenylindole) staining

H. glycines were fixed in Carnoy's fixative (60% ethanol, 30% acetic acid, 10% chloroform) overnight at room temperature (Hedgecock and White, 1985; Flemming, 2000). Nematodes were transferred to 75% ethanol and stained with 0.2–0.5 µg/ml of DAPI overnight in the dark at room temperature. Images were taken using a Zeiss M2 AxioImager with differential interference contrast (DIC) and fluorescence optics. In *C. elegans*, the epidermal nuclei are large and flat, contain large nucleoli, and located in four main cords (Sulston and Horvitz, 1977). The number of epidermal-like nuclei was counted between the metacarpus to anus. The number of epidermal nuclei counted on one side of the animal was doubled to estimate the total number of epidermal nuclei. To estimate the body volume of *H. glycines,* the length of the animal was measured from head to tail and the mean diameter was calculated from three separate measurements (close to the head, the middle part of the body and close to the tail) using FIJI. Volume was estimated based on the calculation of the volume of a cylinder during J2s and J3 and the shape of a sphere in adult females. At least six animals were examined for each developmental stage. The data were log transformed and regression analysis was performed using GraphPad Prism version 7.00 for Windows, GraphPad Software, La Jolla California USA, www.graphpad.com.

The ploidy level of *H. glycines* epidermal nuclei was calculated based on previous methods (Hedgecock and White, 1985; Flemming, 2000). DAPI stained sperm nuclei from adult males were used as a haploid control and included in each experimental session. Fluorescence intensity, exposure time, and all other microscope settings were kept consistent during imaging.

The fluorescence level of the epidermal nuclei and sperm nuclei were measured using ImageJ software. The nuclei of interest were marked and its integrated density (fluorescence in the area of the region of interest × the mean fluorescence of the region of interest) was measured. Than corrected fluorescence intensity was calculated by subtracting the background fluorescence (Fitzpatrik 2014). Eight male animals, eight J2 molting stages animals, and five J3 females, and 13 adult females were examined. In each animal, the fluorescence intensity of ten epidermal nuclei and ten neuronal nuclei was measured.

All other nematodes (*M. incognita, R. reniformis, A. avenae, P. penetrans,* and *Helicotylenchus* sp.) were fixed in Carnoy's fixative for two hours and then transferred to 50% methanol and stained with 0.2–0.5 µg/ml of DAPI overnight in the dark at room temperature until imaging. All images were captured with Zen software on a Zeiss M2 AxioImager with DIC and fluorescence optics and examined in FIJI using ImageJ software. To examine the correlation between body volume and the number of epidermal nuclei among different nematode species, young adult females of *M. incognita* and *R. reniformis,* and J4 molting females of *A. avenae*, *P. penetrans* and *Helicotylenchus* sp. were examined. Nematodes body shapes were considered as a cylinder, and the measurements were taken similarly as in *H. glycines* and the number of epidermal nuclei was counted. At least five animals were examined in each species. The data was log transformed. Regression analysis was performed using GraphPad Prism version 7.00 for Windows, GraphPad Software, La Jolla California USA, www.graphpad.com. Unlike Flemming et al. (2000) we present the number of nuclei as the estimated total number rather than that found on one side of the body. To analyze if *H. glycines* body size and the product of number of epidermal nuclei and ploidy level we compared the *H. glycines* data with the 95% prediction interval from the Flemming et al. (2000) regression model.

Phalloidin staining

Nematodes were fixed in 4% paraformaldehyde overnight at 4°C and washed three times with water. Nematodes were placed in a 3 mm Petri dish and cut open with a 1.2 mm × 25 mm BD precision glide needle (Becton, Dickinson, and Company). Nematodes were then transferred to phalloidin (5-7 unit/ml; Thermo Fisher Scientific) and DAPI (0.2-0.5 μg/ml; Thermo Fisher Scientific) and incubated overnight in the dark at room temperature. The images were taken using a confocal microscope (Zeiss LSM 880 Airyscan) and analyzed using ImageJ software.

Electron microscopy

Synchronized developmental stages of *H. glycines* were collected from soybean roots and stored overnight at 4°C. High-pressure freezing and freeze substitution were modified from previous methods used for *C. elegans* (Han et al. 2018). Metal specimen carriers were coated with 1-hexadecene and a layer of *E. coli* strain OP50. Nematodes were loaded into carriers with 20% bovine serum albumin and frozen in an HPM 010 high-pressure freezer. Freeze substitution was performed in 2% OsO_4 (Electron Microscopy Sciences) and 0.1% uranyl acetate (Polysciences) in 2% H_2O and 98% acetone in an FS-8500 freeze substitution system. Samples were kept at -90°C for 110 hours before being warmed to -20°C over five hours. Samples were then kept at -20°C for 16 hours before being warmed to 0°C over five hours. Samples were washed four times in pre-chilled 100% acetone at 0°C. The last wash was one hour. Samples were then transferred to room temperature and washed two times in 100% acetone. Samples were infiltrated with 1:1 Polybed812 (Polysciences) resin:acetone for 24 hours, 2:1 resin:acetone for 36 hours, 100% resin for 24 hours, and then changed to fresh resin for three days. All infiltration steps were conducted on an orbital shaker at room temperature. Samples were then submerged into embedding molds with resin and hardener and baked at 60°C for two days. 70

nm sections were collected using a PowerTome PC ultramicrotome with a diamond knife and collected onto formvar-coated copper slot grids. Sections were imaged with a Phillips CM200 TEM (Han et al. 2018).

RESULTS

The number of *H. glycines* epidermal nuclei increases following infection: To test if the number of epidermal nuclei increases during development from vermiform J2 to saccate adult female, we examined DAPI stained *H. glycines* at different developmental stages. In pre-infective *H. glycines* J2s there were 44 epidermal nuclei **(Figure 3A)**. Post-infection, the number of epidermal nuclei increases tremendously, 544 in J3 females, 972 in J4 females and 1758 in adult females **(Table 4.1), (Figure 3B)**. The number of epidermal nuclei increases approximately 40 folds from pre-infective J2 to adult female **(Table 4.1)**. In comparison to typical shape *C. elegans,* which has 139 epidermal nuclei (Shemer and Podbilewicz, 2000), saccate shape *H. glycines* adult female has 1752 epidermal nuclei. In nematodes, the variation in the number of epidermal nuclei among nematodes is due to changes in seam cell lineages (Flemming et al. 2000; Azevedo et al. 2000). Thus, we checked for the presence of seam cells in *H. glycines.*

***H. glycines* has seam cell homologs:** The *C. elegans* seam cell divisions contribute to an increase in the total number of nuclei present in the surrounding syncytial epidermis (hyp7) during post-embryonic development (Sulston and Horvitz, 1977). We first asked if seam cell homologs exist in *H. glycines.* The *C. elegans* seam cell have a distinctive eye-shaped appearance using DIC optics; however, due to the highly refractile optical properties of the pre-infective *H. glycines* J2s we were not able to observe any seam cell-like structures. We therefore examined TEM micrograph sections of pre-infective J2s. Similar to *C. elegans* seam cells, we

found electron-dense adherens junctions on each lateral side along the length of *H. glycines* J2 **(Figure 4.4A)**, (Koppen et al. 2001). Within two days post-infection, the refractile optical properties of *H. glycines* J2 using DIC are reduced and we observed a line of elliptical smoothly tapered epidermal cells along the lateral epidermis from the nose to tail **(Figure 4.4B)**. These epidermal cells are morphologically similar to *C. elegans* seam cells (Sulston and Horvitz, 1977). Similar to J1 *C. elegans*, we observed ten seam cells on each side of J2 *H. glycines.* Specifically, we found three seam cell nuclei in the head (one adjacent to the stylet, one adjacent to the metacarpus; one adjacent to the dorsal esophageal gland). Posteriorly, six seam cells lay along the length of the body and a tenth was found in the tail **(Figure 4.4C)**. Thus, using both light microscopy and TEM, we confirmed that *H. glycines* also has seam cells.

***H. glycines* seam cells undergo extensive proliferation following infection and subsequent molts:** We hypothesized that growth of *H. glycines* following infection requires proliferation of the seam cells. As *H. glycines* spends much of its development within the roots of its host, we are unable to follow the cell lineage as it progresses. As an alternative, we dissected nematodes from the roots and examined the seam cells in both live and fixed, DAPI-stained animals at multiple time points following infection. Using DIC optics, we found that, following infection the posterior eight seam cells are in contact with each-other **(Figure 4.5A and B).** Within three days following infection, all seam cells other than the one adjacent to the stylet **(Figure 4.5D)** undergo symmetrical cell division **(Figure 4.5C and D)**. During the J2 stage, these nine seam cells underwent one symmetrical **(Figure 4.6A)** and at least three asymmetrical divisions **(Figure 4.6B-C)**, each seam cell produced four-epidermal daughter cells (seam cell progenitor cells) **(Figure 4.6D)**, oriented dorsoventrally during late J2 stage. In the J2/J3 molt we observed only elliptical shaped nuclei **(Figure 4.6E** pointed with arrow) along the

lateral epidermis and all seam progenitor nuclei migrate dorsoventrally **(Figure 4.6E)**. By the J2/J3 molt, we found on average 246 epidermal nuclei, which was 6 fold more than in pre-infective J2s.

Using DAPI staining, we found that the J3/J4 and J4/adult female molts are each associated with a round of seam cell proliferation and subsequent migration of epidermal daughter nuclei from the lateral epidermis **(Figure 4.7A and B)**. This molt-associated proliferation is similar to that seen in *C. elegans;* however, *C. elegans* seam cells do not divide during the adult molt (Sulston and Horvitz, 1977). In *H. glycines,* the molts were preceeded by an initial proliferation along the lateral ridge and accumulation of daughter cells that was followed by dispersal in the subdorsal and subventral regions. Interestingly, each subsequent round of divisions appeared to produce more daughter cells than the previous.

The proliferation of seam cells during the J3/J4 and J4/adult molts did not occur in a perfectly synchronous pattern. This combined with the difficulties in synchronizing infection, made it impossible to quantify the precise number of daughter cells produced by each seam cell at these later time points. We found that *H. glycines* J3 and J4 females have 544 and 972 epidermal nuclei, respectively **(Table 1)**. In each successive molt, seam cell proliferations almost doubled the number of epidermal nuclei along the lateral epidermis **(Table 1)**. After the final molt, 1758 epidermal nuclei were evenly distributed in an adult female **(Table 1)**, **(Figure 4.3B**), compared with 139 in adult *C. elegans* (Shemer and Podbilewicz, 2000). In short, *H. glycines* seam cells after infection underwent first symmetrical division and multiple asymmetrical divisions by the J2/J3 molt. The number of asymmetrical divisions increases in each successive molts **(Figure 4.8)**.

***H. glycines* has an epidermal organization similar to *C. elegans*:** Most of the post-embryonic *C. elegans* epidermis comprises a multinucleate syncytium that surrounds the lateral seam cells (Podbilewicz and White, 1994). To determine if the *H. glycines* epidermis has a similar organization, we stained post-infective nematodes with the F-actin binding fluorescent probe phalloidin. In phalloidin stain animals, we observed bright fluorescence surrounding each nuclei within the lateral seam, but none in the surrounding epidermis suggesting a similar epidermal syncytial organization to *C. elegans* **(Figure 4.9A, B, C).** To confirm this observation, we examined post-infective juveniles with TEM and found a cluster of nuclei on the lateral margins with distinct cell membranes (Figure 4.9D). This cluster of seam cells was surrounded by a larger epidermal area with periodic nuclei not interrupted with apparent cell membranes (Figure 4.9D). Together, these data suggest that *H. glycines* seam cells are surrounded by an epidermal syncytia.

***H. glycines* male seam cells proliferate less than females:** Similar to J3 females, *H. glycines* J3 males are sausage-shaped. Interestingly, we found that *H. glycines* J3 male seam cells proliferate less than in females **(Figure 4.10A, Figure 4.7A)**. Unlike in J3 females, where seam daughter cells migrate dorsoventrally, in *H. glycines* J3 males, they remain in the lateral epidermis **(Figure 4.10A)**. Using phallodin stain we found that *H. glycines* male seam cells is also surrounded by syncytium like females **(Figure 4.9B)**. By the time of the J3/J4 molt, *H. glycines* males begin remodeling back to a vermiform where they become coiled within the old cuticle **(Figure 4.10B**). Due to the coiling of male J4s and background fluorescence from sperm cells in adults, we were unable to accurately quantify the number of epidermal nuclei **(Figure 4.10C).** Moreover, in live adult male animals it was difficult to locate the position of seam cells because *H. glycines* males have a tendency to lay with a twist in its body.

***H. glycines* epidermal nuclei are polyploid:** In addition to the number of epidermal nuclei, the ploidy of epidermal nuclei is also associated with the nematode body size (Flemming et al. 2000). *C. elegans* epidermal nuclei are polyploid (Flemming et al. 2000; Hedgecock and White, 1985). We measured the DNA content of *H. glycines* epidermal nuclei during the J2/J3 molt, J3 females, and adult females using microdensitometry methods. We found that *H. glycines* epidermal nuclei are polyploid **(Figure 4.11)**. To ensure our methods are reliable, we compared haploid sperm nuclei fluorescent intensity to likely diploid neuronal nuclei (C being haploid DNA content) **(Figure 4.11A)**. The ploidy level of epidermal nuclei during the J2/J3 molt was 8C **(Figure 4.11B)**. By late J3, the ploidy level of the epidermal nuclei in females had increased to 10C **(Figure 4.11C)**. Strikingly, the ploidy level of adult female was 7.7C **(Figure 4.11D)**. While there was substantial variation among individuals, overall our data suggests that *H. glycines* epidermal nuclei are polyploidy.

***H. glycines* number and ploidy level of epidermal nuclei is associated with its body size:** To check if the increasing number of epidermal nuclei and ploidy level at each successive molt have correlation with the increasing body size at different developmental stages of *H. glycines*, we did regression analysis. We found a significant correlation between the number of epidermal nuclei and the estimated body volume ($R^2 = 0.91$; $P < 0.0001$) at different developmental stages (pre-infection J2, J2/J3 molt, J3 and adult female), **(Figure 4.12A)**. Furthermore, we found significant correlation between the product of number and ploidy level of epidermal nuclei and the estimated body volume ($R^2 = 0.86$; $P < 0.0001$) of *H. glycines* at different developmental stages **(Figure 4.12B)**. Our results demonstrate that the growth of *H. glycines* from a vermiform J2 to a saccate adult female is associated with the extensive proliferation of the seam cells and polyploidy. In comparison to the *C. elegans* seam cell lineage,

which contributes 139 nuclei to the epidermal syncytium (Shemer and Podbilewicz, 2000), the *H. glycines* female seam cell lineage contributes 1758 epidermal nuclei.

***H. glycines* number and ploidy level of epidermal nuclei does not fit in a published model on bacterial feeder vermiform nematodes body size:** Flemming et al. (2000) examined 12 free-living nematode species of the order Rhabditia and proposed that nematode body size is correlated to the product of the number and ploidy of epidermal nuclei. We mapped the data from *H. glycines* onto the previously proposed regression line (Flemming et al., 2000). Interestingly, we found *H. glycines* lay outside of 95% prediction interval in their regression model for vermiform species **(Figure 4.13)**. This indicates, saccate shaped *H. glycines* may have different method of body size evolution.

Because *H. glycines* lay outside the prediction interval established by Flemming et al (2000), we were curious whether this was due to a clade-wide change in the relationship of epidermal nuclei and ploidy to body size. We, therefore, examined the number and ploidy of epidermal nuclei in vermiform species within other Tylenchomorpha species. The *Helicotylenchus* sp. (family Hoplolaimidae) is a sister group to *H. glycines* Heteroderidae **(Figure 4.1)**, it is vermiform throughout its life cycle. We observed seam cells along the lateral epidermis, morphologically similar to *H. glycines* and *C. elegans,* in *Helicotylenchus* sp. **(Figure 4.14A**), (Sulston and Horvitz, 1977). We found that J4 female *Helicotylenchus* sp. contained 194 epidermal nuclei with a ploidy of 3.4C. Similarly, in *Aphelenchus avenae*, the intraclade outgroup vermiform species (Figure 4.1), we observed seam cells along the lateral epidermis morphologically similar to *H. glycines* and *C. elegans* **(Figure 4.14B)**, (Sulston and Horvitz, 1977). Furthermore, in J4 female *A. avenae*, we found only 220 epidermal nuclei and 3.3C in J4 females. Together, these data suggest that the epidermal proliferation of *H. glycines* was not due

to an earlier evolutionary event leading to a general increase in epidermal nuclei in all species within the Tylenchomorpha.

Divergent division patterns acting on conserved seam cells gave rise to independently evolved saccate body shapes: Saccate body shapes evolved multiple times among nematodes. To determine if the saccate shape in other nematodes is also correlated with seam cell proliferation, we examined the independently evolved saccate nematode *M. incognita* **(Figure 4.1)**. We hypothesized that, despite their independent origins *H. glycines* and *M. incognita* would use a similar pattern of seam cell proliferation to increase the number of epidermal nuclei and ploidy level associated with their increased volumes. To determine if the number and ploidy of epidermal nuclei is associated with an independently-derived saccate body form, we examined the young adult females of *M. incognita*. We counted 598 epidermal nuclei and a mean ploidy level of 4.67C in *M. incognita*. As a closely related vermiform control **(Figure 4.1)**, we found that *Pratylenchus penetrans* J4 females have 100 epidermal nuclei. Due to background fluorescence in *P. penetrans,* we were unable to accurately measure the ploidy level in this species. Our results suggest that, similar to *H. glycines*, *M. incognita* proliferation of epidermal nuclei is associated with a saccate body shape.

Unlike *H. glycines,* which grows throughout each juvenile stage, much of the growth in *Meloidogyne* spp. occurs during J2 following infection with very little increase in size occurring during the J3 and J4 stages (Triantyphylou and Hirschmann, 1960). Similar to *H. glycines* we found that J2 *M. incognita* extracted soon after infection have a line of epidermal cells along the lateral seam morphologically similar to *H. glycines* and *C. elegans* seam cells (Sulston and Horvitz, 1977), **(Figure 4.15A)**. To further examine the proliferation of epidermal nuclei in *M. incognita,* we conducted an analysis of DAPI stained juveniles at successive time points

following infection. In late J2s, we observed 240 epidermal nuclei **(Figure 4.15B)**. Following the J2/J3 molt, we did not observe a clustering of nuclei along the lateral ridge as observed during *H. glycines.* Interestingly, staining with phalloidin revealed putative cell junctions in the subventral and subdorsal quadrants and an unusual pattern of cell junctions along the lateral seam **(Figure 4.16A)**. While our time points are insufficient to propose a comprehensive model of epidermal division in *M. incognita,* the pattern of divisions appears to deviate substantially from *H. glycines*.

***R. reniformis* does not use seam cell proliferation method to increase their body size:** *R. reniformis* is a saccate-shaped nematode and phylogenetically proximal to *H. glycines* **(Figure 4.1)**. Unlike *H. glycines,* the adult female of *R. reniformis* is the infective stage and becomes saccate following infection. The mature saccate *R. reniformis* female is smaller in volume compared with *H. glycines*. We, therefore, hypothesized that *R. reniformis* would have an intermediate number of nuclei between *H. glycines* and *Helicotylenchus* sp. Similar to *H. glycines* and *C. elegans,* we found a line of laterally positioned epidermal nuclei consistent with seam cells **(Figure 4.17)**, (Sulston and Horvitz, 1997). Amazingly, the *R. reniformis* adult parasitic female has only 50 epidermal nuclei and a ploidy level of 5.2C. We conducted a time-course analysis, but did not observe any epidermal divisions following infection. Rather, we observed swelling of the body occurred adjacent to and concurrent with the enlarging gonad **(Figure 4.18)**. This result suggests that epidermal proliferation is not strictly required for the development of a saccate body shape.

Atypical body shape in nematodes is not strictly associated with the number or ploidy level of epidermal nuclei: We examined the relationship between the body volume and the number and ploidy level of epidermal nuclei across species (*H. glycines*, *M. incognita*, *R.*

reniformis, *A. avenae*, and *Helicotylenchus* sp.). We found no significant association between the estimated body volume and the product of number and ploidy level of epidermal nuclei across species ($R^2 = 0.22$; $P = 0.41$), **(Figure 4.19A)**. This finding, while contradictory to Flemming et al (2000), is in agreement with recent results showing a large size difference between *C. elegans* and a newly described *Caenorhabditis* sp. that does not correlate with changes in epidermal nuclear number or ploidy (Woodruff et al., 2018). We mapped *A. avenae* and *Helicotylenchus* sp. data onto the previously proposed regression line (Flemming et al., 2000). Interestingly both vermiform species lay within the 95% prediction interval in their regression model, but very close to the border **(Figure 4.13)**.

DISCUSSION

Our results suggest that the stem cell-like seam cells are conserved in the Tylenchomorpha nematodes. Similar to *C. elegans,* we found that the lateral ridge of *H. glycines* comprises elliptical-shaped cells with proliferative capacity. Furthermore, using TEM we observed characteristic adherens junctions along the lateral ridge in transverse sections. Using light microscopy, we found similar cells in all nematodes examined here. While we did not conduct TEM on other species, an examination of published and unpublished data suggests that adherens junctions along the later ridge are also present in *Meloidogyne incognita* and *Pratylenchus penetrans* (Endo, 1997). Seam cells are present in bacterial feeding nematodes *Panagrellus redivivus* and *Pristionchus pacificus* (Sternberg and Horvitz, 1982). Similarly, the seam cells were found in a group of diverse bacterial feeding nematodes (Flemming et al, 2000). We hypothesize that seam cells have been conserved within the crown clades of Chromadoria (Holterman et al., 2006; Van Megen et al., 2009).

We show that epidermal proliferation is extensive in *H. glycines.* Most *C. elegans,* seam cell divisions lead to the formation of a single Hyp 7 epidermal nucleus and a posterior seam cell (Sulston and Horvitz, 1977). In contrast, we found that seam cell proliferation in *H. glycines* increases at each successive molt **(Figure 4.7)**. Occasionally, the *C. elegans* seam lineage leads to the formation of glia or neuronal daughters. For example, the seam cell V5 leads to the formation of the post-deirid neurons prior to the L2 molt. Due to the parasitic nature of *H. glycines* development we were unable to follow the precise lineage; however, we did not observe DAPI-stained nuclei with a neuron-like morphology.

Our results may suggest that epidermal proliferation and the increase in epidermal ploidy causes the increase in body volume of *H. glycines*. We found a strong correlation between the product of epidermal nuclear number by ploidy and the body volume. Interestingly, we also found that the marked sexual dimorphism in *H. glycines* is represented by the different number of epidermal nuclei found during the J3 stages of each sex. The primary control strategy for *H. glycines* is host resistant. *H. glycines* females are smaller on resistant varieties than susceptible (Noel et al. 1983). It will be interesting to know if this size difference is due to decreased seam cell proliferation or epidermal ploidy.

A question our data still does not answer is why epidermal proliferation in *H. glycines* does not simply lead to long vermiform nematodes that grow proportionally in length and width? In *C. elegans*, the elongation of embryos beyond the twofold stage requires the contraction of body wall muscles (Williams and Waterston, 1994). Ablation of *C. elegans* body wall muscle leads to swelling around the destroyed cells (Plunkett et al., 1996). We recently demonstrated that *H. glycines* and *M. incognita* undergo progressive muscle atrophy with the onset of the sedentary life cycle (Han et al. 2018).This atrophy corresponds with the increase in size. We

speculate that in *H. glycines* and *M. incognita,* the atrophy of body wall muscles following infection prevents the maintenance of a vermiform shape by eliminating the lengthening forces found in other nematodes.

Body size in nematodes was considered to have evolved based on the number of epidermal nuclei and their ploidy (Flemming et al. 2000). Our data do not strictly fit that model. While we found a significant correlation between these the number and ploidy of epidermal nuclei and *H. glycines* body size during post-embryonic development, our *H. glycines* data lay outside of the 95% prediction interval proposed by Flemming et al. (2000). Indeed, based on the number and ploidy of epidermal nuclei in adult *H. glycines* females, the predicted body volume should be 100-fold greater than found. We previously showed that the *H. glycines* increases in thickness following infection (Han et al., 2018). Also, post-infective *H. glycines* secrete exudates from the cuticle that are proposed to originate from the thickened epidermis (Endo, 1993). Perhaps rather than increased body volume, the unexpectedly large number of epidermal nuclei and increased ploidy in *H. glycines* may be used to provide increased epidermal thickness and protein synthesis.

Our results suggest that multiple mechanisms may lead to a saccate body shape. Similar to *H. glycines, M. incognita* undergoes extensive epidermal proliferation and epidermal polyploidy. However, the apparent organization of seam cells differs from that observed in *H. glycines.* The presence of phalloidin-stained structures similar to seam cells in the subdventral and subdorsal quadrants of *M. incognita* in post-infective stages could point to the formation of a separate seam cell pool. This will require further examination using both additional light microscopy and TEM. As *H. glycines* and *M. incognita* likely evolved into saccate shapes independently, we suggest that this serves as an example of parallel evolution where a similar

parasitic environment led to selection for increased proliferation on the seam cells through distinct mechanisms.

The evolution from vermiform to saccate nematode may have occurred through an intermediate transitional stage as represented by *R. reniformis,* which showed no obvious epidermal proliferation. The increase in *R. reniformis* body volume from vermiform to saccate is substantially smaller than that found in *H. glycines. H. glycines* produces more offspring than *R. reniformis* (Turner and Subbotin, 2006; Robinson et al. 1997) and it is generally accepted that saccate nematodes have a greater reproductive potential than vermiform species. We observed that the swelling of *R. reniformis* began proximal to the growing gonad. We speculate that the increased fecundity of saccate nematodes began with the evolution of a larger gonad size similar to *R. reniformis.* This was followed by proliferation of the epidermis allowing for larger gonads with additional reproductive capacity. This hypothesis will require extensive examination of saccate species from additional clades.

TABLE AND FIGURES

Table 4.1. The total number of epidermal nuclei on *Heterodera glycines* epidermis at different developmental stages.

Developmental stages	No. of epidermal nuclei	Sample size	Range
Pre infective-J2	44	11	40-48
J3 female	544	7	492-656
J4 female	972	7	750-1194
Adult female	1758	6	1436-2020

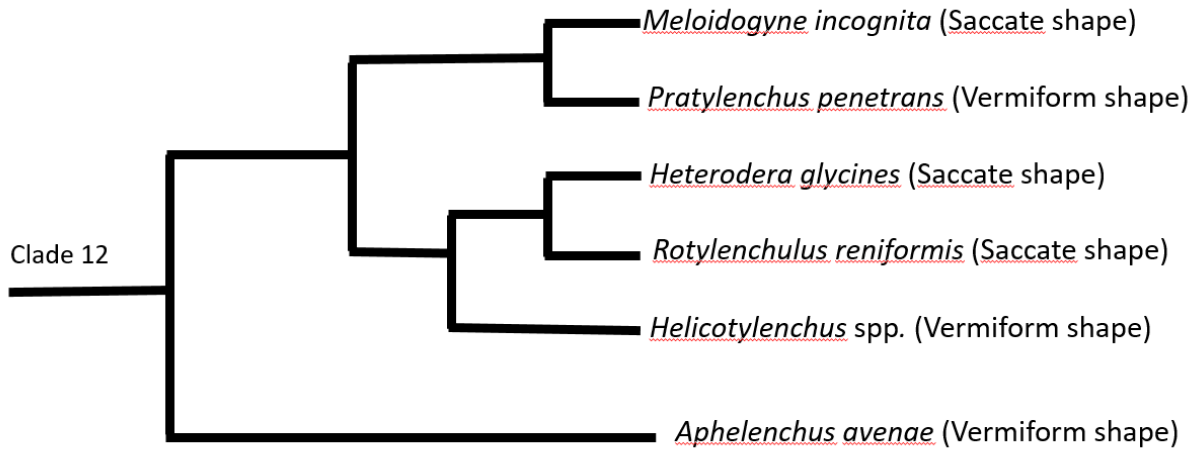

Figure 4.1. Phylogeny of the genera of nematode discussed in this study. The phylum nematode is currently divided into 12 clades (van Megan et al. 2009).

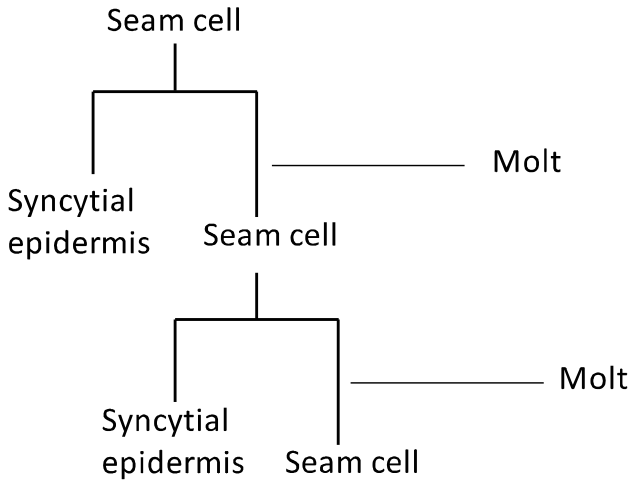

Figure 4.2. *Caenorhabditis elegans* seam cell divide once during each molt. Most seam cell divisions generate an anterior daughter cell that fuses with the hyp 7 (syncytium in *C. elegans*) and a posterior daughter cell that becomes a seam cell division during each molt (Sulston and Horvitz 1997; Shemer and Podbilewicz, 2000).

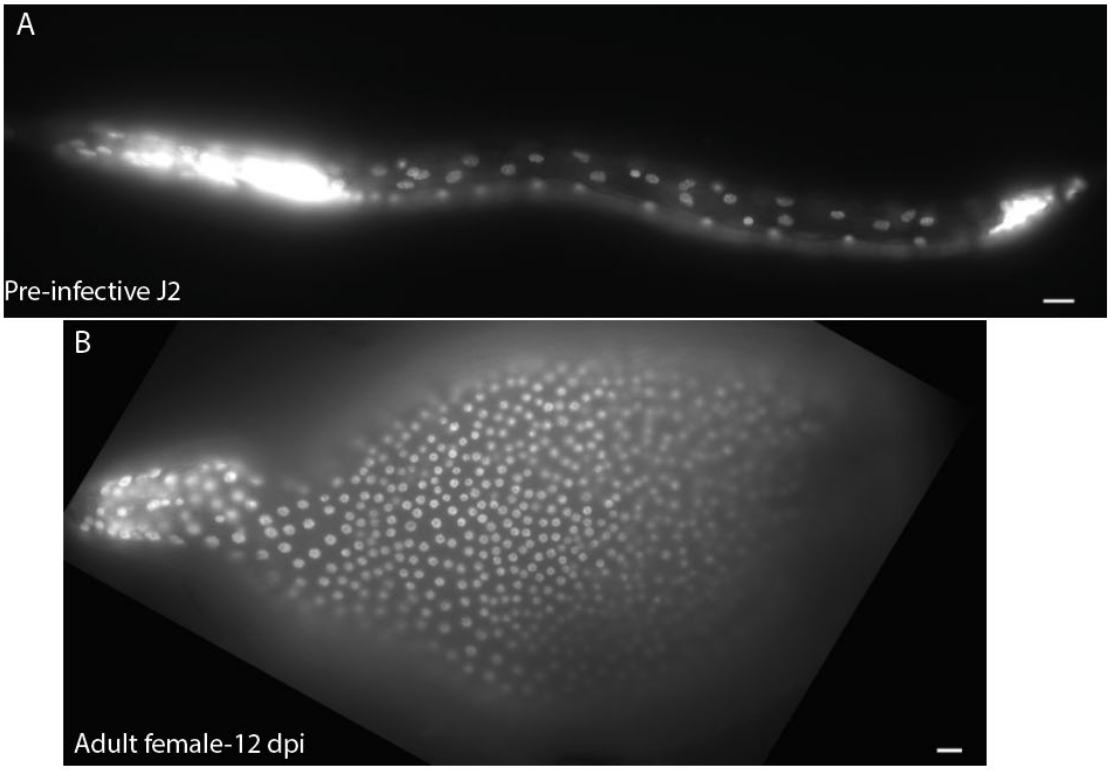

Figure 4.3. *Heterodera glycines* number of epidermal nuclei increases tremendously post-infection. Lateral view of DAPI micrographs (A) pre-infective J2; (B) adult female. Scale bars = 10 µm.

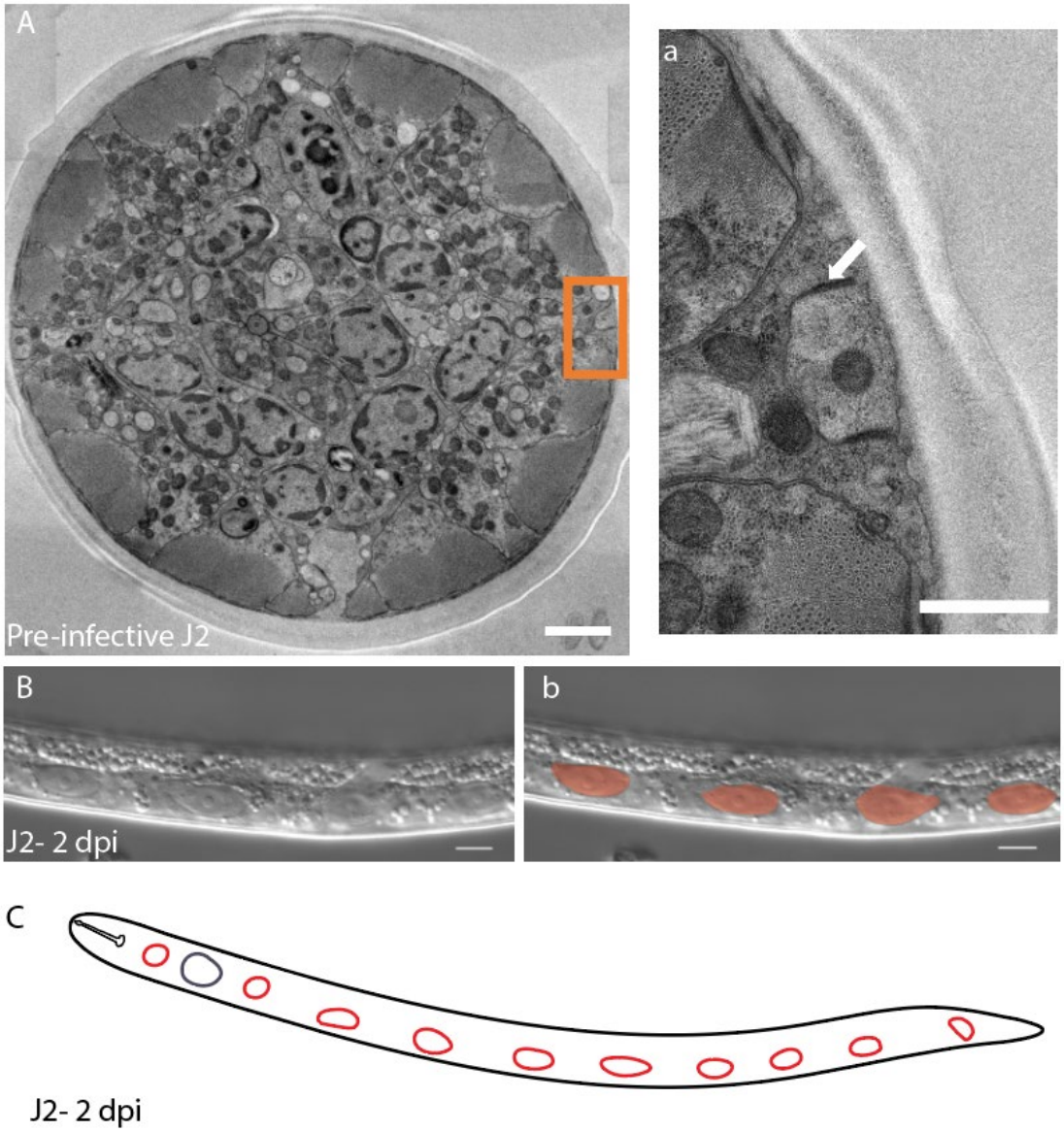

Figure 4.4. *Heterodera glycines* has seam cell homologs. (A) A cross-section TEM micrograph of pre-infective J2. (a) High magnification on the lateral side of the cross-section, arrow indicate electron-dense adherence junctions of seam cell enclosing a nuclei. (B) DIC micrograph of two days post-infection (dpi) J2 with a line of elliptical smoothly tapered epidermal cells along the lateral epidermis. (b) Pseudo orange color overlays on seam cells. (C) Cartoon represents of a two dpi J2 with 10 seam cells along the lateral epidermis (Three in the head, adjacent to the stylet, adjacent to the metacarpus; adjacent to the dorsal esophageal gland; Six along the length of the body; Tenth in the tail). Both TEM image and light microscopy confirmed *H. glycines* has seam cells similar to *C. elegans* (Sulston and Horvitz, 1977). Scale bars = TEM (A)-2 µm; TEM (a)-500 µm DIC-10 µm.

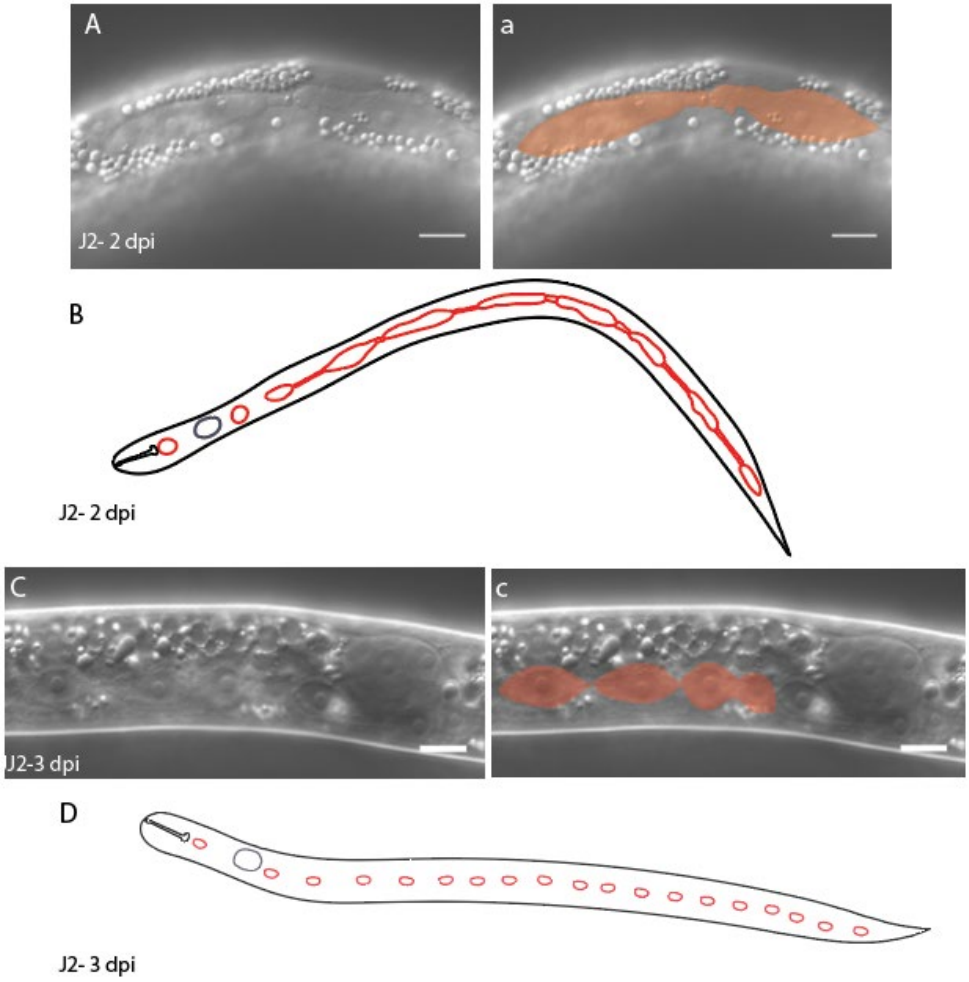

Figure 4.5. DIC micrographs of lateral epidermis of *Heterodera glycines* showing seam cell connection and symmetrical division in J2s post-infection. (A) J2 two days post-inoculation (dpi) showing seam cells making contact with each-other, (a) Pseudo orange color overlays on two connected seam cells. (B) Cartoon represent of (A), expect two seam cells over the head, seam cells are connected. (C) J2 three (dpi) showing seam cells after symmetrical division, (c) Pseudo orange color overlays on seam cells. (D) Cartoon represent of (C), showing seam cells after symmetrical division, other than the anterior. Scale bars = 10 µm.

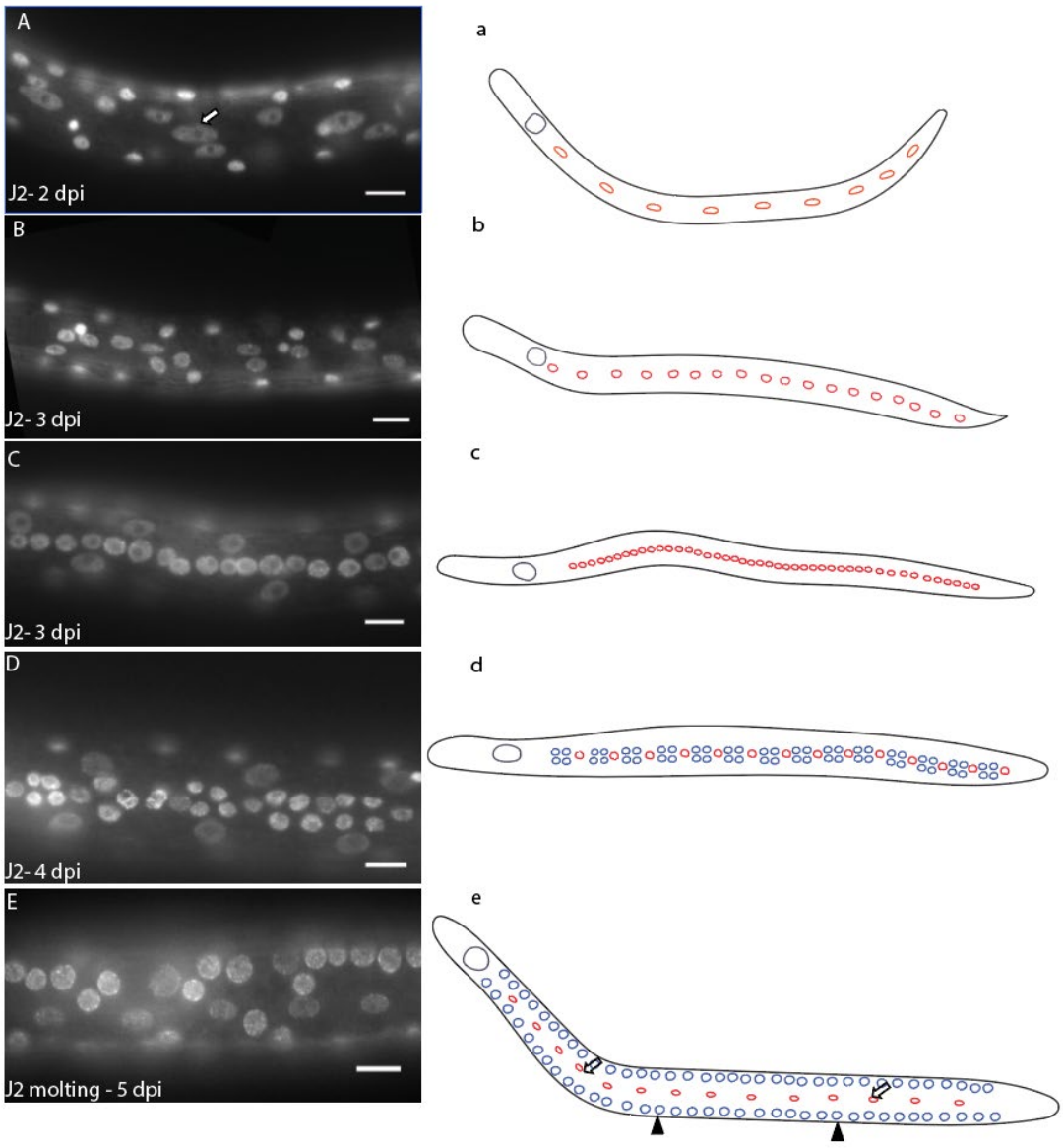

Figure 4.6. DAPI micrographs of lateral epidermis of *Heterodera glycines* showing selected seam cell divisions during post-infection J2 stages. (A) J2 two days post-inoculation (dpi) shows the flat epidermal seam cell nuclei, (a) cartoon represent of the animal (A) showing all seam nuclei other than the most anterior in the head. (B) J2 three (dpi) shows first symmetrical division, (b) cartoon represent of the animal (B) showing all seam nuclei after first symmetrical division. (C) J2 three (dpi) underwent few asymmetrical division producing more epidermal nuclei, (c) cartoon represent of (C). (D) J2-close to molt, four (dpi) by this stage each seam cell nuclei produced four epidermal nuclei (seam progenitor nuclei) oriented dorsoventrally, (d) cartoon represents of (D). (E) J2 molting stage animal, five (dpi) all seam progenitor nuclei migrated dorsoventrally (arrowheads in cartoon represent, e), only elliptical shape seam nuclei stay along the lateral epidermis (arrows in cartoon represent, e). Scale bars = 10 µm.

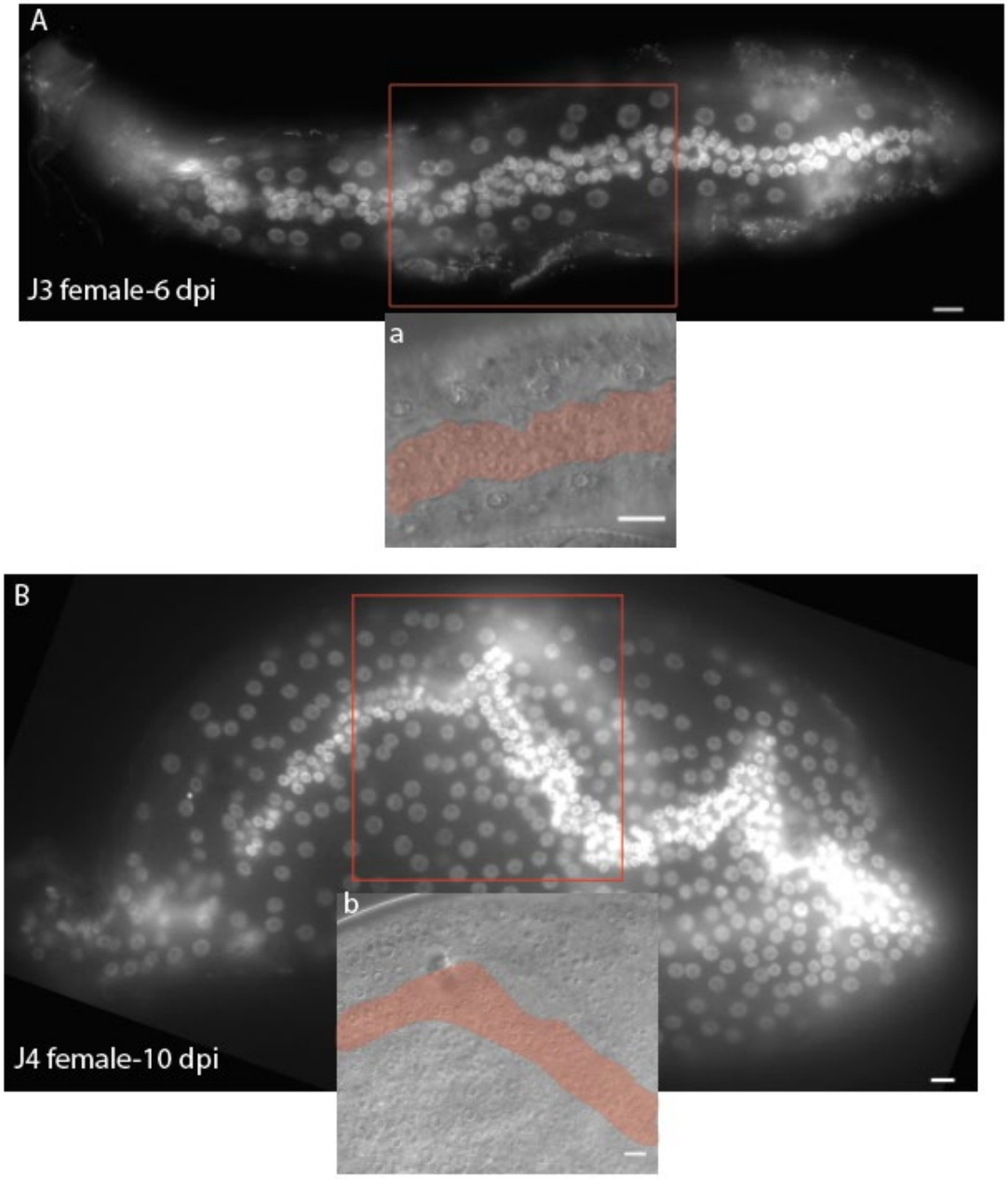

Figure 4.7. DAPI micrographs of lateral epidermis of *Heterodera glycines* showing seam cell proliferations in molting females. (A) J3 female six days post-inoculation (dpi) showing seam cells proliferations, (a) DIC overlays of the same animal. (B) J4 female ten days dpi has more epidermal nuclei along the lateral epidermis than in J3 female, (b) DIC overlays of the same animal. (C) Adult female 12 days dpi, epidermal nuclei evenly distributed. Scale bars = 10 µm.

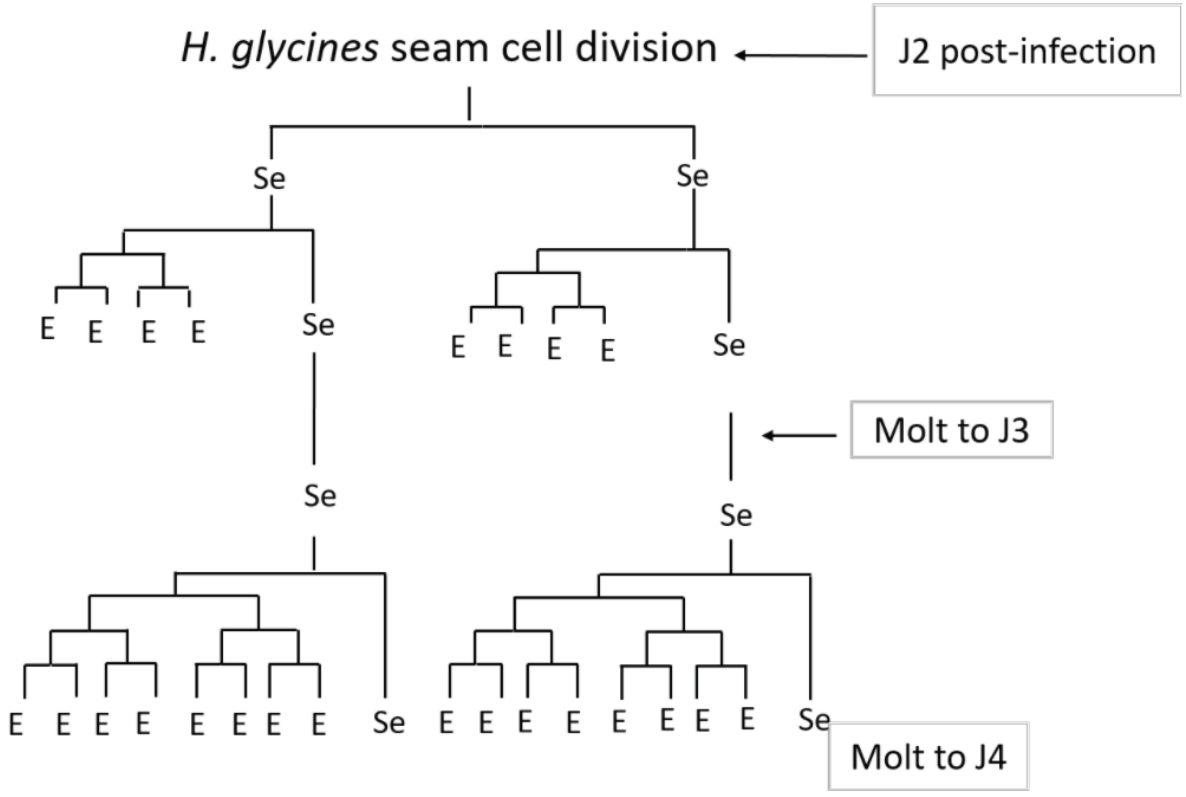

Figure 4.8. Working model of *Heterodera glycines* female seam cell division post-infection. Both live and DAPI stained animals were examined. In J2 stage post-infection first seam cells divide symmetrically, than underwent few asymmetrical division before J2 molting stage. In *Caenorhbditis elegans* seam cells divide once during each molt (Sulston and Horvitz, 1997). The number of asymmetrical division increases during each successive molt. After the final molt approximately 1800 epidermal nuclei were produced in *H. glycines* in comparison to 140 in *C. elegans* (Shemer and Podbilewicz, 2000).

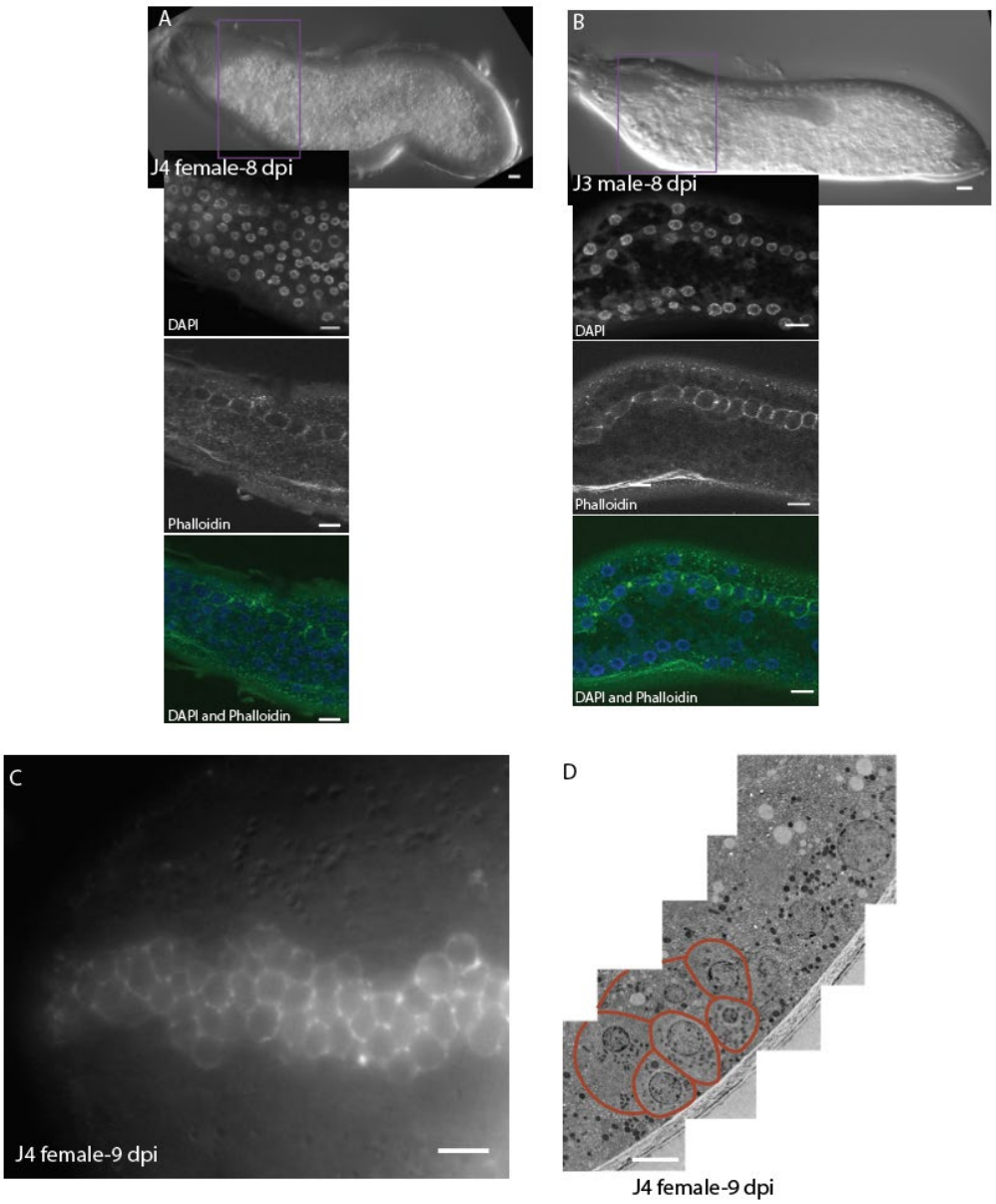

Figure 4.9. *Heterodera glycines* epidermis is a syncytium like *Canorhdbitis elegans.* **(A)** DIC micrograph of seven days post infection (dpi) early J4 female stained with both Phalloidin and DAPI. Phalloidin is an actin binding stain and can marked actin-enriched cell membrane. Phalloidin fluorescence was observed surrounding each nucleus within the lateral seam, but none in the surrounding epidermis. DAPI, a nuclear stain showed the presence of nuclei all over the epidermis. (B) DIC micrograph of seven dpi J3 male stained with both Phalloidin and DAPI. Similar to female phalloidin fluorescence was observed surrounding each nucleus within the lateral seam, but none in the surrounding epidermis. (C) Fluorescent micrographs of phalloidin-stained nine dpi female with phalloidin fluorescence within the lateral seam. (D) TEM micrograph of nine dpi female with a cluster of nuclei on the lateral margins with distinct cell membranes. Scale bars = DIC, DAPI, Phalloidin micrographs-10 µm; TEM-200 µm.

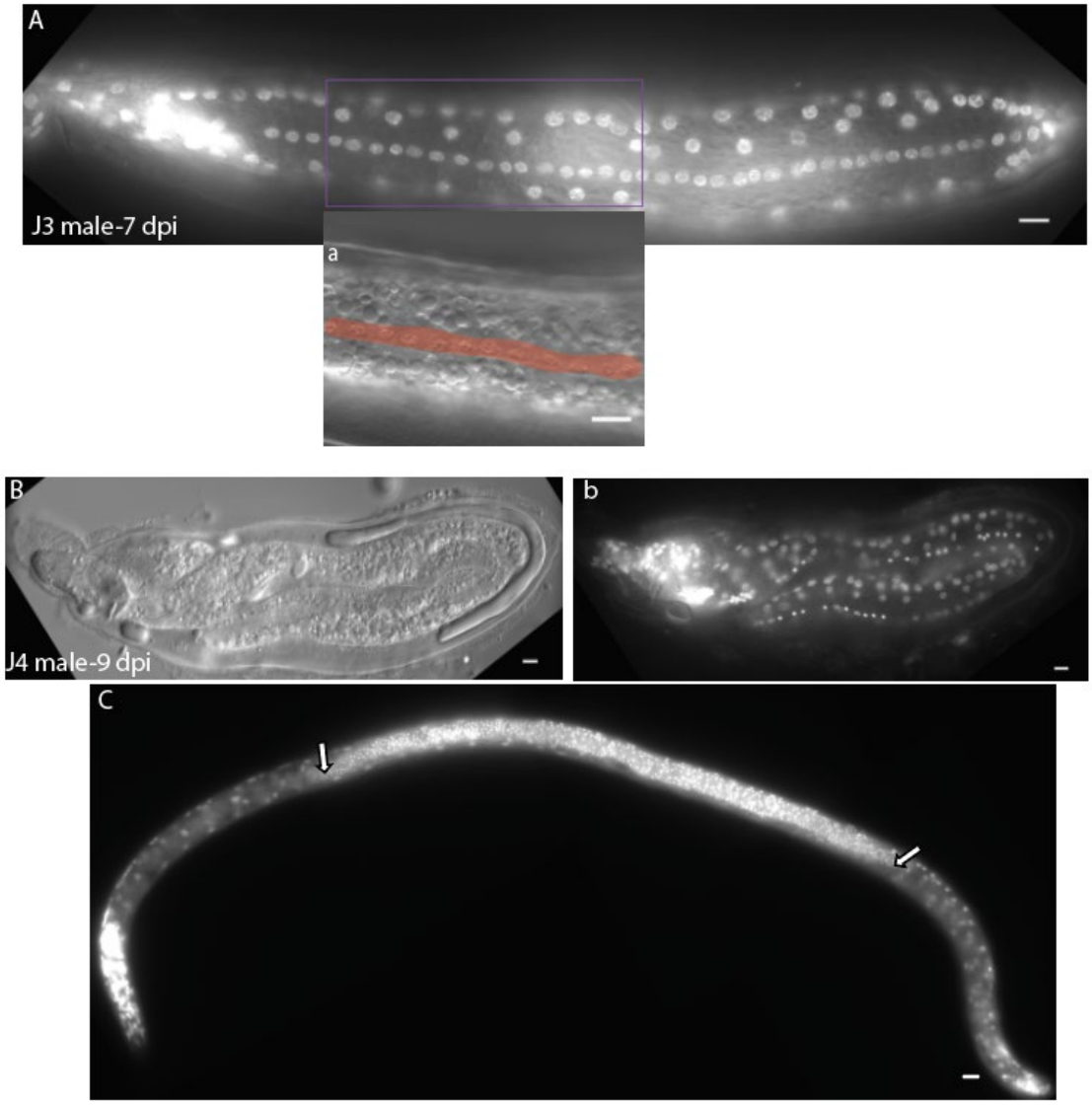

Figure 4.10. *Heterodera glycines* male seam cells proliferate less than females. (A) Lateral view of DAPI stained fluorescent micrograph of J3 male seven days post-infection (dpi). Nuclei along the lateral side are produced during J3 stage through seam cell division, (a) DIC overlay micrograph of (A) with orange pseudo color along the lateral line. (B) DIC micrograph of a nine dpi vermiform shape J4 female coiled within the old cuticle, (b) DAPI micrograph of the same animal, epidermal nuclei was difficult to follow because of the coiling. (C) DAPI stained fluorescent micrograph of the adult male with bright fluorescence from the sperm nuclei, make it hard to follow epidermal nuclei in adult male. Scale bars = 10 µm.

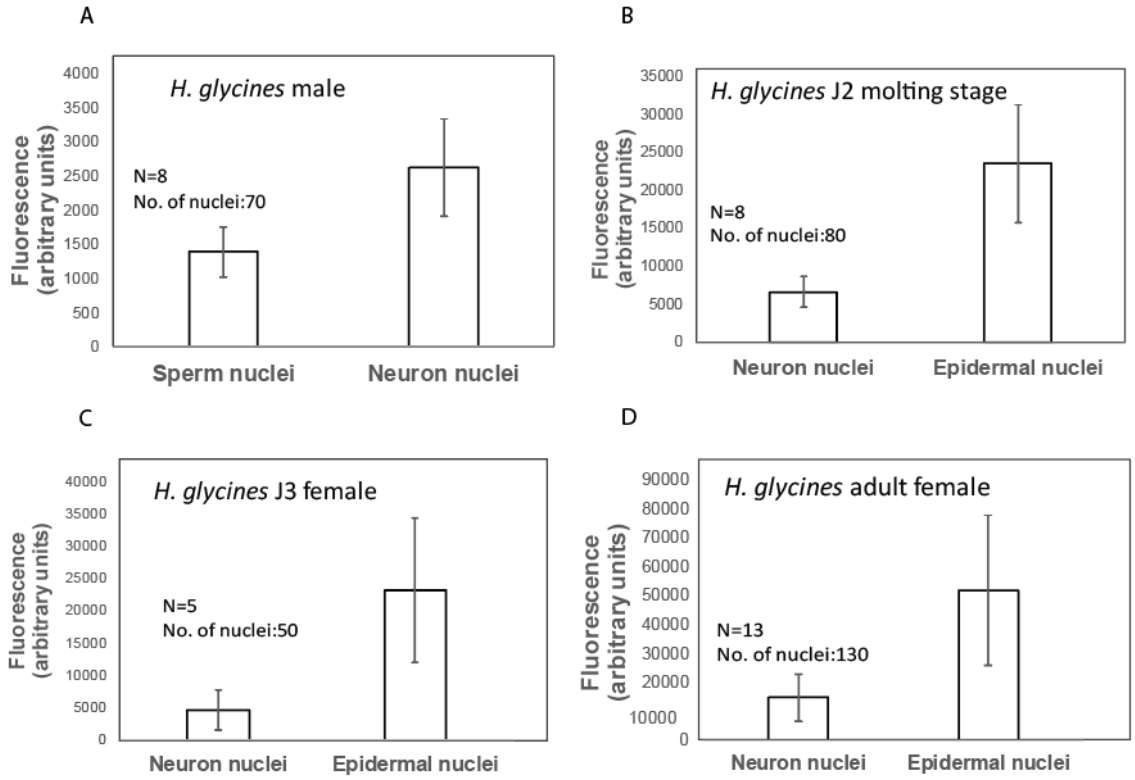

Figure 4.11. *Heterodera glycines* epidermal nuclei are polyploid. The DNA content of the *H. glycines* epidermal nuclei of J2 molting staged animals, J3 females, and adult females was measured in DAPI stained animals using microdensitometry methods. (A) In male animals, the ratio of fluorescence intensity measured in sperm nuclei and neuronal nuclei was approximately 2, neuronal nuclei are diploid (2C). (B). In J2 molting stage animals, the DNA content of epidermal nuclei was 4C. (C) In female J3 stage the DNA content of epidermal nuclei was 10C. (D) The DNA content of adult female was 7.7C.

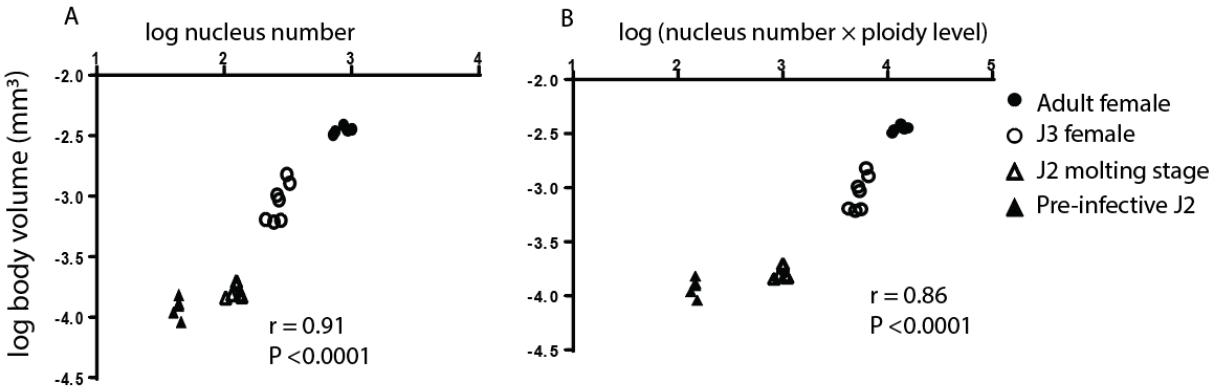

Figure 4.12. *Heterodera glycines* number and ploidy level of epidermal nuclei is correlated to its body size at different stages of development (pre-infective J2, molting stage, J3 female and adult female). The shape of pre-infective J2, J2/J3 molt s and J3 female animals were considered as a cylinder and adult female as a sphere to estimate their body volume. The number of epidermal nuclei counted on one side was doubled to get total count. (A) The significant correlation between the estimated body volume and the number of epidermal nuclei at different developmental stages ($R^2 = 0.91$; $P < 0.0001$). (B) The significant correlation between the estimated body volume and the product of the number of epidermal nuclei and the ploidy level at different developmental stages ($R^2 = 0.86$; $P < 0.0001$).

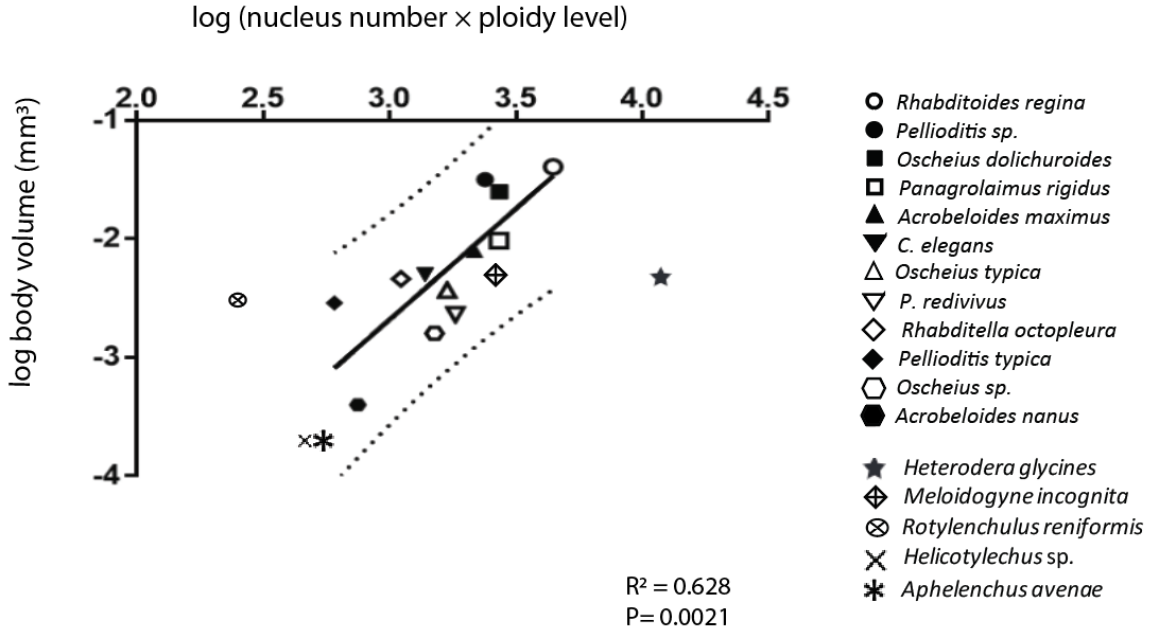

Figure 4.13. The tylenchomorpha body size relation with the product of the number and ploidy level of epidermal nuclei do not fit in the regression model given for vermiform nematode species (Flemming et al. 2000). The number of epidermal nuclei given by Flemming et al. 2000 for each nematode species was doubled to get the total count and ran a regression with 95% prediction interval. *Heterodera glycines* lay outside the 95% prediction interval in their regression model for vermiform species suggests that the number and ploidy level of the epidermal nuclei may regulate other aspects of the development.

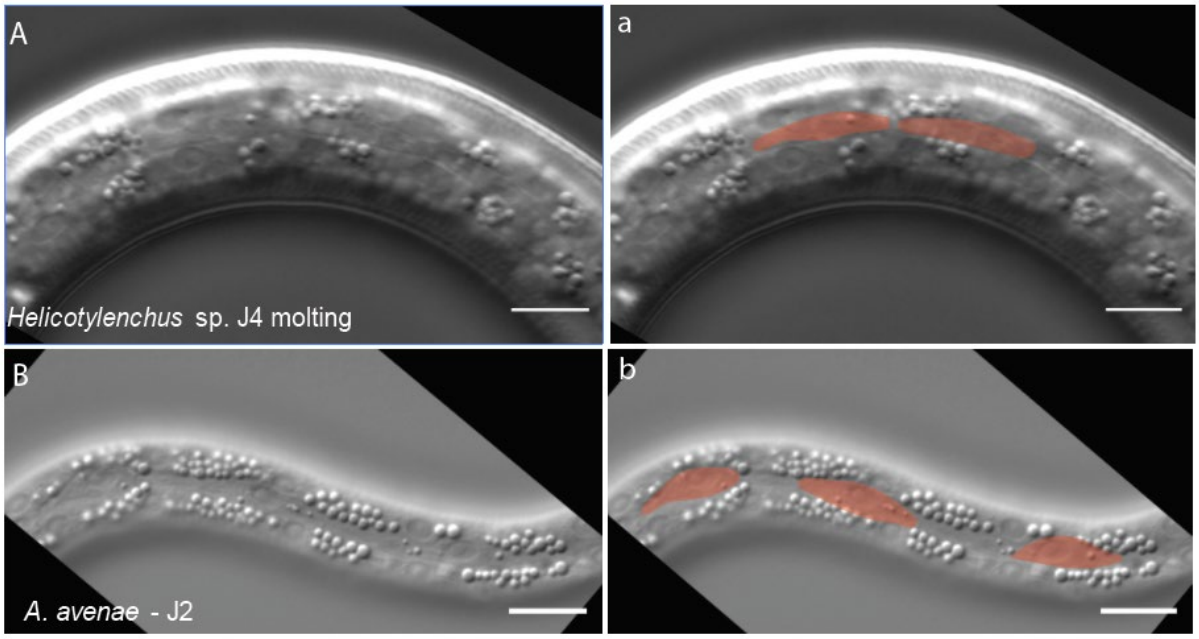

Figure 4.14. *Helicotylenchus* sp. and *Aphelenchus avenae* has seam cell homologs. (A) Lateral view DIC micrograph of J4 molting stage *Helicotylenchus* sp**.** with a line of elliptical smoothly tapered epidermal cells along the lateral epidermis, (a) Pseudo orange color overlays on seam cells. (B) Lateral view DIC micrograph of J2 stage *A. avenae* with a line of elliptical smoothly tapered epidermal cells along the lateral epidermis, (b) Pseudo orange color overlays on seam cells. Seam cells morphology on both species is similar to *C. elegans* (Sulston and Horvitz, 1977).Scale bars = 10 µm.

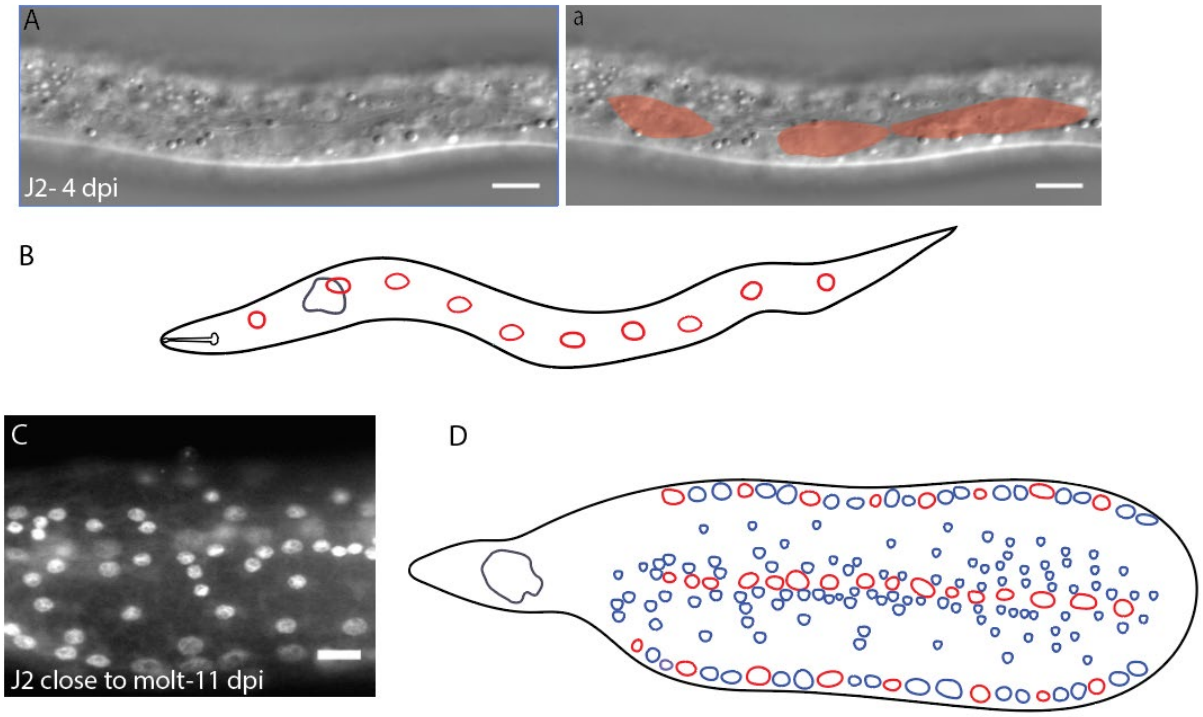

Figure 4.15. *Meloidogyne incognita* has seam cell homologs. These seam cells proliferates post-infection. (A) Lateral view DIC micrograph of a J2 four days post-infection (dpi) with a line of elliptical smoothly tapered epidermal cells along the lateral epidermis, (a) Pseudo orange color overlays on seam cells. (B) The cartoon represents of animal (A) showing ten seam cells along the lateral epidermis. (C) DAPI micrograph of lateral epidermis of late J2 11 dpi animal, (D) The cartoon represents of animal (C). *M. incognita* has seam cells morphologically similar to *C. elegans* (Sulston and Horvitz, 1977). Scale bars = 10 µm.

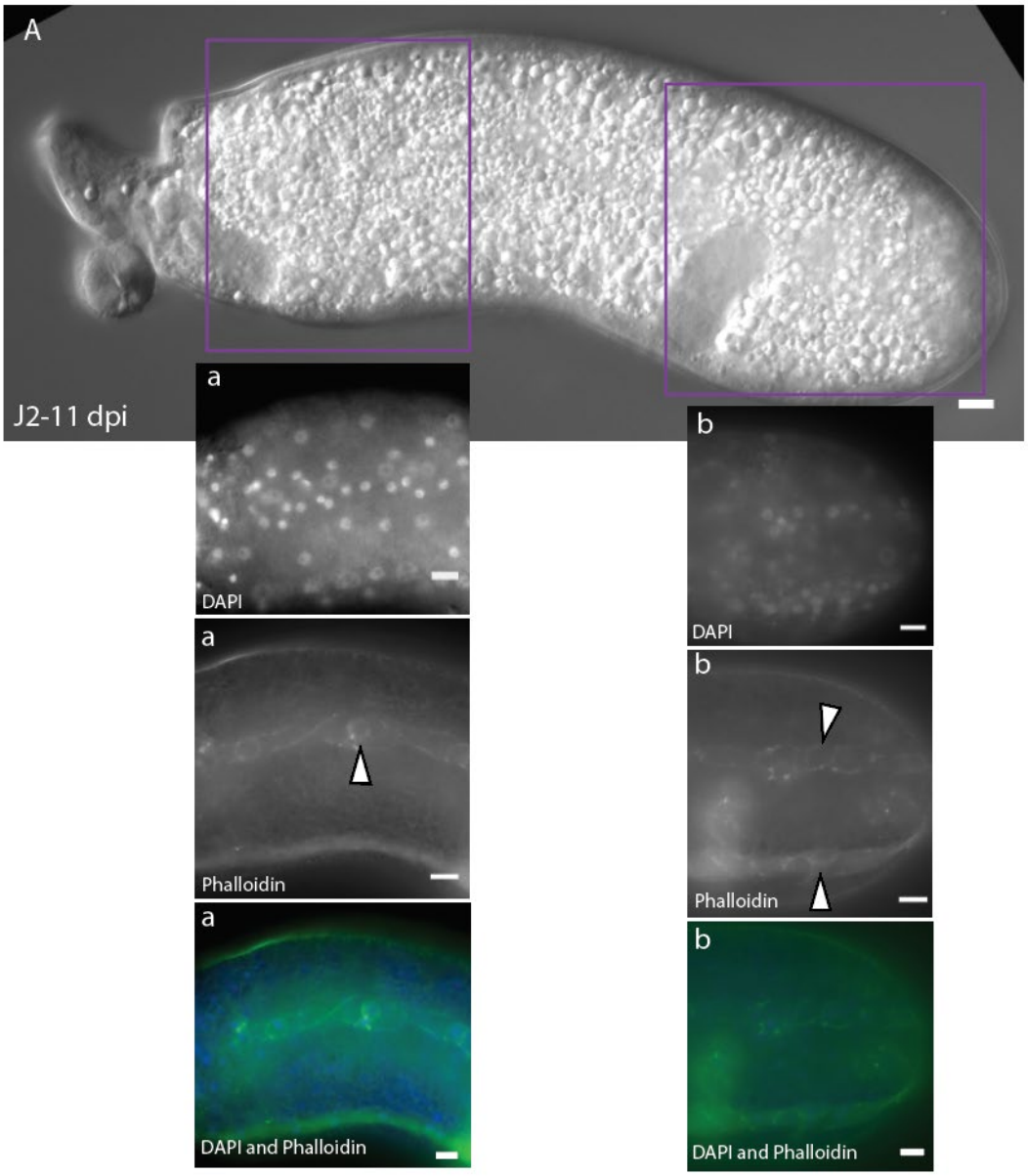

Figure 4.16. *Meloidogyne incognita* seam cell division followed different pattern than *Heterodera glycines*. (A) DIC micrograph of 11 days post-infection (dpi) J2 stained with both Phalloidin and DAPI. Phalloidin is an actin binding stain and can marked actin-enriched cell membrane. Phalloidin fluorescence was observed surrounding each nucleus within the lateral seam, but none in the surrounding epidermis. DAPI, a nuclear stain showed the presence of nuclei all over the epidermis, (a) The anterior part of the animal (A), (b) The posterior part of the animal, arrowheads pointed phalloidin fluorescence along the subventral and subdorsal cords. In *H. glycines* phalloidin fluorescence was observed only along the lateral seam. Scale bars = 10 µm.

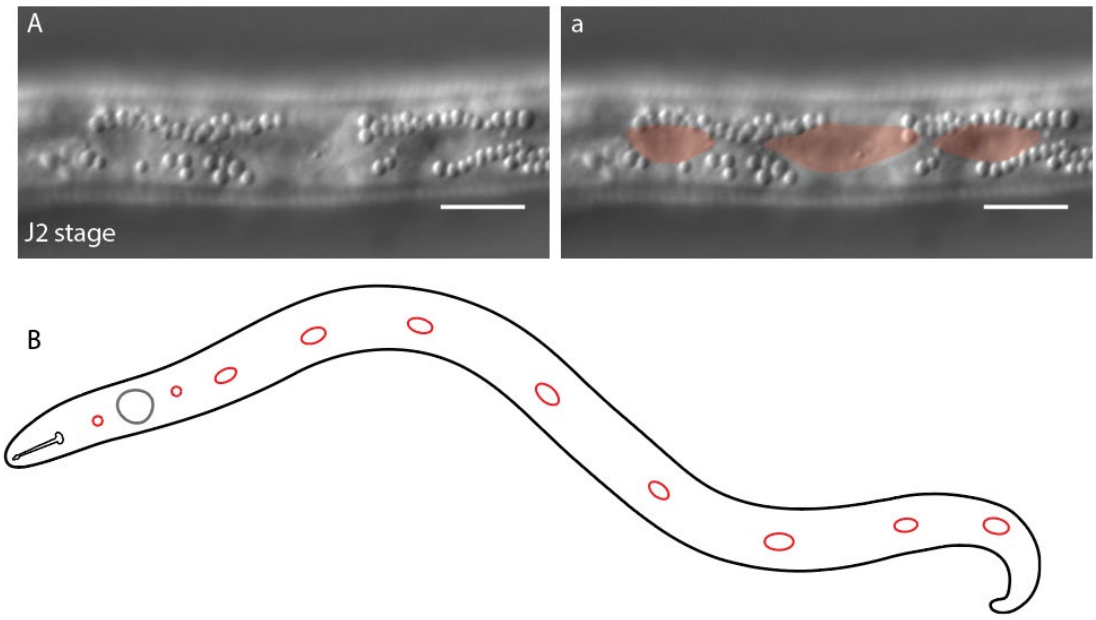

Figure 4.17. *Rotylenchulus reniformis* has seam cell similar to *H. glycines*. (A) Lateral view DIC micrograph of a J2 stage animal with a line of elliptical smoothly tapered epidermal cells along the lateral epidermis, (a) Pseudo orange color overlays on seam cells. (B) The cartoon represents of animal (A) showing ten seam cells along the lateral epidermis. *R. reniformis* has seam cells morphologically similar to *C. elegans* (Sulston and Horvitz, 1977). Scale bars = 10 µm.

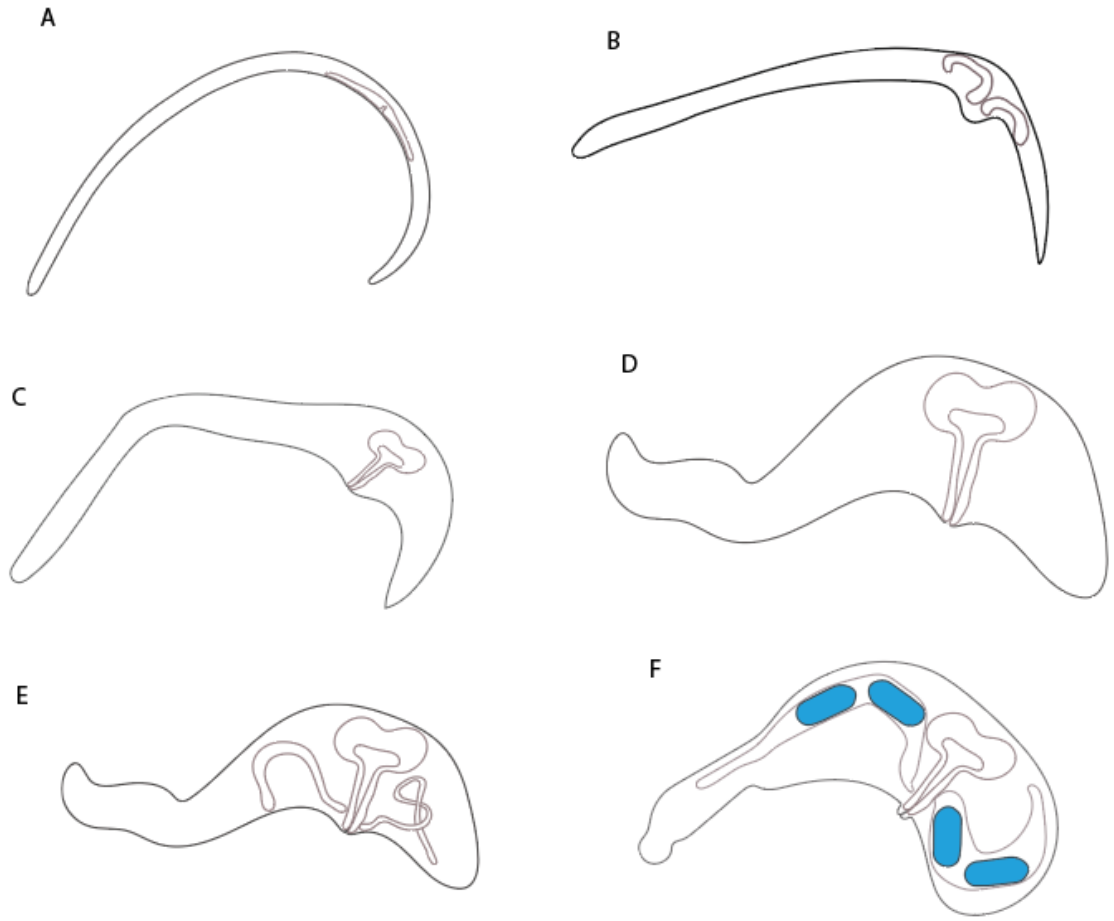

Figure 4.18. *Rotylenchulus reniformis* female gonad growth correlates with their body swelling or shape change. We conducted a time-course analysis using both DIC and DAPI stained animals and drew cartoon represents of the growing gonads. (A) Pre-parasitic adult female. (B-E) Different phases of gonad growth in parasitic adult females after infection. (F) Adult reproductive female with four eggs inside.

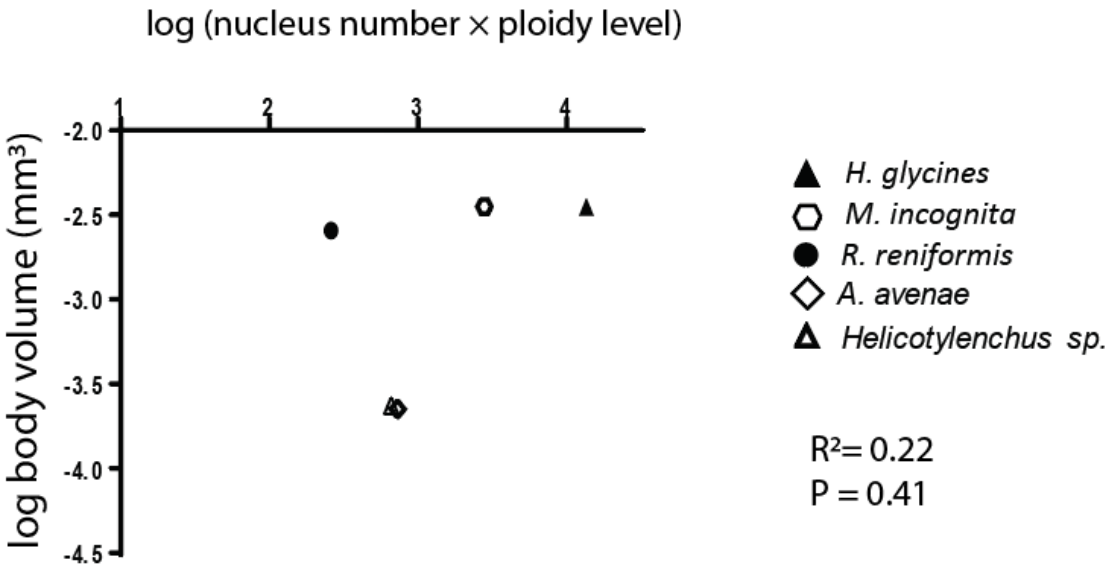

Figure 4.19. Atypical body shape in nematodes is not strictly associated with the number or ploidy level of epidermal nuclei. (A) There is no significant association between estimated body volume and the product of number of epidermal nuclei and ploidy level across species (*Heterodera glycines*, *Meloidogyne incognita*, *Rotylenchulus reniformis*, *Aphelenchus avenae*, and *Helicotylenchus* sp.) ($R^2 = 0.22$; $P = 0.41$).

REFERENCES

Adamson M. L., Deets G. B. & Benz G. W. 1987. Description of the male and redescription of female *Phlyctainophora squuli* Mudrey and Dailey, 1969 (Nematoda; Dracunculoidea) from elasmobranchs. *Canadian Journal of Zoology* 65: 30063010.

Azevedo, R. B., Cunha, A., Emmons, S. W., & Leroi, A. M. (2000). The demise of the platonic worm. *Nematology*, *2*(1), 71-79.

Bird, A. F. (1984). Growth and moulting in nematodes: Moulting and development of the hatched larva of *Rotylenchulus reniformis*. *Parasitology*, *89*(1), 107-120.

De Soyza, K. (1973). Energetics of *Aphelenchus avenae* in monoxenic culture. *Proceedings of the Helminthological Society of Washington*, *40*, 1-10.

Dong, L., Li, X., Huang, L., Gao, Y., Zhong, L., Zheng, Y., & Zuo, Y. (2013). Lauric acid in crown daisy root exudate potently regulates root-knot nematode chemotaxis and disrupts Mi-flp-18 expression to block infection. *Journal of Experimental Botany*, *65*(1), 131-141.

Dunn, R. A. (1973). Extraction of eggs of *Pratylenchus penetrans* from alfalfa callus and relationship between age of culture and yield of eggs. *Journal of Nematology*, *5*(1), 73.

Endo, B. Y. (1993). Ultrastructure of cuticular exudates and related cuticular changes on juveniles in *Heterodera glycines*. Journal of the Helminthological Society of Washington (USA).

Fitzpatrick, M. (2014). Measuring cell fluorescence using ImajeJ. https://theolb.readthedocs.io/en/latest/imaging/measuring-cell-fluorescence-using-imagej.html

Flemming, A. J., Shen, Z. Z., Cunha, A., Emmons, S. W., & Leroi, A. M. (2000). Somatic polyploidization and cellular proliferation drive body size evolution in nematodes. *Proceedings of the National Academy of Sciences*, *97*(10), 5285-5290.

Ganji, S., Wubben, M. J., & Jenkins, J. N. (2013). Two simple methods for the collection of individual life stages of reniform nematode, *Rotylenchulus reniformis*. *Journal of Nematology*, *45*(2), 87.

Han, Z., Thapa, S., Reuter-Carlson, U., Reed, H., Gates, M., Lambert, K. N., & Schroeder, N. E. (2018). Immobility in the sedentary plant-parasitic nematode *H. glycines* is associated with remodeling of neuromuscular tissue. *PLoS Pathogens*, *14*(8), e1007198.

Hastings, R. J. (1939). The biology of the meadow nematode *Pratylenchus pratensis* (de Man) Filipjev 1936. *Canadian Journal of Research*, *17*(2), 39-44.

Hedgecock, E. M., & White, J. G. (1985). Polyploid tissues in the nematode *Caenorhabditis elegans*. *Developmental Biology*, *107*(1), 128-133.

Holterman, M., van der Wurff, A., van den Elsen, S., van Megen, H., Bongers, T., Holovachov, O., Bakkar, J., & Helder, J. (2006). Phylum-wide analysis of SSU rDNA reveals deep phylogenetic relationships among nematodes and accelerated evolution toward crown clades. *Molecular Biology and Evolution*, *23*(9), 1792-1800.

Jones, J. T., Haegeman, A., Danchin, E. G., Gaur, H. S., Helder, J., Jones, M. G., Kikuchi, T., Manzanilla-López, R., Palomares-Rius, J.E., Wesemael, W.M. & Perry, R. N. (2013). Top 10 plant-parasitic nematodes in molecular plant pathology. *Molecular Plant Pathology*, *14*(9), 946-961.

Köppen, Mathias, Jeffrey S. Simske, Paul A. Sims, Bonnie L. Firestein, David H. Hall, Anthony D. Radice, Christopher Rongo, and Jeffrey D. Hardin. "Cooperative regulation of AJM-1 controls junctional integrity in *Caenorhabditis elegans* epithelia." *Nature Cell Biology* 3, no. 11 (2001): 983.

Lauritis, J. A., Rebois, R. V., & Graney, L. S. (1983). Development of *Heterodera glycines* Ichinohe on soybean, Glycine max (L.) Merr., under gnotobiotic conditions. *Journal of Nematology*, *15*(2), 272.

Lucius, R., & Poulin, R. (2016). General Aspects of Parasite Biology. *The Biology of Parasites*.

Plunkett, J. A., Simmons, R. B., & Walthall, W. W. (1996). Dynamic Interactions between Nerve and Muscle in *Caenorhabditis elegans*. *Developmental Biology*, *175*(1), 154-165.

Podbilewicz, B., & White, J. G. (1994). Cell fusions in the developing epithelia of *Caenorhabditis* elegans. *Developmental Biology*, *161*(2), 408-424.

Raski, D. J. (1950). The life history and morphology of the sugar-beet nematode, *Heterodera schachtii* Schmidt. *Phytopathology*, *40*(2), 135-152.

Rebois, R. V., & Huettel, R. N. (1986). Population dynamics, root penetration, and feeding behavior of *Pratylenchus agilis* in monoxenic root cultures of corn, tomato, and soybean. *Journal of Nematology*, *18*(3), 392.

Robinson, A. F., Inserra, R. N., Caswell-Chen, E. P., Vovlas, N., & Troccoli, A. (1997). Rotylenchulus species: Identification, distribution, host ranges, and crop plant resistance. *Nematropica*, *27*(2), 127-180.

Schmidt, G. D. (1962). *Tetrameres coloradensis* sp. n., a nematode parasite of the common snipe *Capella gallinago delicata*. *Journal of Parasitology*, *48*(6), 850-851.

Shemer, G., & Podbilewicz, B. (2000). Fusomorphogenesis: cell fusion in organ formation. *Developmental Dynamics: an Official Publication of the American Association of Anatomists*, *218*(1), 30-51.

Stiernagle, T. (2006). Maintenance of C. elegans (February 11, 2006), WormBook, ed. The *Caenorhabditis* elegans Research Community, WormBook, doi/10.1895/wormbook. 1.101. 1.

Sulston, J. E. (1976). Post-embryonic development in the ventral cord of *Caenorhabditis elegans*. *Philosophical Transaction of the Royal Society B*, *275*(938), 287-297.

Sulston, J. E., & Horvitz, H. R. (1977). Post-embryonic cell lineages of the nematode, *Caenorhabditis elegans*. *Developmental Biology*, *56*(1), 110-156.

Triantaphyllou, A. C., & Hirschmann, H. (1960). Post infection development of *Meloidogyne incognita* Chitwood 1949 (Nematoda-Heteroderidae). In *Annales de l'Institut Phytopathologique Benaki,*3(1),1-11.

Turner, S.J & Rowe, J.A. (2006) Cyst nematodes. In: *Plant Nematology* (Perry, R.N. and Moens, M., eds), pp. 90–122. Wallingford, Oxfordshire: CAB International.

Turner, S. J., & Subbotin, S. A. (2006). Cyst nematodes. In: Perry, R. N., & Moens, M. (eds) *Plant Nematology*, pp. 101-143. Wallingford, Oxfordshire: CAB International.

Tyler, J. (1933). Development of the root-knot nematode as affected by temperature. *Hilgardia*, *7*(10), 389-415.

van Megen, H., van den Elsen, S., Holterman, M., Karssen, G., Mooyman, P., Bongers, T., Holovachov, O., Bakker, J. & Helder, J. (2009). A phylogenetic tree of nematodes based on about 1200 full-length small subunit ribosomal DNA sequences. *Nematology*, *11*(6), 927-950.

Wang, C., Bruening, G., & Williamson, V. M. (2009). Determination of preferred pH for root-knot nematode aggregation using pluronic F-127 gel. *Journal of Chemical Ecology*, *35*(10), 1242-1251.

Williams, B. D., & Waterston, R. H. (1994). Genes critical for muscle development and function in *Caenorhabditis elegans* identified through lethal mutations. *The Journal of Cell Biology*, *124*(4), 475-490.

Woodruff, G. C., Willis, J. H., & Phillips, P. C. (2018). Dramatic evolution of body length due to postembryonic changes in cell size in a newly discovered close relative of *Caenorhabditis elegans*. *Evolution Letters*, *2*(4), 427-441.

CHAPTER 5: CONCLUSION AND FUTURE DIRECTION

Plant-parasitic nematodes are estimated to cause $80 billion of crop loss worldwide annually (Nicol et al. 2011). Among, plant-parasitic nematodes sedentary nematodes are more fecund and considered more damaging than their phylogenetically closest migratory relatives (Jones et al. 2013; Hasting 1939). Sedentary nematode *Heterodera glycines* alone can cause $469 to $818 million soybean yield loss annually in the United States (Matthews and Youssef 2016). Few options are available for *H. glycines* control. Additional control strategies are required to supplement existing control strategies. *H. glycines* has interesting but complicated hatching behavior. Further, in the post-infection sedentary part of the life cycle, *H. glycines* shows sex-specific body size and motility differences, which are not common in most nematodes. During my PhD, I studied *H. glycines* hatching behaviors and sex-specific developmental differences, which could serve as specific targets of its control.

H. glycines has complicated hatching behavior. Numerous studies have demonstrated that *H. glycines* hatching increases in the presence of a host plant or other stimulants (Perry 2002; Teft and Bone 1985; Teft, Rende and Bone 1982; Clark and Shepherd 1966), whereas some individual eggs will hatch in the absence of any stimulant. The presence of hatching stimulus ensures that actively growing roots are present for nematodes to infect and feed on (Jones et al. 1998). An allelopathic compound found in kidney bean (*Phaseolus vulgaris* L.) roots, glycinoeclepin A, is a natural hatching stimulus of *H. glycines* (Masamune et al.1982). In chapter 2, I found that hatching stimulants do not enhance embryogenesis process. My results suggest it may influence the hatching decision once J2 development is complete. In potato cyst nematode many researchers had found that stimulating hatching under inappropriate conditions using host

stimulants and starved the hatched J2s can be one possible control (Byrne et al. 2001; Devine et al. 2001; Ryan and Devine 2005). Majority of *H. glycines* eggs hatch in the presence of host cue, more greenhouse and field based research on stimulating hatching under inappropriate conditions may provide more information on *H. glycines* management too.

The nervous system of nematodes has been the primary target for nematode control (Holden-Dye and Walker 2011). However, our knowledge on the nervous system of sedentary plant-parasitic nematodes is very limited compared to the model nematode, *Caenorhabditis elegans.* Following infection and the establishment of a feeding site, sedentary nematodes become immobile. Interestingly, in some sedentary nematodes like *H. glycines*, loss of mobility after infection is reversed in adult males while females never regain mobility. In *C. elegans*, contraction and relaxation of most body wall muscles are regulated by motor neurons within the ventral nerve cord (VNC). In chapter 3, I found that VNC neurons degeneration is correlated with nematode sedentary behavior. Acetylcholinesterase (AChE) is involved in the termination of impulse transmission by rapid hydrolysis of the neurotransmitter acetylcholine (ACh) in numerous cholinergic pathway in the central and peripheral nervous system (Colovic et al. 2013). The activity of AChE is more in the nervous system, higher in motor neurons than in sensory neurons (Colovic et al. 2013). Atkinson et al. (2013) reported disturbing neuropeptides in a cyst nematode *Globodera pallida* could alter their movement and infection. My findings on neuronal remodeling behavior of *H. glycines* are not common behavior among nematodes. My results may be used to develop targeted control strategies for those economically important plant-parasitic nematodes with similar neuron remodeling behavior while avoiding off-target effects to beneficial nematodes and humans.

The sedentary life-style within the phylogenetic clade comprising the most plant-parasitic nematodes has arisen at least twice (Van Megen et al., 2009). Unlike most nematodes, sedentary nematode like *H. glycines* females grow disproportionately greater in width than in length developing into a saccate shaped adult. In the nematode *C. elegans,* body size is correlated with stem-cell-like divisions of laterally positioned stem cell-like 'seam' cells that contribute to an increase in the total number of epidermal nuclei (Sulston and Horvitz, 1977; Flemming et al. 2000). In chapter 4, I found that following infection, *H. glycines* seam cells proliferate extensively during each developmental stage. *H. glycines* adult female epidermis comprises a syncytium of approximately 1800 epidermal nuclei, in comparison to approximately 140 in *C. elegans* (Shemer and Podbilewicz 2000). I found that seam cells occupy major part of the *H. glycines* epidermis. In *C. elegans* seam cells are required for the formation of stage-specific cuticles. Fibrillar exudate has been found on the post-infection *H. glycines* cuticle surface (Endo 1933). We also observed fibrillar exudate in post-infection *H. glycines* (Figure 5.1). Aumann et al. (1991) reported fibrillar exudate may have some role in host-parasite interaction. *H. glycines* epidermal syncytium is made of seam cell daughter nuclei, it is possible that seam cells are responsible for producing fibrillar exudate and play some role in host-pathogen interaction. Furthermore, in chapter 4, I found that *Meloidogyne incognita* another saccate shape nematode also shows seam cell proliferation after infection, while the pattern of the division was very different than in *H. glycines*. Interestingly, *Rotylenchulus reniformis* seam cells do not proliferate after infection. My results suggest distinct mechanisms evolved to produce a similar phenotype from a common ancestor.

FIGURE

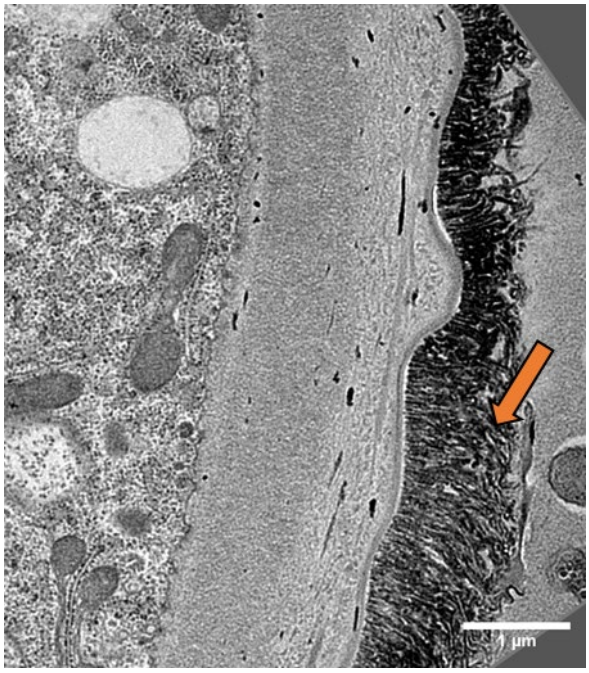

Figure 5.1. TEM micrograph of *Heterodera glycines* J4 female. Arrow fibrillar exudate.

REFERENCES

Atkinson, L. E., Stevenson, M., McCoy, C. J., Marks, N. J., Fleming, C., Zamanian, M., Day, T.M., Kimber, M.J., Maule, A.G., & Mousley, A. (2013). flp-32 Ligand/receptor silencing phenocopy faster plant pathogenic nematodes. *PLoS Pathogens*, *9*(2), e1003169.

Aumann, J., Robertson, W. M., & Wyss, U. (1991). Lectin binding to cuticle exudates of sedentary *Heterodera schachtii* (Nematoda: Heteroderidae). *Revue Nématol*, *14*(1), 113-118.

Byrne, J. T., Maher, N. J., & Jones, P. W. (2001). Comparative responses of *Globodera rostochiensis* and *G. pallida* to hatching chemicals. *Journal of Nematology*, *33*(4), 195.

Colovic, M. B., Krstic, D. Z., Lazarevic-Pasti, T. D., Bondzic, A. M., & Vasic, V. M. (2013). Acetylcholinesterase inhibitors: pharmacology and toxicology. *Current Neuropharmacology*, *11*(3), 315-335.

Devine, K. J., Byrne, J., & Jones, P. W. (2001). In-vitro studies on the relative availability and mobility in soil of natural hatching factors for the potato cyst nematodes, *Globodera rostochiensis* and *G. pallida*. *Nematology*, *3*(1), 75-83.

Endo, B. Y. (1993). Ultrastructure of cuticular exudates and related cuticular changes on juveniles in *Heterodera glycines*. *Journal of the Helminthological Society of Washington (USA)*.

Hastings, R. J. (1939). The biology of the meadow nematode *Pratylenchus pratensis* (de Man) Filipjev 1936. *Canadian Journal of Research*, *17*(2), 39-44.

Holden-Dye, L., & Walker, R. J. (2011). Neurobiology of plant parasitic nematodes. *Invertebrate Neuroscience*, *11*(1), 9-19.

Jones, P. W., Tylka, G. L. .& Perry, R.N. (1998). Hatching. In: Perry, R.N. & Wright, D.J. (Eds).The Physiology and Biochemistry of free living and Plant-parasitic nematodes. Wallingford, UK, CABI Publishing, pp. 181-121.

Masamune, T., Anetai, M., Takasugi, M., & Katsui, N. (1982). Isolation of a natural hatching stimulus, glycinoeclepin A, for the soybean cyst nematode. *Nature*, *297*(5866), 495.

Matthews, B. F., & Youssef, R. M. (2014). Soybean cyst nematode, *Heterodera glycines*, infection assay using soybean roots. *Molecular Plant Pathology*.

Nicol, J. M., Turner, S. J., Coyne, D. L., Nijs, L. Den, Hockland, S., Tahna Maafi, Z., et al. (2011). Genomics and Molecular Genetics of Plant-Nematode Interactions. In *Genomics and Molecular Genetics of Plant-Nematode Interactions*, p. 21–43. Available at: http://link.springer.com/10.1007/978-94-007-0434-3.

Perry, R.N. (2002). Hatching. In Lee, D, ed. The biology of nematodes. New York; Taylor and Francis. 147-69.

Shemer, G., & Podbilewicz, B. (2000). Fusomorphogenesis: cell fusion in organ formation. *Developmental Dynamics: An Official Publication of the American Association of Anatomists*, *218*(1), 30-51.

Sulston, J. E., & Horvitz, H. R. (1977). Post-embryonic cell lineages of the nematode, *Caenorhabditis elegans*. *Developmental Biology*, *56*(1), 110-156.

Ryan, A., & Devine, K. J. (2005). Comparison of the in-soil hatching responses of *Globodera rostochiensis* and *G. pallida* in the presence and absence of the host potato crop cv. British Queen. *Nematology*, *7*(4), 587-597.

Tefft, P. M., & Bone, L. W. (1985). Plant-induced hatching of eggs of the soybean cyst nematode *Heterodera glycines*. *Journal of Nematology*, *17*(3), 275.

Tefft, P. M., Rende, J. F., & Bone, L. W. (1982). Factors Influencing Egg Hatching of the Soybean Cyst Nematode. In *Proceeding of Helminthology Society of Washington,* 49(2), 258-265.

van Megen, H., van den Elsen, S., Holterman, M., Karssen, G., Mooyman, P., Bongers, T., Barkar, J., & Helder, J. (2009). A phylogenetic tree of nematodes based on about 1200 full-length small subunit ribosomal DNA sequences. *Nematology*, *11*(6), 927-950.